The Pennsylvania State University

The Graduate School

Department of Chemistry

# ANTIBACTERIAL POLYMERS,

# RECYCLABLE PALLADIUM CATALYSTS FOR COUPLING REACTIONS, AND

# CATALYTIC CONVERSION OF CELLULOSE INTO LIQUID FUELS

A Dissertation in

Chemistry

by

Shikchya Tandukar

© 2009 Shikchya Tandukar

Submitted in Partial Fulfillment
of the Requirements
for the Degree of

Doctor of Philosophy

May 2009

The dissertation of Shikchya Tandukar was reviewed and approved* by the following:

Ayusman Sen
Professor of Chemistry
Head of the Department of Chemistry
Dissertation Advisor
Chair of Committee

John V. Badding
Professor of Chemistry

Alan J. Benesi
Senior Lecturer in Chemistry
Director of NMR facility

T. C. (Mike) Chung
Professor of Materials Science and Engineering

*Signatures are on file in the Graduate School

## ABSTRACT

This thesis is focused mainly on two areas of chemistry- polymers and catalysis. In **chapter 2**, I have discussed the fundamentals of the chemical structure on the antibacterial activity of the imidazolium salts and polymers. The study correlates the effect of chemical nature of the alkyl tail and the positive charge on the potency of the antibacterial compounds studied. In **chapter 3**, I have reported the design and synthesis of silica nanoparticles supported N-heterocyclic carbene-palladium complexes and their application in carbon-carbon coupling reactions. The catalysts are air and moisture stable and because of the large surface to volume ratio of the nanoparticles, the catalyst sites are readily accessible to the reactants. Thus, they are effective catalyst for a wide range of substrates. However, conventionally, heterogeneous catalyst preparation is a multistep process including ligand synthesis, forming ligand-metal complex and then immobilization on to a solid support. In **chapter 4**, I have described a simple one step synthesis of heterogeneous palladium catalyst by crosslinking commercially available poly(allylamine) with a palladium salt. This method cuts down the time and cost involved otherwise and the catalyst proved to be an efficient catalyst for a number of carbon-carbon bond forming reactions. It was also easy to separate the catalyst and reused them without losing any activity. Further, in **chapter 5**, a mild reaction protocol for the synthesis of ether is reported. Finally, in **chapter 6**, I have discussed a thermo-catalytic method for converting cellulose into liquid fuels. This method used $H^+$ ions formed from water at high temperature to bring about the acid hydrolysis of cellulose into dehydrated hexitols and finally into liquid fuels like dimethytetrahydrofuran and other $C_5$ and $C_6$ compounds. As no mineral acid is used, the acid recovery and disposal is no longer an issue.

## TABLE OF CONTENTS

## LIST OF FIGURES

## LIST OF TABLES

## ACKNOWLEDGEMENTS

My first words of gratitude go to my advisor Dr. Ayusman Sen. Without his encouragement and support, both intellectual as well as financial, this journey would have been impossible. My sincere thanks for all he has done. I would also like to thank my committee members Dr. John V. Badding, Dr. Alan J. Benesi and T. C. (Mike) Chung for their valuable time and support. I should not forget to thank Dr. Blake Peterson for the use of the lab facilities for biological studies. I would like to thank Dr. Bob Minard for always being eager to help in deciphering the mass spectra.

During my graduate research, I learned a lot of experimental skills from Dr. Minren Lin, Dr. Myeongsoon Kang, Dr. Varun Sambhy and Dr. Megan M. MacBride. I also want to thank Dr. Sachin Borkar and Dr. Angel Ugrinov for their advice and suggestions. Thanks also go to current and former members of Sen's group for being supportive and creating a nice working environment. I would also like to thank Missy Hazen at electron microscopy facility, Dr. Allen Kimel at Material Science and Engineering, James Miller and Dr. Bob Minard at mass spectroscopy facility for being helpful as I was learning the analytical skills.

I am also very fortunate to have a Nepali community in State College that is like a home away from home. I am thankful to Dr. Prem Bhandari and family, Dr. Sundar Shrestha and family, Deepu and Nellie Bhattarai, and Aryendra Chakraborty who made me feel like a part of their family. My friends Soma, Sabi, British and Rajan deserve thanks for always lending an ear to me.

My family has been my solid ground for all the years in grad school. I would like to thank my father, Bhai Kaji Tandukar for his guidance and for having faith in me. He is the one who steered me towards chemistry. I would also like to remember my mother, late Vijaya Laxmi Tandukar. I miss her and I am always grateful for her love and support. I also want to thank my

brother, Dewas Tandukar and his family Susan and Sydney for supporting my decisions and being there for me. I am also grateful to my aunt Vishow Laxmi Tandukar and my cousins Sagun, Nirjal, and Lina and all my extended family members for their encouragement. Last but not the least; I would like to thank my husband Omkar Raman Parajuli for his love and encouragement. He has been a friend and a critique. I will always be indebted to him for his selfless support during the tumultuous period in my life when I first came to Penn State. Thank you.

## Chapter 1

# Introduction

Antibacterial compounds are being increasingly used as cleaning products in everyday life because of the increase in the public health awareness. It is highly desirable to use them as a simple coating on surfaces for contact killing the nuisance microorganisms. Antimicrobial coatings on hospital surfaces, medical devices and implants can prevent the life threatening microbial infections in patients who have compromised immune system. They also find application in food processing and packaging industries.**[1],[2]** Recent outbreak of *E. coli* in spinach and ground beef**[3],[4]** and *Salmonella* in packaged goods like peanut butter and fresh produce like jalapeno peppers and tomatoes**[5]** emphasize the importance of a sterile environment during food production and packaging. This has driven the research in making the most effective antibacterial material and for designing them, it is essential to understand the mode of action of these antibacterial compounds and how their chemical structure affect the antibacterial activity. In **chapter 2**, I have discussed the structure activity relationships in imidazolium small molecules and polymers. Imidazole derivatives are bioactive compounds and are increasingly used in pharmaceutical companies and hence, it is relevant to consider imidazole based antibacterial compound for this study. The dependence of the antibacterial activity in the nature of the alkyl tail and the amount of the positive charge is studied in the first chapter.

Transition metal catalyzed coupling reactions like Suzuki, Heck and Sonogashira are extensively used in industries.**[6],[7]** The invention of these methods has simplified the carbon-carbon bond formation. However, transition metals, like Pd, Pt, Rh, Ru used for the catalysis, are expensive. Homogeneous catalysts that are often employed are difficult to separate from the product. The trace metal contamination is not desirable, especially when the final product is a

drug component. Heterogeneous catalysts, in which the transition metal species are anchored onto a solid support, can be easily separated and reused several times. Polymer supported recyclable heterogeneous catalysts have been reported,**[8],[9],[10],[11]** but in these cases, some of the active sites are embedded in the polymer matrix and cannot participate in the reaction. It is essential to have all the active sites on the surface of the support for an efficient catalyst. In **chapter 3**, I have discussed the synthesis of N-heterocyclic carbene-palladium complex (NHC-Pd) immobilized on ~10 nm silica particles.**[12]** In the last decade, N-heterocyclic carbene (NHC) has gained considerable attention as an alternative to the widely used phosphine ligand. NHC exhibits air and moisture stability that is lacked by phosphine ligands. Further, because of the very high surface area of the silica nanoparticles, these catalysts remain suspended in a variety of solvents with the catalyst sites readily accessible to the reactants. The silica nanoparticle supported NHC-Pd catalyst was applied for Suzuki and Heck coupling reactions using a wide range of substrate in benign, non-conventional solvents including water. They were also easily separated by filtration and reused repeatedly.

In **chapter 4**, I have reported a simple one step synthesis of heterogeneous palladium catalyst by crosslinking commercially available poly(allylamine) with a palladium salt. This method minimized the time and cost involved in the tedious multistep conventional routes employed for heterogeneous catalyst preparation. The resulting Pd cross-linked polymer PAA-Pd catalyst was air and moisture stable and insoluble in the reaction solvents used. PAA-Pd effectively catalyzed Suzuki, Heck and Sonogashira coupling in benign solvents, including water. They were separated easily and used multiple times without the loss of activity. Based on the easy preparation and long lifetime of the catalyst, a continuous reactor system was also designed for easy separation of the product.

In **chapter 5**, I have reported a mild reaction condition for the synthesis of unsymmetrical ethers. Ketones and phenols react with primary and secondary alcohols to yield a

range of unsymmetrical ether. The reaction was catalyzed by catalytic amounts of mineral as well as solid acid.

Finally, in **chapter 6**, I have further employed the catalytic method in the thermo-chemical conversion of cellulose into biofuel. The worldwide energy crisis has catapult much research in alternate fuel sources. Cellulose, which is the most abundant form of biomass, is gaining popularity as a renewable resource for making biofuel. This resource has no net effect in the greenhouse gas as the $CO_2$ produced from fuel consumption is subsequently used during the regrowth of the plants.**[13]** However, the two methods that are commonly used for converting cellulose into liquid fuel have their own limitations. The acid hydrolysis is a corrosive method and the recovery and proper disposal of the acid is always an issue. Enzymatic method is carried out in a milder condition, but the process is slow and the enzymes are expensive.**[14]** In this chapter, I have discussed the method in which cellulose is converted into dehydrated hexitols and finally into fuels using reversibly formed acid from water at high temperature. The reaction is catalyzed by Rh catalyst. The most appealing aspect of this process is that no mineral acid is used for hydrolysis. Rather, acid hydrolysis of the celluloses is performed by $H^+$ ions generated from water at high temperature. At ambient temperature, these in situ formed $H^+$ ions disappear thereby eliminating the need for acid recovery and disposal.**[15]**

**References**

**1.** Nuzzo, R. G. *Nat. Mater*. **2003**, *2*, 207-208.

**2.** Greenberg, C. B.; Steffek, C. *Thin Solid Films* **2005**, *484*, 324-327.

**3.** http://www.cdc.gov/ecoli/june2008outbreak/

**4.** http://www.cdc.gov/ecoli/2006/september/

**5.** http://www.cdc.gov/salmonella/saintpaul/

**6.** Tsuji, J. *Palladium Reagents and Catalysts: Innovations in Organic Synthesis*; Wiley: Chichester, 1995.

**7.** Heck, R. F. *Comprehensive Organic Synthesis*; Trost, B. M.; Fleming, I., Eds.; Pergamon: Oxford, 1991.

**8.** Kim, J-H.; Kim, J-W.; Shokouhimehr, M.; Lee, Y-S. *J. Org. Chem*. **2005**, *70*, 6714-6720.

**9.** Schwarz, J.; Bohm, V. P. W.; Gardiner, M. G.; Grosche, M.; Harrmann, W. A.; Hieringer, W.; Raudaschl-Sieber, G. *Chem. Eur. J*. **2000**, *6*, 1773-1780.

**10.** Byun, J-W.; Lee, Y-S. *Tetrahedron Lett*. **2004**, *45*, 1837-1840.

**11.** Kim, J-W.; Kim, J-H.; Lee, D-H.; Lee, Y-S. *Tetrahedron Lett.* **2006**, *47*, 4745-4748.

**12.** Tandukar, S.; Sen, A. *J. Mol. Catal. A:Chem*. **2007**, *268*, 112-119.

**13.** Klass, D. L. *Biomass for Renewable Energy, Fuels, and Chemicals*, Academic Press: San Diego, 1998.

**14.** U. S. Department of Energy, Energy Efficiency and Renewable Energy. http://www.eere.energy.gov/biomass (accessed on January 24, 2007).

**15.** (a) Chamblee, T. S.; Weikel, R. R.; Nolen, S. A.; Liotta, C. L.; Eckert, C. A. *Green Chem*. **2004**, *6*, 382-386. (b) Nolen, C. A.; Liotta, C. L.; Eckert, C. A.; Glaserb, R. *Green Chem*. **2003**, *5*, 663-669.

# Chapter 2

# Structure-Activity Relationships in Antibacterial Imidazolium Compounds

## 2.1 Introduction

The demand for materials that kill harmful microbes is increasing due to the increase in the public health awareness. Quaternary ammonium compounds (QAC) including pyridinium and imidazolium groups are potent towards both gram positive and gram negative bacteria.**[1],[2]** These antibacterial compounds carry a positive charge, usually on the quaternary nitrogen, and a hydrophobic unit, a hydrocarbon tail. The lethal action of QAC is proposed to be because of the disruption of the bacterial cell membrane.**[3]** All cell membranes are made up of lipid molecules arranged into a bilayer structure as shown in (Figure **2-1**). The lipid molecule consists of a polar head and a hydrophobic alkyl tail.**[4]** At physiological pH, the bacterial cell surface is considered to be negatively charged due to the phosphatidic groups of the lipid bilayer structure. The positively charge QAC binds electro-statically to the negatively charged bacterial cell surface. The hydrocarbon tail of the QAC then interacts with the inner lying hydrophobic group of the lipid bilayer structure, thereby disrupting the cell membrane. This leads to the leakage of cytoplasmic contents and finally results in the cell death. Electron scanning microscopy has been used to confirm these morphological changes in the bacterial cell membrane after treating with antibacterial compound (Figure **2-2**).**[5]**

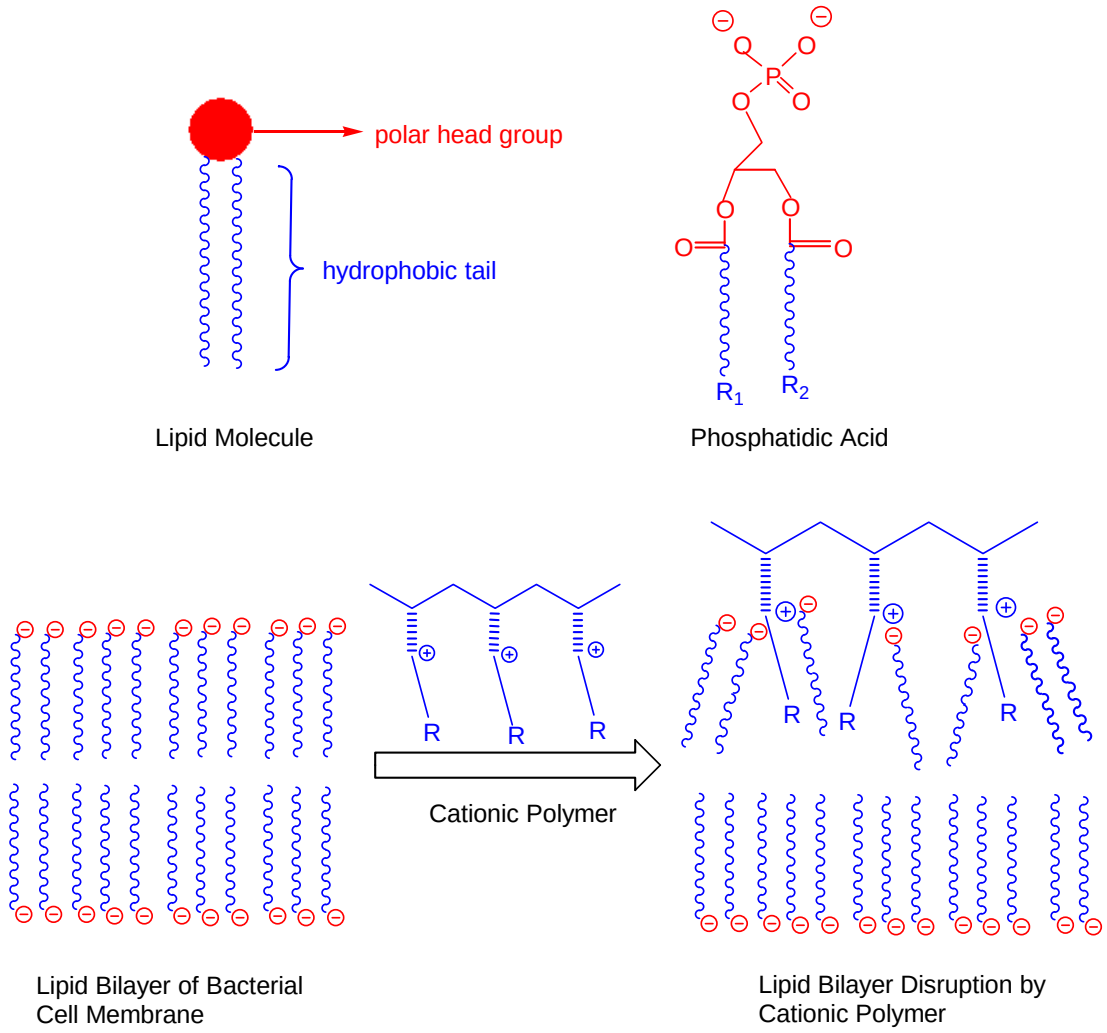


Figure **2-1**: Schematic representation of the membrane disruption by antibacterial cationic polymer.

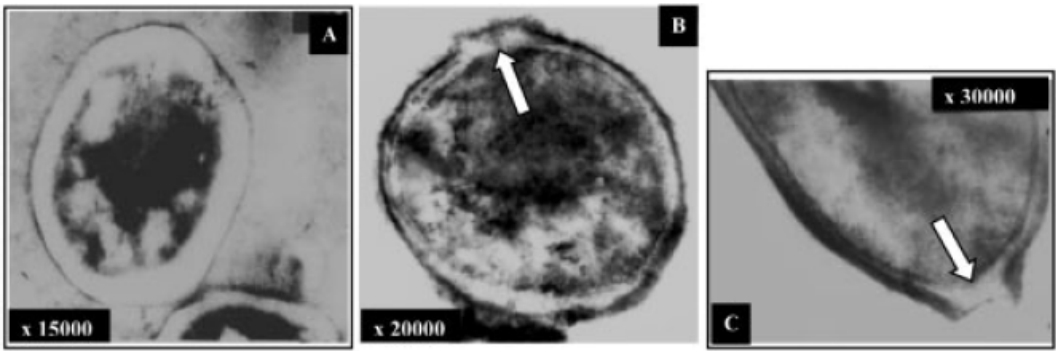


Figure **2-2**: Electron Scanning Micrograph of: (A) Normal *Staphylococcus aureus* cell. (B) and (C) *Staphylococcus aureus* cell after treating with cationic polymer, in which disruption in the cell membrane as well as irregular cell shape are seen.**[5]**

The cationic polymers have enhanced antibacterial activity than the small molecules.**[3]** The higher potency of the cationic polymer is interpreted to be due to the increase in the charge density. From the commercial point of view, the polymers can be used as antimicrobial coating on everyday use surfaces like door knobs, keyboards, kitchen surfaces, hospital surfaces, clothing, etc. A large number of antibacterial polymers have been synthesized from conventional polymers like poly(vinyl pyridine), poly(vinyl alcohol), polyacrylate, polymethacrylate, polystyrene and poly(methyl methacrylate).**[6]**

Imidazole derivatives are bioactive compounds. It is increasingly being used in pharmaceuticals as antifungal, antimicrobial**[7]** and antitumor medications.**[8]** It is also used as hypocholesterolaemic agent.**[9]** The antibacterial activity of the quaternary imidazolium compound have been studied extensively and the concentration as low as 4 μg/mL is effective in killing the bacteria.**[10]** However, only few references are available that covers the antibacterial activity of imidazolium polymers.**[11]** The activity of cationic polymer was found to be considerably more than the corresponding small molecule for gram negative bacteria. It is known that the antibacterial effect of the cationic polymer depends on the polymer structure. The length

of the alkyl tail in the imidazolium unit plays a vital role in determining the potency of the antibacterial compound. The antibacterial activity increases with the increase in the tail length for quaternary imidazolium compounds. However, the cationic polymers do not follow this general trend because of the localization of the active sites in the polymer. It is very important to understand the structure-activity of the cationic polymer for designing the effective antibacterial material.

In this chapter, the structure-activity relationship of the imidazolium salts and polymers will be discussed. The antibacterial activity of the imidazolium salts were correlated with the length of alkyl tail. These alkyl tails are almost always linear for penetrating the cell surface. Branching in the tail is said to decrease the efficacy of the compounds.**[12]** The activity was also established between the linear and the branched alkyl tail. The antibacterial activity of the imidazolium polymers were correlated to the length of the alkyl tail, degree of N-alkylation, charge density and polymer chain length. The antibacterial activity of these imidazolium polymers were tested against both types of bacterial strains- gram positive *Bacillus cereus* and gram negative *Escherichia coli*.

## 2.2 Results and Discussion

### 2.2.1 Synthesis of N-Alkylated Imdazolium Salts and Polymers

1-Alkyl-3-vinyl imidazolium bromides ($C_n$VIB) were synthesized by heating N-vinyl imidazole with alkyl bromides. The synthetic scheme is shown in (Figure **2-3**). The nitrogen atom at position **1** was alkylated with short (propyl), moderately long (butyl, hexyl, octyl) and long (decyl, dodecyl, tetradecyl and hexadecyl) linear hydrocarbon tails. Bioactive compounds with quaternary nitrogen almost always have a linear alkyl tail for disrupting the cell surface. The branched alkyl tail is said to have lower antibacterial efficacy. The effect of the branched alkyl tail in the antibacterial activity was also studied. For this, N-vinyl imidazole was alkylated with 1-bromo-3,5,5-trimethyl hexane and 1-bromo-2-ethyl hexane. The resulting series were characterized by $^1$H NMR and the upfield shift of the singlet for hydrogen at position C-2 of the imidazolium ring from 7.8 ppm to 10.9 ppm ensured the alkylation.

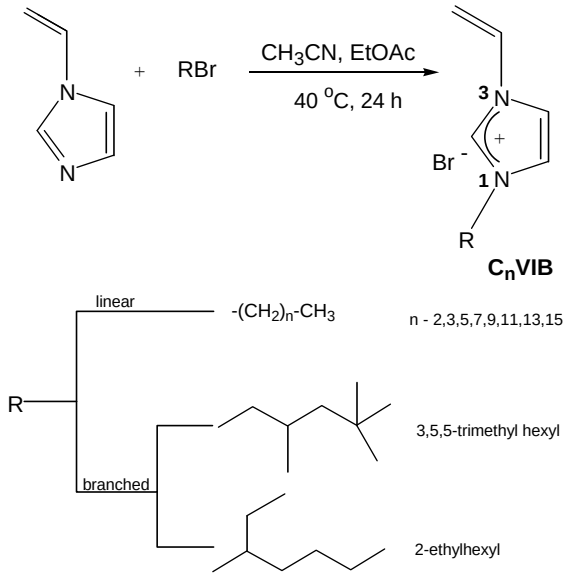


Figure **2-3**: Synthesis of a library of 1-alkyl-3-vinyl imidazolium bromide.

It has been reported that cationic polymers with moderately long alkyl tail ($C_{4-8}$) show higher potency than polymers with short ($C_{1-3}$) and long ($C_{10}$ and above) alkyl tails. The polymer with long alkyl moieties tend to stick to each other due to hydrophobic interaction. However, in polymers with moderately long alkyl moieties, such interaction is not strong enough to overcome the electrostatic repulsion due to the positive charge of the polymer. **[1a]** There seems to be an optimum tail length for effectively disrupting the cell membrane while preventing the hydrophobic inter-chain aggregation of the polymer.**[13]** So, 1-hexyl-3-vinyl imidazolium bromide ($C_6$VIB) and 1-octyl-3-vinyl imidazolium bromide ($C_8$VIB) with moderately long alkyl tail were considered for the synthesis of cationic polymers. $C_6$VIB and $C_8$VIB were each randomly polymerized by free radical method. Three different types of polymers were made:

(i) a homopolymers of $C_n$VIB {where n-6,8} (Figure **2-4**),

(ii) a copolymer of $C_n$VIB with n-vinyl imidazole (VI) (Figure **2-5**) and

(iii) a copolymer of $C_n$VIB with 1-propyl-3-vinyl imidazolium bromide ($C_3$VIB) to retain the charge density in the polymer chain (Figure **2-6**).

The N-alkylated active sites in the copolymers were maintained at 10 and 25 % by varying the molar ratio of $C_n$VIB. The monomers to initiator concentration ratio $[M_o]/[I]$ was maintained at either 20 or 50 for varying the polymer chain length.

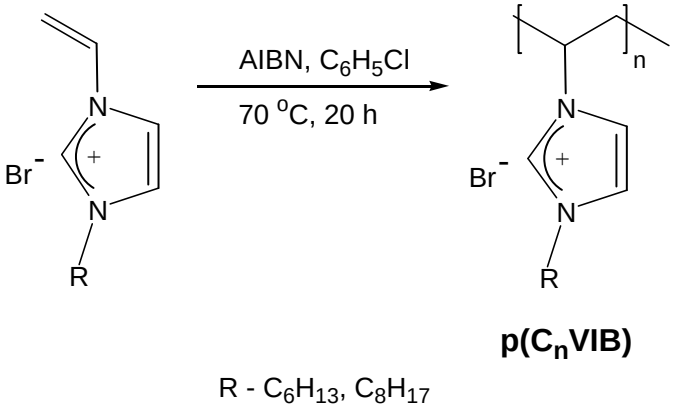


Figure **2-4**: Free radical polymerization of 1-alkyl-3-vinyl imidazolium bromide.

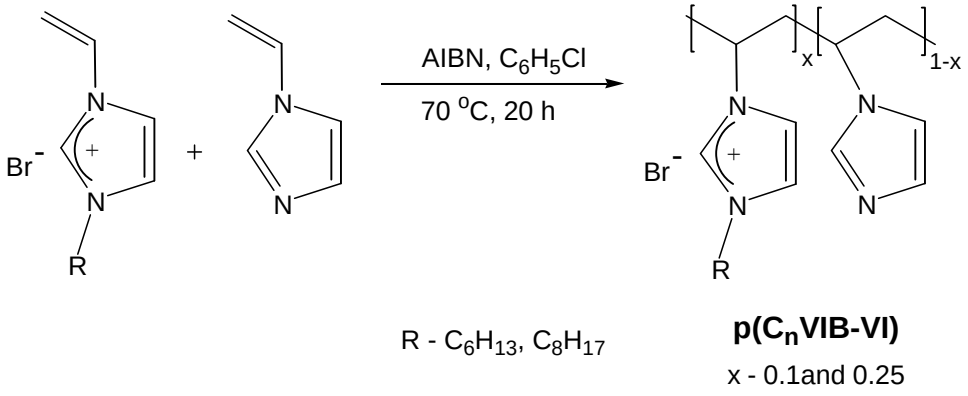


Figure **2-5**: Copolymerization of 1-alkyl-3-vinyl imidazolium bromide with vinyl imidazole.

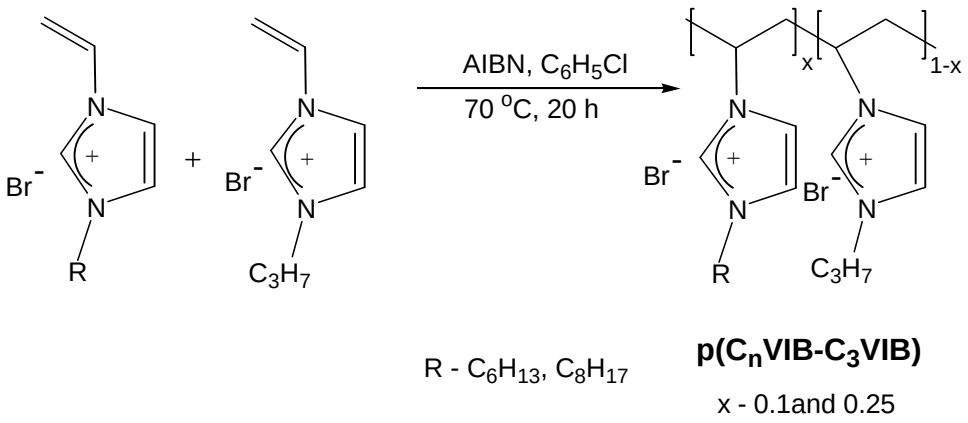


Figure **2-6**: Copolymerization of 1-alkyl-3-vinyl imidazolium bromide with 1-propyl-3-vinyl imidazolium bromide.

### 2.2.2 Antibacterial Assay using Microdilution Method

The antibacterial activity of the imidazolium salts and the cationic polymer were studied by modified microdilution broth assay method.**[14]** The activity is reported as Minimum Inhibitory Concentration (MIC), which is the lowest concentration required to kill greater than 99% of the added bacteria. The lower the MIC value for a compound, higher is the antibacterial activity. The schematic representation of the antibacterial assay is shown in (Figure **2-7**).**[15]** In a 96 well polystyrene tray, an appropriate volume of the Luria-Bertani (LB) nutrient broth, aqueous solution of the compound and the bacterial cell solution was taken. The initial innoculum concentration was approximately $5x10^5$ cfu/mL and the concentration of the compound in the wells ranged from $4x10^{-3}$ to 3.0 mg/mL. The tray was then incubated for ~ 18 h at the appropriate temperature.

The bacterial growth was analyzed by recording the absorbance at 590 nm at the beginning and the end of incubation. The difference in the absorbance is correlated to the change in the cell density in each well. The wells were also visually analyzed for turbidity. If the compounds are ineffective, the bacterial colonies grow and the clear LB test solution turns turbid. The lack of turbidity can be due to either the death of bacteria (bactericidal effect) or minimum bacterial growth (bacteriostatic effect). The bactericidal or bacteriostatic effect of the polymer is determined by the spread count method.**[16]** Aliquots were taken from the wells showing no cell growth and plated on to the LB-agar plates. The plates were incubated overnight at the appropriate temperature and the colonies were quantified. The bacterial colonies on the plate indicate the growth was only stopped in the aliquots, i.e., bacteriostatic effect. If the compound is bactericidal, no/few colonies can be seen. The tests were done in duplicate to check the accuracy of the results.

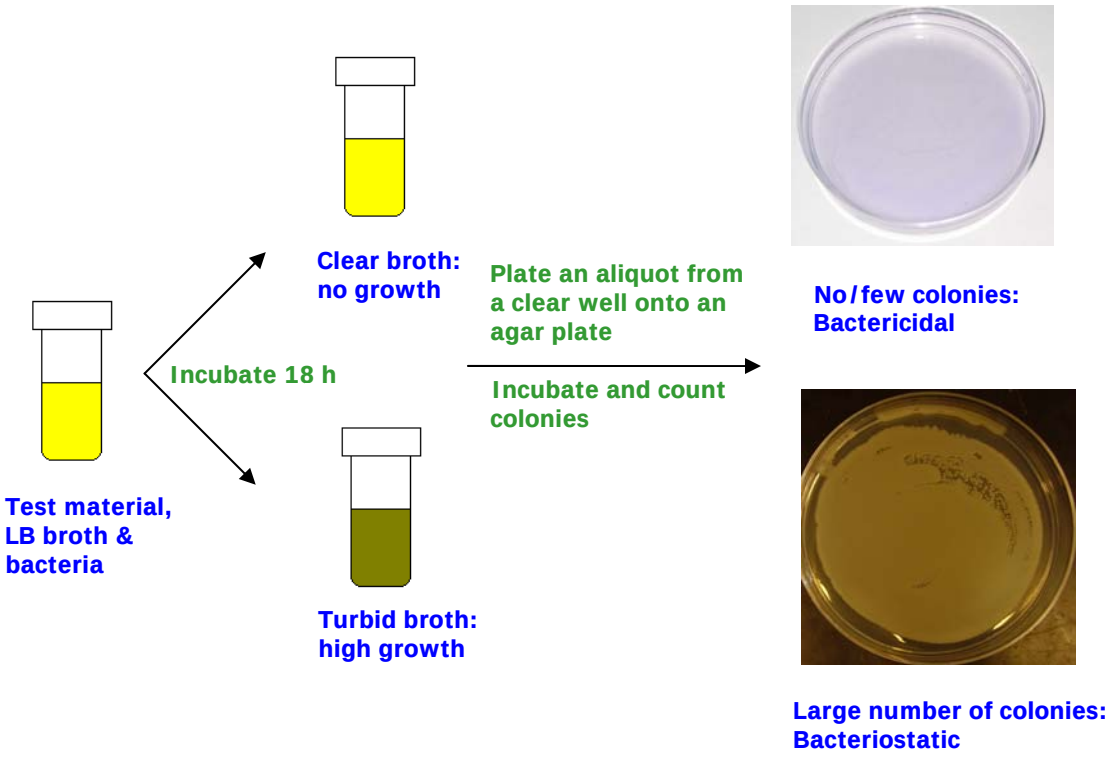


Figure **2-7**: Schematic representation for determining the antibacterial activity of N-alkylated imidazolium salts and polymers by microdilution method.**[15]**

### 2.2.3 Antibacterial Activity of 1-Alkyl-3-Vinyl Imidazolium Bromide

All small molecules synthesized were soluble in water and their antibacterial activities were tested against gram negative *E. coli* and gram positive *B. cereus* using microdilution broth assay method described earlier. The MIC values of the tested imidazolium salts against *E. coli* and *B. cereus* as a function of the alkyl tail length is given in (Table **2-1**). A clear relation between the lengths of the alkyl tail and the antibacterial effect was observed for linear 1-alkyl-3-vinyl imidazolium bromides ($C_n$VIB). The imidazolium salts with short alkyl tails, $C_3$VIB and $C_4$VIB were ineffective against the tested bacteria. Henceforth, the MIC values decreased with the increase in the length of the alkyl tail from $C_6$ to $C_{16}$. 1-tetradecyl and 1-hexadecyl -3-vinyl imidazolium bromide have the lowest MIC of 4 μg/mL against both *E. coli* and *B. cereus*. Among the quaternary salts tested, the longer tail should have allowed better disruption of the bacterial cell membrane. It should also be assumed that the electrostatic repulsion between these molecules overcome the hydrophobic interaction thereby preventing the aggregation of the compounds.**[1a]**

The branching in the alkyl tail did not decrease the antibacterial activity of the studied imidazolium salts. The linear $C_6$VIB and branched 1-(3,5,5-trimethylhexyl)-3-vinyl imidazolium bromide (T $C_6$VIB) and 1-(2-ethylhexyl)-3-vinyl imidazolium bromide (E$C_6$VIB) showed similar activity towards *E. coli* whereas, 1-(3,5,5-trimethylhexy)l-3-vinyl imidazolium bromide showed enhanced activity than $C_6$VIB towards *B. cereus.* The branching in the tail at the terminal end might have eased the penetration of the thick peptidoglycan layer in the cell membrane of the gram positive bacteria. 1-(2-ethylhexyl)-3-vinyl imidazolium bromide which is branched close to the positive charge of the imidazolium ring shows similar activity as $C_6$VIB.

Table **2-1**: Antibacterial activity of 1-alkyl-3-vinyl imidazolium bromide.

| entry | sample | MIC (mg/mL) | |
|---|---|---|---|
| | | ***E. coli*** | ***B. cereus*** |
| 1 | $C_3$VIB | - | - |
| 2 | $C_4$VIB | - | - |
| 3 | $C_6$VIB | 2.6 | 2.6 |
| 4 | $C_8$VIB | 0.3 | 2.9 |
| 5 | $C_{10}$VIB | 0.3 | 0.3 |
| 6 | $C_{12}$VIB | 0.03 | 0.03 |
| 7 | $C_{14}$VIB | 0.004 | 0.004 |
| 8 | $C_{16}$VIB | 0.004 | 0.004 |
| 9 | $TC_6$VIB | 3.0 | 0.3 |
| 10 | $EC_6$VIB | 2.9 | 2.9 |

**$TC_6$VIB**=1-(3,5,5-trimethylhexyl)-3-vinyl imidazolium bromide
**$EC_6$VIB**=1-(2-ethylhexyl)-3-vinyl imidazolium bromide

### 2.2.4 Antibacterial Activity of Cationic Imidazolium Polymers

Antibacterial activity is said to be enhanced in cationic polymers due to the increased charge density. As discussed earlier, imidazolium salts with moderately long alkyl tail $C_6$VIB and $C_8$VIB were considered for polymerization. (Table **2-2**) shows a library of polymer synthesized to study the structure-activity relationship.

Table **2-2**: A list of copolymers synthesized to study the structure-activity relation.

| entry | polymer | ratio of $C_n$VIB[a] | $[M_o]$:[I][b] |
|---|---|---|---|
| 1 | p( $C_6$VIB-$C_3$VIB) | 0.25 | 50:1 |
| 2 | p( $C_6$VIB-$C_3$VIB) | 0.10 | 50:1 |
| 3 | p( $C_6$VIB-$C_3$VIB) | 0.10 | 20:1 |
| 4 | p( $C_6$VIB-VI) | 0.10 | 50:1 |
| 5 | p( $C_6$VIB-VI) | 0.10 | 20:1 |
| 6 | p( $C_8$VIB-$C_3$VIB) | 0.25 | 50:1 |
| 7 | p( $C_8$VIB-$C_3$VIB) | 0.10 | 50:1 |
| 8 | p( $C_8$VIB-$C_3$VIB) | 0.10 | 20:1 |
| 9 | p( $C_8$VIB-VI) | 0.10 | 20:1 |

[a] n – 6,8. [b] $[M_o]$ is the total monomer concentration in moles and [I] is initiator concentration.

The homopolymers p($C_6$VIB) and p($C_8$VIB) were completely ineffective in killing/inhibiting the bacteria up to the tested MIC of 2.5 mg/mL. Their copolymers with vinyl imidazole in which the N-alkyl moieties were reduced to 50 % were also ineffective (data not included). In the studied polymers, the local concentration of the alkyl tails in the polymer chain must be high enough for the hydrophobic aggregation.**[17],[18]** Thus, it was necessary to decrease the N-alkyated sites in the cationic polymer. However, this also minimizes the charge density in the polymer. The electrostatic adsorption of the positively charged polymer to the negatively charged bacterial cell surface is vital for the cell death. So, in the next step, $C_6$VIB and $C_8$VIB were individually copolymerized with $C_3$VIB. As discussed earlier, $C_3$VIB has no antibacterial activity and would only retain the charge density in the polymer. The molar ratio of the active monomer to $C_3$VIB was varied to be 1:9 and 1:3 for 10 and 25 % N-alkyaltion respectively. The chain length was varied by varying the monomers to initiator concentration ratio $[M_o]/[I]$ to 20 and 50. The active monomers were also polymerized with vinyl imidazole in the ratio of 1:9 and $[M_o]/[I]$ ratio of 20 and 50.

The MIC values of the polymers against gram negative *E. coli* are shown in (Table **2-3**). The $C_6$VIB based copolymers have MIC values lower than that of the monomer confirming the enhanced antibacterial property of the polymer. However, $C_8$VIB based copolymers have MIC values higher than the corresponding monomer. The six carbon tail seems to be an optimum tail length to cause the effective membrane disruption.

The antibacterial activity of $C_6$VIB based copolymers with 10 and 25 % N- hexyl tails were identical (entries 1 and 2). This result shows that 10 % active sites in the polymer is sufficient to kill the bacteria. The activity seems to be independent of the percent N-hexyl tails beyond this limit. Among the $C_6$VIB based copolymers tested, poly($C_6$VIB-VI) has the lowest MIC of 0.25 mg/mL (entries 4 and 5). The lower MIC value of poly($C_6$VIB-VI) than poly($C_6$VIB-$C_3$VIB) (entries 2 and 3) indicates that maintaining the charge density in the polymer

does not necessarily improve the antibacterial activity. The results show that even a small percent of positive charge is sufficient to effectively bind the polymer to the bacterial cell surface and cause membrane disruption. The decreased activity of poly($C_6$VIB-$C_3$VIB) can be due to the additional propyl tails in the polymer chain which can lower the mobility of hexyl tails needed for membrane disruption. The activity of poly($C_6$VIB-$C_3$VIB) (entry 3) with shorter polymer chain was slightly lower than that of poly($C_6$VIB-$C_3$VIB) (entry 2) with longer polymer chain while such effect of the polymer chain length was not observed in the case of poly($C_6$VIB-VI) (entries 4 and 5).

Table **2-3**: Antibacterial activities of the copolymers against gram negative *E. coli*.

| **entry** | **polymer** | **ratio of $C_n$VIB**[a] | **$[M_o]$:[I]**[b] | **MIC** (mg/mL) | **monomer MIC** (mg/mL) |
|---|---|---|---|---|---|
| 1 | p( $C_6$VIB-$C_3$VIB) | 0.25 | 50:1 | 1.0 | |
| 2 | p( $C_6$VIB-$C_3$VIB) | 0.10 | 50:1 | 1.0 | |
| 3 | p( $C_6$VIB-$C_3$VIB) | 0.10 | 20:1 | 1.5 | |
| 4 | p( $C_6$VIB-VI) | 0.10 | 50:1 | 0.25 | 2.6 |
| 5 | p( $C_6$VIB-VI) | 0.10 | 20:1 | 0.25 | |
| 6 | p( $C_8$VIB-$C_3$VIB) | 0.25 | 50:1 | 1.0 | |
| 7 | p( $C_8$VIB-$C_3$VIB) | 0.10 | 50:1 | 1.0 | |
| 8 | p( $C_8$VIB-$C_3$VIB) | 0.10 | 20:1 | 1.0 | 0.3 |
| 9 | p( $C_8$VIB-VI) | 0.10 | 20:1 | >1.0 | |

[a] n – 6,8. [b] $[M_o]$is the total monomer concentration in moles and [I] is initiator concentration.

Based on the previous result, only $C_6$VIB based copolymers were tested against gram positive *B. cereus* and the MIC values are shown in (Table **2-4**). The MIC values are lower than that of the corresponding monomer. Poly($C_6$VIB-VI) has the lowest MIC of 1.0 mg/mL. Poly($C_6$VIB-VI) has higher activity than poly ($C_6$VIB-$C_3$VIB) as in the case of *E. coli*. They also show similar trend for the polymer chain length.

Table **2-4**: Antibacterial activities of the copolymers against gram positive *B. cereus*.

| **entry** | **polymer** | **ratio of $C_n$VIB**[a] | **$[M_o]$:[I]**[b] | **MIC** (mg/mL) | **monomer MIC** (mg/mL) |
|---|---|---|---|---|---|
| 1 | p( $C_6$VIB-$C_3$VIB) | 0.10 | 50:1 | 2.0 | |
| 2 | p( $C_6$VIB-$C_3$VIB) | 0.10 | 20:1 | 2.5 | |
| 3 | p( $C_6$VIB-VI) | 0.10 | 50:1 | 1.0 | 2.6 |
| 4 | p( $C_6$VIB-VI) | 0.10 | 20:1 | 1.0 | |

[a] n – 6,8. [b] $[M_o]$is the total monomer concentration in moles and [I] is initiator concentration.

### 2.2.5 Rate of Bacterial Cell Death

It is desirable that these antibacterial polymers rapidly kill bacteria. The kill kinetics of poly($C_6$VIB-VI) with 10 % N-alkylation and monomers to initiator concentration ratio {[$M_o$]:[I]} of 20 and 50 were investigated against *B. cereus*. These two polymers have the same MIC of 1.0 mg/mL but differ only in the polymer chain length. The 1.0 mg/mL polymer solution in LB broth and the bacterial cell solution with an initial innoculum of $5x10^5$ cfu/mL were taken in a 15 ml culture tube and incubated at 30 ˚C. Small aliquots were taken at different time intervals to count the viable cells by spread count method described previously. A plot of viable *B. cereus* cells in the culture against time is shown in (Figure **2-8**). Both polymer showed similar activity and 99 % of bacteria was killed within 2 minutes of coming in contact with the polymer.

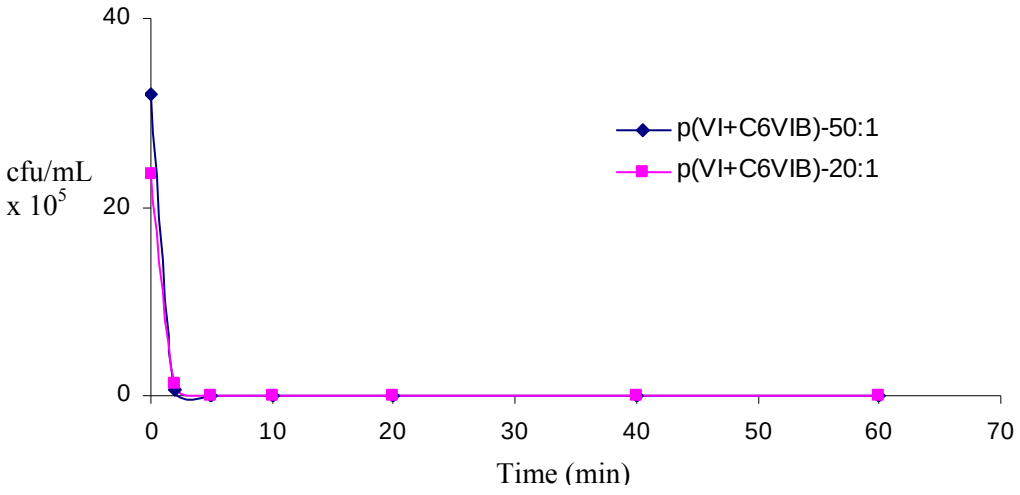


Figure **2-8**: Rate of *B. cereus* cell death in the presence of p($C_6$VIB-VI).

## 2.3 Conclusion

The structure-activity relationship of different N-alkylated imidazolium salts and cationic polymers were established. The antibacterial activity of the N-alkylated imidazolium salts increased with the increase in the alkyl tail and the branching in the tail did not decrease the potency of the compound, in fact, the branching at the tip of the tail increased the potency of the compound. The antibacterial activity of the cationic imidazolium polymers were also correlated to the length of the alkyl tail, degree of N-alkylation, charge density and the polymer chain length. It was observed that the $C_6$VIB based copolymers had lower MIC than their corresponding monomer. Poly ($C_6$VIB-VI) were most effective in killing the bacteria and as low as 10 % loading of the active sites in the polymer is sufficient to be potent. It was also seen that maintaining the charge density over the entire polymer chain did not increased their antibacterial activity. The effect of the polymer chain length on the activity was not observed. Poly ($C_6$VIB-VI) killed bacteria within 2 minutes of contact. This structure-activity relationship study established for the imidazolium compounds would help in designing effective and powerful antibacterial materials.

## 2.4 Experimental

### 2.4.1 Materials and Instrumentation

N-vinyl imidazole, 1-bromopropane, 1-bromobutane, 1-bromohexane, 1-bromooctane, 1-bromodecane, 3,5,5-trimethyl-1-hexanol and 1-bromo-2-ethyl hexane were purchased from Aldrich Chemical Co. 1-bromododecane was purchased from Avocado. 1-bromotetradecane and 1-bromohexadecane were purchased from Acros Organics. N-vinyl imidazole was distilled prior to use while all other reagents were used as received. Luria-Bertani (LB) broth (Lennox modification) and agar were purchased from DIFCO. 96 well polystyrene plates were purchased from Nunc. $^{1}$H NMR spectra were collected on a Bruker DPX300 (300 MHz) and DRX400 (400MHz) spectrometers. Perkin Elmer HTS 7000 bioassay reader was used to measure absorbance during bioassay.

### 2.4.2 Synthesis of 1-Bromo-3,5,5-Trimethylhexane

To the hydrobromic acid (0.13 mol, 47-49 %), in a round bottom flask, concentrated sulfuric acid (0.032 mol) was added drop wise with continuous stirring.**[19]** 3,5,5-trimethyl-1-hexanol (0.05 mol) was added, followed by the sulfuric acid (0.026 mol). The reaction mixture was refluxed for 3 h. A dark brown layer formed above the acid is separated and washed with water. The dried liquid is then purified by column chromatography using 4:1 hexane and dichloromethane as the mobile phase and silica gel (300 g, 0.035-0.070 mm, pore diameter 9 nm) to yield 68 % of the product as a clear liquid.

$^{1}$H NMR (300 MHz, $CDCl_3$, ppm): 3.35 (m, 2H), 1.81 (m, 1H), 1.65 (m, 2H), 1.15 (dd, 1H), 1.05 (dd, 1H), 0.9 (d, 3H), 0.86 (s, 9H).

### 2.4.3 Synthesis of 1-Alkyl-3-Vinyl Imidazolium Bromide

A general method for preparing different N-alkylated imidazolium salts is described. In a round bottom flask, N-vinyl imidazole (0.05 mol) and 1-alkyl bromide (0.06 mol) was added to 1:3 ratio of acetonitrile and ethyl acetate and heated at 40 ˚C for 24 h. The product, separated out as a viscous liquid, was washed with ethyl acetate and dried under vacuum to yield 52-75 % product as a clear yellow liquid.

The $^{1}$H NMR spectrum of N-vinyl imidazole is shown in (Figure **2-9**). The singlet for the C-2 proton (a) of the imidazole ring is at 7.75 ppm and the protons at C-4 and C-5 (b) appears at 7.30 and 7.23 ppm respectively. The vinyl protons (c and d) appear between 4.88 and 7.10 ppm. In the $^{1}$H NMR spectrum of 1-hexyl-3-vinyl imidazolium bromide (Figure **2-10**), the singlet of the C-2 proton appears at 10.80 ppm (a) due to de-shielding by the positive nitrogen. The peaks of the remaining protons in the ring (b and c) as well as the vinyl protons (d and e) move up-field. The peak of the α-methylene proton appears at 4.37 ppm (f) while the remaining methylenes and the terminal methyl from the hexyl tail appear downfield between 0.65-1.9 ppm (g).

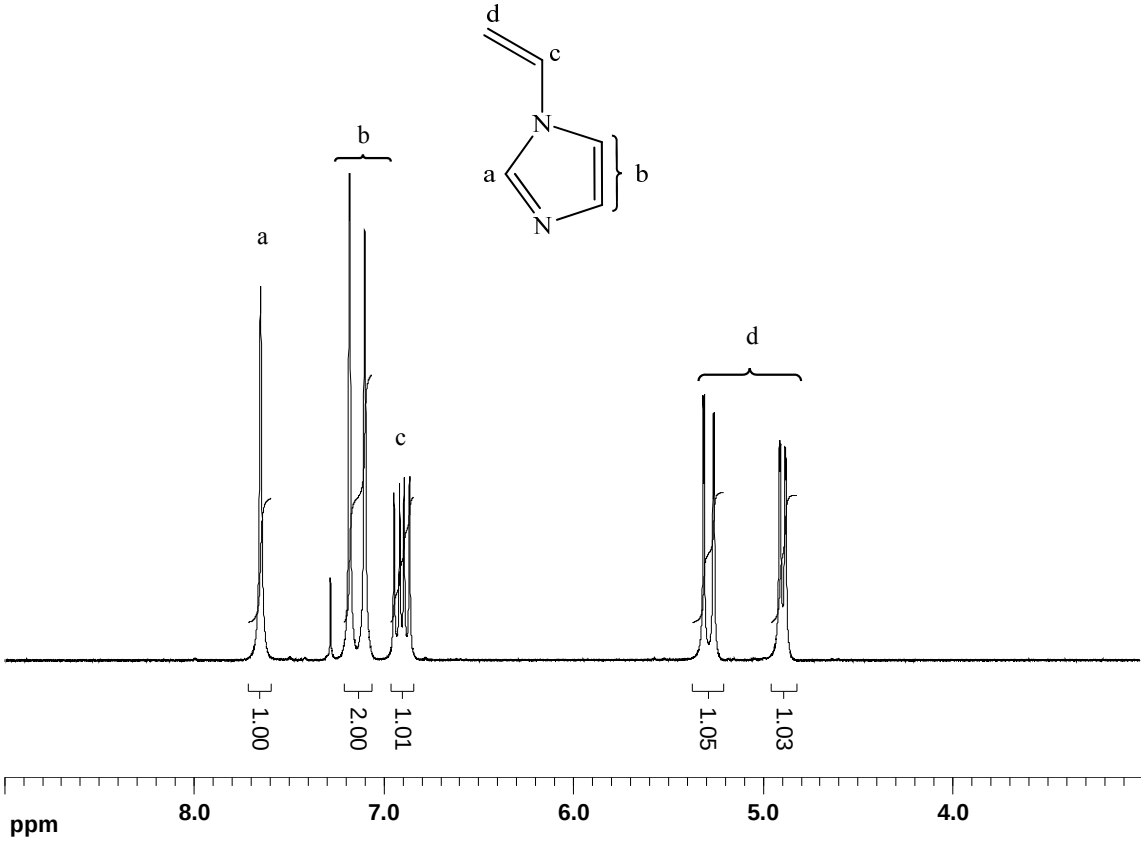


Figure **2-9**: $^{1}H$ NMR (300 MHz, $CDCl_3$) spectrum of N-vinyl imidazole.

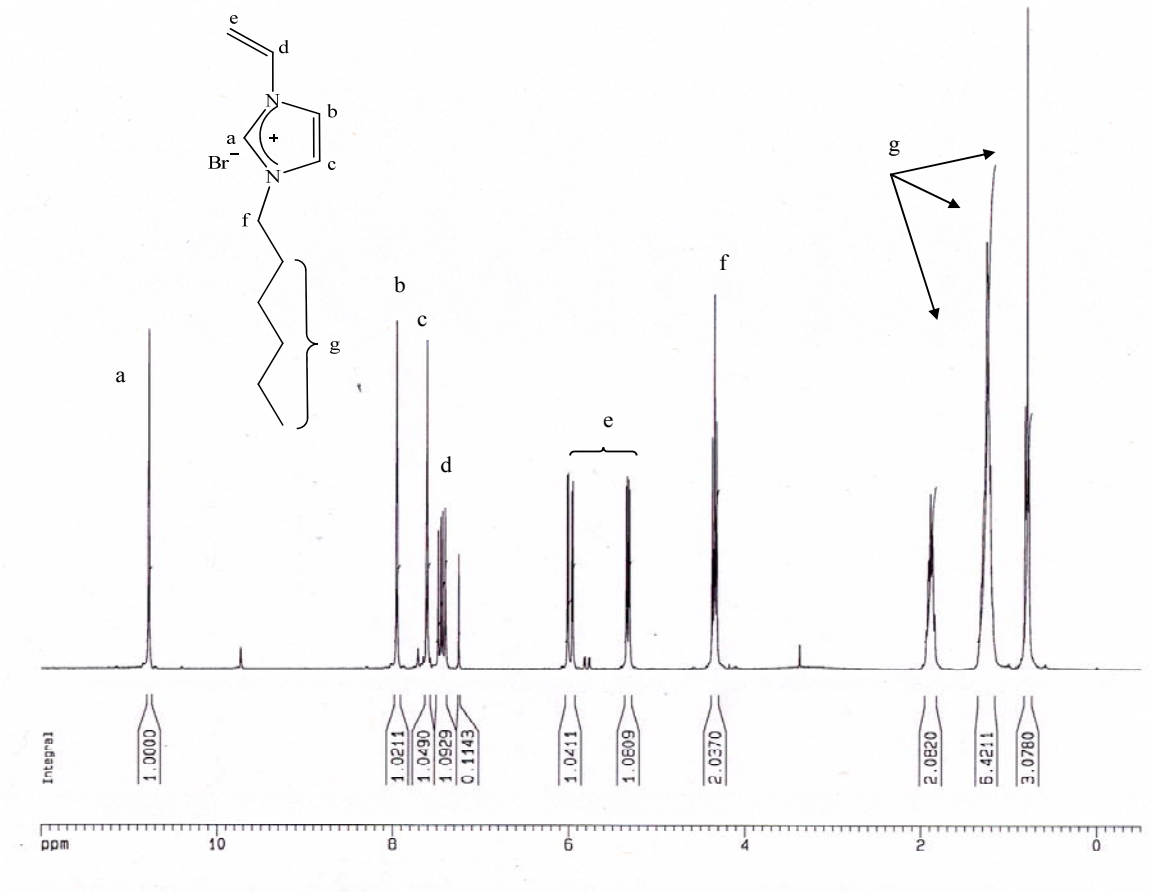


Figure **2-10**: $^{1}$H NMR (300 MHz, $CDCl_3$) spectrum of 1-hexyl-3-vinyl imidazolium bromide.

The peak positions of $^{1}$H NMR spectra of the various 1-alkyl-3-vinyl imidazolium bromides synthesized are listed below:

**1-propyl-3-vinyl imidazolium bromide:** $^{1}$H NMR (300 MHz, $CDCl_3$, ppm): 10.82 (s, 1H), 7.90 (s, 1H), 7.65 (s, 1H), 7.40 (dd, 1H), 5.99 (d, 1H), 5.34 (d, 1H), 4.35 (t, 2H), 1.93 (m, 2H), 0.96 (t, 3H).

**1-butyl-3-vinyl imidazolium bromide:** $^1$H NMR (300 MHz, $CDCl_3$, ppm): 10.96 (s, 1H), 7.85 (s, 1H), 7.56 (s, 1H), 7.40 (dd, 1H), 5.96 (d, 1H), 5.32 (d, 1H), 4.33 (t, 2H), 1.88 (m, 2H), 1.32 (m, 2H), 0.89 (t, 3H).

**1-octyl-3-vinyl imidazolium bromide:** $^1$H NMR (300 MHz, $CDCl_3$, ppm): 10.86 (s, 1H), 7.95 (s, 1H), 7.63 (s, 1H), 7.46 (dd, 1H), 5.96 (d, 1H), 5.30 (d, 1H), 4.35 (t, 2H), 1.89 (m, 2H), 1.25 (m, 10H), 0.79 (t, 3H).

**1-decyl-3-vinyl imidazolium bromide:** $^1$H NMR (400 MHz, $CDCl_3$, ppm): 10.81 (s, 1H), 7.83 (s, 1H), 7.48 (s, 1H), 7.42 (dd, 1H), 5.93 (d, 1H), 5.30 (d, 1H), 4.35 (t, 2H), 1.90 (m, 2H), 1.20 (m, 14H), 0.75 (t, 3H).

**1-dodecyl-3-vinyl imidazolium bromide:** $^1$H NMR (300 MHz, $CDCl_3$, ppm): 10.92 (s, 1H), 7.92 (s, 1H), 7.59 (s, 1H), 7.54 (dd, 1H), 6.03 (d, 1H), 5.43 (d, 1H), 4.46 (t, 2H), 1.95 (m, 2H), 1.33 (m, 18H), 0.88 (t, 3H).

**1-tetradecyl-3-vinyl imidazolium bromide:** $^1$H NMR (300 MHz, $CDCl_3$, ppm): 10.66 (s, 1H), 7.72 (s, 1H), 7.36 (s, 1H), 7.27 (dd, 1H), 5.82 (d, 1H), 5.19 (d, 1H), 4.13 (t, 2H), 1.69 (m, 2H), 1.09 (m, 22H), 0.66 (t, 3H).

**1-hexadecyl-3-vinyl imidazolium bromide:** $^1$H NMR (300 MHz, $CDCl_3$, ppm): 10.97 (s, 1H), 7.89 (s, 1H), 7.50 (s, 1H), 7.45 (dd, 1H), 5.99 (d, 1H), 5.40 (d, 1H), 4.34 (t, 2H), 1.95 (m, 2H), 1.25 (m, 26H), 0.84 (t, 3H).

**1-(3,5,5-trimethylhexyl)-3-vinyl imidazolium bromide:** $^1$H NMR (300 MHz, $CDCl_3$, ppm): 10.78 (s, 1H), 7.80 (s, 1H), 7.40 (m, 2H), 5.86 (d, 1H), 5.22 (d, 1H), 4.25 (t, 2H), 1.66 (m, 2H), 1.41 (m, 1H), 1.07 (dd, 1H), 1.00 (dd, 1H), 0.88 (d, 3H), 0.70 (s, 9H).

**1-(2-ethylhexyl)-3-vinyl imidazolium bromide:** $^1$H NMR (300 MHz, $CDCl_3$, ppm): 10.95 (s, 1H), 7.94 (s, 1H), 7.55 (dd, 1H), 7.49 (s, 1H), 6.06 (d, 1H), 5.45 (d, 1H), 4.34 (d, 2H), 1.96 (m, 1H), 1.30 (m, 8H), 0.95 (t, 3H), 0.88 (t, 3H).

### 2.4.4 Synthesis of Cationic Imidazolium Polymer

The poly(1-alkyl-3-vinyl imidazolium bromide), with $C_6$ or $C_8$ tail, was synthesized by the free radical polymerization using azobisisobutyronitrile (AIBN) as the initiator. To the degassed chlorobenzene, in a dry sealed round bottom flask, $C_n$VIB (5 mmol) and AIBN was added and heated at 70 ˚C for 20 h. The product formed was dialyzed in a dialysis membrane (MW cut off 6000-8000) against water and MeOH and dried to yield 60-86 % of yellowish solid. The spectrum of p($C_6$VIB-$C_3$VIB) with 1:3 ratio of the monomers is shown in (Figure **2-11**). The aromatic region consists of peaks for the protons on the imidazolium ring (a,a',b,b') and the characteristic peaks for the vinyl protons is absent. The peak for α–methylene proton of the hexyl tail and α'-methine protons of the polymer backbone (c and c') appears at 4.05 ppm and the remaining methylenes, the terminal methyl and the polymer backbone proton (d and d') appears between 0.80 and 2.10 ppm.

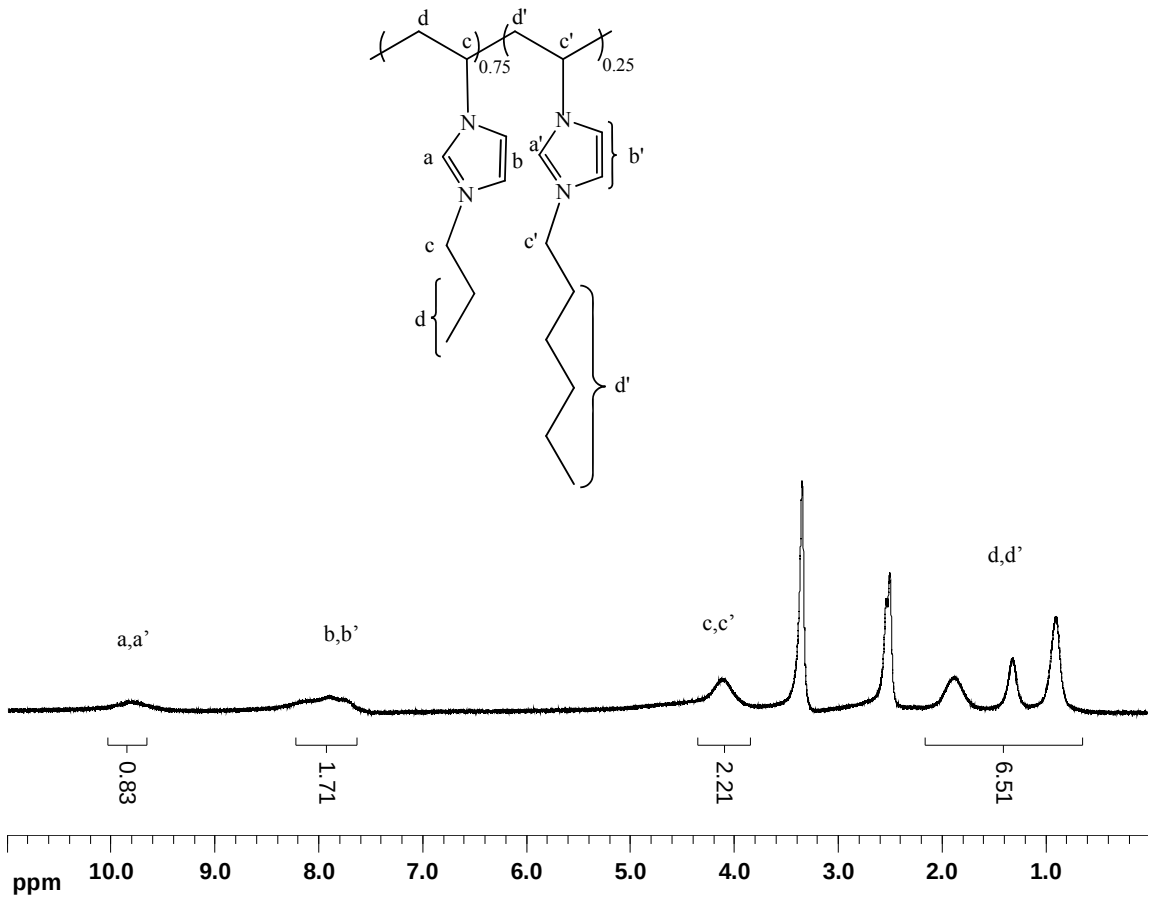


Figure **2-11**: $^{1}$H NMR (300 MHz, DMSO) spectrum of p($C_6$VIB-$C_3$VIB).

The various copolymers of 1-alkyl-3-vinyl imidazolium bromide with (i) vinyl imidazole and (ii) 1-propyl-3-vinyl imidazole were also made by the free radical polymerization method described earlier. $C_6$VIB and freshly distilled VI or $C_3$VIB were added in the molar ratio of 1:3 and 1:9, so that the final monomer concentration was 5 mmol. 0.05 or 0.02 molar equivalents of AIBN with respect to the final monomer concentration was used to vary the polymer chain length. The reaction mixture was heated at 70 ˚C for 20 h and the product dialyzed for purification.

### 2.4.5 Antibacterial Assay using Microdilution Method

*E. coli* (DH5-α, Clontech) were grown at 37 ˚C while *B. cereus* (UW85, ATCC 53522, a gift of Dr. J. Handelsman) were grown at 30 ˚C and maintained on LB plates. The ratio between absorbance at 590 nm ($OD_{590}$) and colony forming units (cfu) per mL was determined using the spread count method. For assays, bacteria were cultured for 16-18 h in LB broth and cell counts were quantified by $OD_{590}$ measurement. The cultures were then diluted in LB broth to yield the approximate cfu/mL.

Small molecules and cationic polymers were tested for antimicrobial activity using a modified microdilution broth assay in 96 well polystyrene plates. For small molecules, 220 μL of LB broth, 25 μL of the compound in water at 10x final concentrations and 5 μL of the bacterial cell solution at $2.5x10^7$ cfu/mL were added to each well. For polymers, 245 μL of the polymer in LB broth and 5 μL of the cell solution were added to each well. Water substituted the compound solution in the negative control well. The final volume of the well was 250 μL with an initial inoculum of $5 \times 10^5$ cfu/mL. The concentration of the tested compounds ranged from $4x10^{-3}$ to 3.0 mg/mL. The plates were incubated at 37 ˚C for *E. coli* and 30 ˚C for *B. cereus* at 230 rpm for about 18 h. The absorbance at 590 nm was quantified immediately after the cell addition and again after the incubation period to determine the change in cell density. In order to determine whether the compounds were bactericidal or bacteriostatic, aliquots were taken from wells showing little or no cell growth and plated on LB plates. These were incubated overnight at the appropriate temperature and the colonies were quantified.

### 2.4.6 Rate of Bacterial Cell Death

To 2 mL of 2x final concentration of cationic polymer in LB broth taken in a sterile culture tube, 2 mL of bacterial cell solution was added for an initial inoculum of $5x10^5$ cfu/mL. The tubes were incubated at 30 ˚C for *B. cereus*. At certain times, 20 µL of the assay was removed and serially diluted with LB broth. 100 µL of diluted solution was then plated on the LB plates. These were incubated for 18 h at the appropriate temperature and the colonies were quantified. Colony forming units per milliliter and % reduction over time were then calculated.

## 2.5 References

**1. (a)** Tiller, J. C.; Liao, C. J.; Lewis, K.; Klibanov, A.M. *PNAS* **2001**, *98*, 5981-5985. **(b)** Sambhy, V.; MacBride, M.; Peterson, B. R.; Sen, A. *J. Am. Chem. Soc*. **2005**, *128*, 9798-9808.

**2. (a)** Milovic, N. M.; Wang, J.; Lewis, K.; Klibanov, A. M. *Biotech. Bioeng*. **2005**, *90*, 715-722. **(b)** Haldar, J.; Kondaiah, P.; Bhattacharya, S. *J. Med. Chem*. **2005**, *48*, 3823-3831. **(c)** Cheng, Z.; Zhu, X.; Shi, Z. L.; Neoh, K. G.; Kang, E. T. *Ind. Eng. Chem. Res*. **2005**, *44*, 7098-7104. **(d)** Lee, S. B.; Koepsel, R. R.; Morley, S. W.; Matyjaszewski, K.; Sun, Y.; Russell, A. J. *Biomacromolecules* **2004**, *5*, 877-882.

**3.** Tashiro, T. *Macromol. Mat. Eng*. **2001**, *286*, 63-87.

**4.** Collins, Y. E.; Stotzky, G. *Can. J. Microbiol*. **1996**, *42*, 621-627.

**5.** Kenaway, R.; Mahmoud. Y. A. G. *Macromol. Biosci*. **2003**, *3*, 107-116.

**6.** Kuroda, K.; DeGrado, W. F. *J. Am. Chem. Soc*. **2005**, *127*, 4128-4129.

**7. (a)** Wang, P-L.; Ito, M.; Igarashi, Y. *Eur. Pat. Appl*. **2005**, EP 1508329. **(b)** Sobue, S.; Sekiguchi, K. *Biol. Pharm.l Bull*. **2004**, *27*, 1428-1432. **(c)** Uchida, K.; Nishiyama, Y.; Yamaguchi, H. *J. Infect. Chemother*. **2004**, *10*, 216-219. **(d)** Hashiguchi, T.; Kodama, A.; Ryu, A.; Otagiri, M. *Int. J. Pharm*. **1998**, *161*, 195-204. (e) Melander, C.; Cavanagh, J.; Huigens, R. W.; Ballard, T. E.; Richards, J. J. *U.S. Pat. Appl*. **2008**, US 2008181923.

**8.** Huesca, M.; Al-Qawasmeh, R.; Young, A. H.; Lee, Y. *PCT Int. Appl.* **2005**, WO 2005047266.

**9.** Evans, E. W.; Snyder, E. A.; Mirro, E. J.; Merrill, C. *U.S. Pat*. **2001**, US 6297268.

**10. (a)** Demberelnyamba, D.; Kim, K. S.; Choi, S.; Park, S. Y.; Lee, H.; Kim, C. J.; Yoo, I. D. *Bioorg. Med. Chem*. **2004**, *12*, 853-857. **(b)** Docherty, K. M.; Kulpa, Jr. C. F. *Green Chemistry* **2005**, *7*, 185-189. **(c)** Demberelnyamba, D.; Ariunaa, M.; Shim, Y. K. *Int. J. Mol. Sci*. **2008**, *9*, 807-820. **(d)** Melaiye, A.; Sun, Z.; Hindi, K.; Milsted, A.; Ely, D.; Reneker, D. H.; Tessier, C. A.; Youngs, W. J. *J. Am. Chem. Soc.* **2005**, *127*, 2285-2291.

**11. (a)** Secken, T.; Bulent, A.; Cetinkaa, E.; Ozdemir, I. *Poly. Bull*. **1996**, *37*, 443-450. **(b)** Eastwood, I. M.; Padget, J. C.; Gerrard, J. J.; Yeates, T. *PCT Int. Appl.* **1997**, WO 9705182. **(c)** Fujisawa, K.; Goshima, T.; Nakamura, M. *PCT Int. Appl.* **2008**, WO 2008038719.

**12.** Silverman, R. B. *The Organic Chemistry of Drug Design and Drug Action*, 2nd ed., Elsevier Academic Press, 2004.

**13.** Lewis, K.; Klibanov, A. M. *Trends. Biotechnol.* **2005,** *23(7*), 343-348.

**14.** NCCLS Approved Standard, M7-A6. **2003**, Villanova,PA.

**15.** Sambhy, V. *Antibacterial Polymers and Functional Nanocomposites; Cabondioxide Poisoning in Alkaline Fuel Cells* Ph.D. Dissertation, December **2007**.

**16.** Herigstad, B.; Hamilton, M.; Heersink, J. *J. Microbiol. Meth*. **2001**, *44*, 121-129.

**17.** In *Polymer-Surfactant Systems* Surfactant Science Series Kwak, J. C. T. Eds. Marcel Dekker Inc. New York, 1998.

**18.** Turner, M. S.; Joanny, J. F. *J. Phys. Chem*. **1993**, *97*, 4825-4831.

**19.** Furniss, B. S.; Hannaford, A. J.; Rogers, V.; Smith, P. W. G.; Tatchell, A. R. *Vogel's Textbook of Practical Organic Chemistry*, 4th ed.; Longman Inc., NY, 1986.

# Chapter 3

# N-Heterocyclic Carbene Palladium Complex Immobilized on Silica Nanoparticles. Recyclable Catalyst for Suzuki and Heck Coupling Reactions under Mild Conditions

## 3.1 Introduction

N-Heterocyclic carbenes (NHCs) were first isolated by Arduengo et al. in 1991[**1**] and since then, they have gained considerable attention as an alternative to phosphine ligands in transition metal catalysis. NHCs are air and moisture stable which is lacked in phosphines. They also exhibit high thermal stability and resistance to ligand dissociation from the metal center.[**2**] In the past decade, NHCs have been used as a ligand in a number of transition metal catalyzed organic reactions.

Carbon-carbon bond formation reactions, such as Suzuki and Heck coupling that are catalyzed by palladium complexes are used widely in a variety of synthetic and industrial applications.[**2-13**] However, the homogeneous catalysts that are often employed are difficult to separate and reuse. This is not desirable from economic and environmental standpoint as the catalyst synthesis involves multistep routes and expensive transition metals. Polymer-supported recyclable heterogeneous catalysts have been employed.[**9-12**] In these cases, some of the catalytic sites are buried within the polymer matrix and cannot participate in the reactions. It is desirable to have all the active sites on the surface of the support for higher efficiency. The use of palladium complex formed in situ on the surface of a silica gel for Heck reaction has also been reported.[**13**] Here, we report on Suzuki and Heck reactions catalyzed by N-heterocyclic carbene-palladium (NHC-Pd) complexes immobilized on ~ 10 nm silica nanoparticles.[**14**] Because of the very high surface area and small size, these nanoparticles remain suspended in a variety of solvents with the catalyst sites readily accessible to the reactants. Thus, they are effective

catalysts for a wide range of substrates in benign non-conventional solvents, including water. Moreover, they are readily separated by filtration and can be reused repeatedly.

## 3.2 Results and Discussion

### 3.2.1 Preparation of 1-Decyl-3-(Triethoxysilyl Propyl) Imidazolium Salts Immobilized on Silica Nanoparticles

The synthesis of carbene ligand precursor is shown in (Figure **3-1**). Imidazole was deprotonated by sodium hydride and then alkylated with decyl bromide in THF.[**15**] N-decyl imidazole was then quaternized with neat chloropropyl triethoxy silane. The resulting clear viscous ionic liquid 1-decyl-3-(triethoxysilyl propyl) imidazolium chloride was covalently linked with nano-sized silica support by condensation with surface silanol groups.[**16**] The chloride ions were subsequently replaced by either dodecane sulfonate or para-toluene sulfonate ions by heating with corresponding sodium salt in an aqueous medium to yield silica supported NHC precursor **1** and **2**. TEM image of the chloride analog of the precursor (Figure **3-2**) showed individual particles with an average diameter of 10.5 nm.

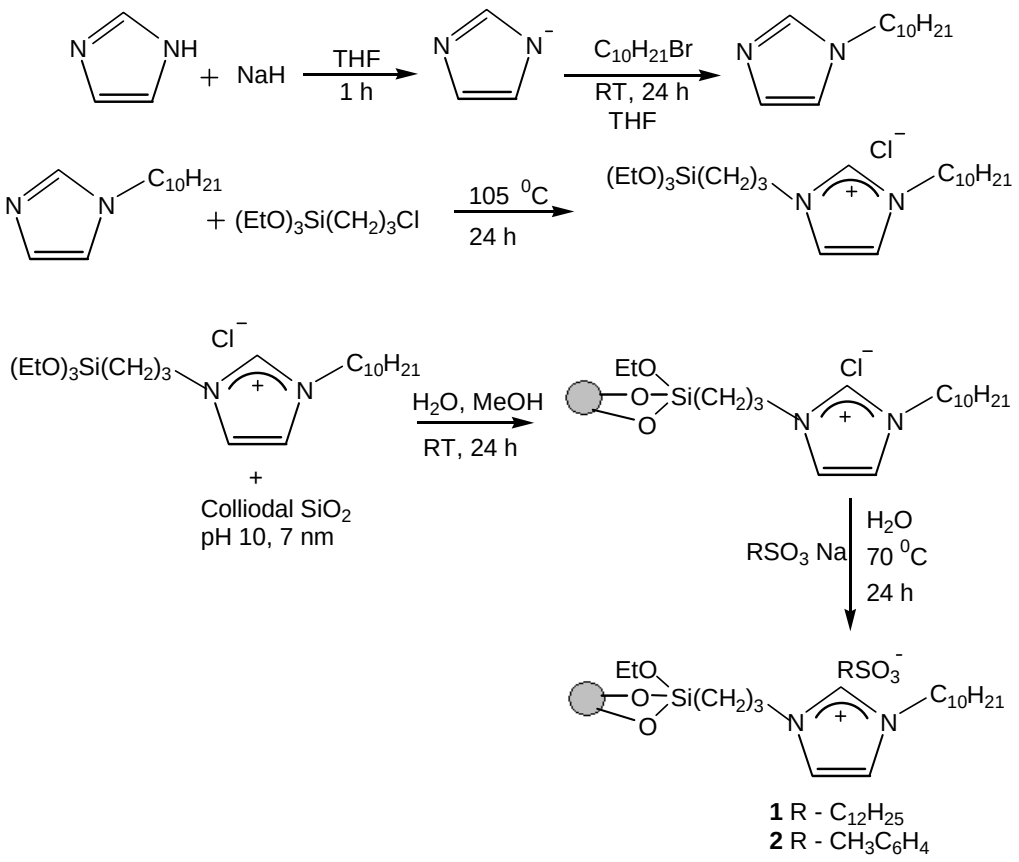


Figure **3-1**: Synthesis of silica nanoparticle immobilized NHC precursor.

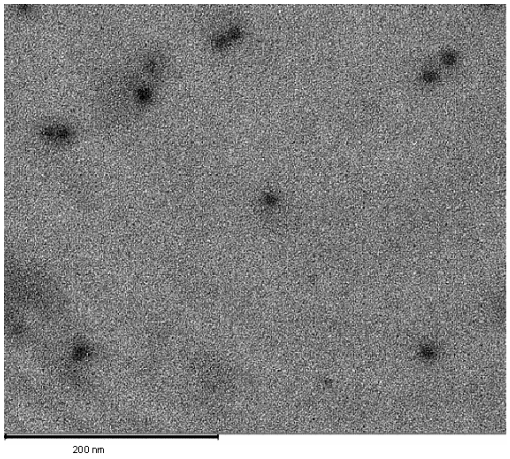


Figure **3-2**: TEM image of silica nanoparticle supported NHC precursor.

### 3.2.2 In Situ Preparation of Silica Nanoparticle Supported N-Heterocyclic Carbene-Pd Complex

The catalyst was synthesized by heating silica supported NHC precursor **1** or **2** with $Pd(OAc)_2$ in toluene at 50 ˚C for 8 h to obtain corresponding light brown colored catalyst **3** or **4** (Figure **3-3**). The amount of palladium in the catalysts was determined by inductively coupled plasma-atomic emission spectroscopy (ICP-AES). The amount of Pd was found to be 0.239 mmol/g and 0.235 mmol/g for catalyst **3** and **4** respectively. Further, TEM images of **3** (Figure **3-4**) showed that the particles did not aggregate with the immobilization of the metal and the average diameter was measured to be 9.8 nm.

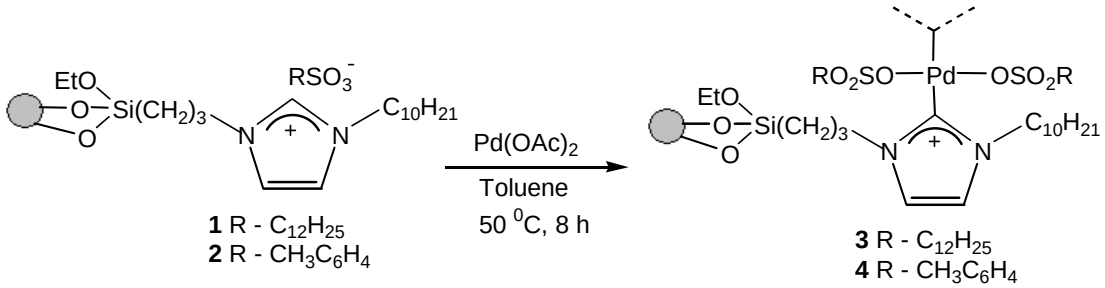


Figure **3-3**: Synthesis of silica supported NHC-Pd complex.

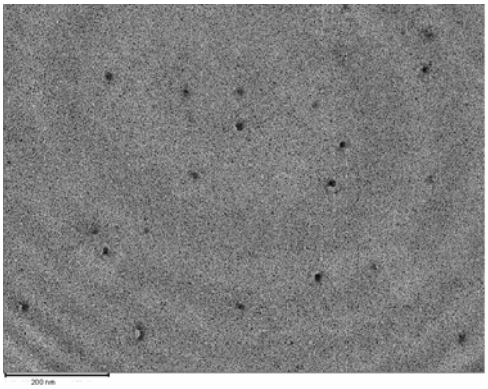

Figure **3-4**: TEM image of silica supported NHC-Pd catalyst **3**.

### 3.2.3 Heterogeneous Suzuki Cross-Coupling Reaction

The catalytic activity of silica nanoparticle supported NHC-Pd complexes **3** and **4** were initially analyzed by reacting aryl iodides with phenylboronic acid. 2 mol % of either catalyst **3** or **4** was used for the reaction and gave excellent yields within 2 h at 50 ˚C (Table **3-1**). Typically, toxic organic solvents like dimethylformamide (DMF) or N-methylpyrrolidone (NMP) are employed in such coupling reactions. However, we employed a more benign solvent system: 1:1 (v/v) mixture of isopropanol ($^{i}$PrOH) and water. The obtained yields were at least as good as those obtained in traditional organic solvents.**[8]**

Table **3-1**: Suzuki cross-coupling reactions catalyzed by **3** and **4**[a].

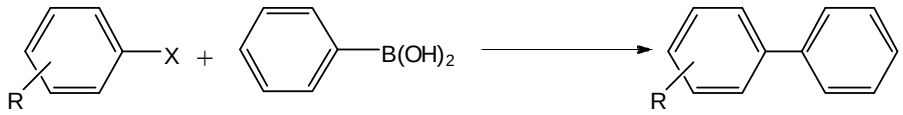


| Entry | aryl halide | Product | yield (%)[b] [catalyst] |
|---|---|---|---|
| 1 | 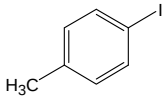 | 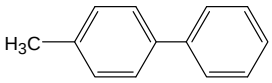 | 94 [**3**] |
| 2 | | | 89 [**4**] |
| 3 | 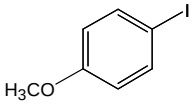 | 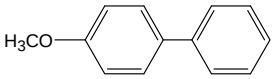 | 89 [**3**] |
| 4 | | | 90 [**4**] |

[a]Conditions: aryl halide (0.75 mmol), phenylboronic acid (0.9 mmol), catalyst (2 mol % Pd), $Na_2CO_3$ (3.75 mmol), $^{i}$PrOH/$H_2O$ (1:1, v/v), 50 ˚C, 2 h. [b]Isolated by column chromatography.

The complex **3** was then chosen for the heterogeneous cross coupling reaction of a range of aryl halides with phenylboronic acid (Table **3-2**). Excellent yields were obtained with both aryl iodides and aryl bromides. The catalyst was equally effective in catalyzing the substrates with electron withdrawing functional groups like nitro, aldehyde and ketone (entries 3, 8, and 9) as well as electron donating functionalities like methyl and methoxy (entries 4, 6, and 7). The activity of the catalyst was also not affected by the position of the functional group in the aryl ring (entries 12 and 14). The catalyst was also active towards sterically hindered aryl bromide (entry 16). However, a low yield was obtained when chlorobenzene was used as the substrate (entry 17).

Table **3-2**: Suzuki cross-coupling reaction of aryl halides with phenyl boronic acid catalyzed by Pd complex **3**[a].

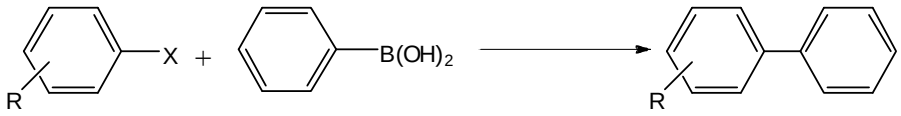


| entry | R | X | time (h) | yield (%)[b] |
|---|---|---|---|---|
| 1[c] | H | I | 2 | 91 |
| 2 | $CH_3$ (4-) | I | 2 | 94 |
| 3[d] | $NO_2$ (4-) | I | 1 | 94 |
| 4 | $OCH_3$ (4-) | I | 2 | 89 |
| 5 | H | Br | 12 | 91 |
| 6 | $CH_3$ (4-) | Br | 12 | 76 |
| 7 | $OCH_3$ (4-) | Br | 6 | 91 |
| 8[e] | CHO (4-) | Br | 6 | 92 |
| 9 | $COCH_3$ (4-) | Br | 6 | 93 |

| | | | | |
|---|---|---|---|---|
| 10 | OH (4-) | Br | 6 | 90 |
| 11 | $NO_2$ (4-) | Br | 6 | 98 |
| 12 | CN (4-) | Br | 6 | 93 |
| 13 | $C(O)OCH_3$ (4-) | Br | 6 | 88 |
| 14 | $OCH_3$ (2-) | Br | 12 | 93 |
| 15 | CN (2-) | Br | 6 | 92 |
| 16 | Naphthalene | Br | 12 | 82 |
| 17 | H | Cl | 11 | 29 |

[a]Conditions: aryl halide (0.75 mmol), phenylboronic acid (0.9 mmol), **3** (2 mol % Pd), $Na_2CO_3$ (3.75 mmol), $^i$PrOH/$H_2O$ (1:1, v/v) (10 mL), 50 ˚C. [b]Isolated by column chromatography. [c]$K_2CO_3$ as base. [d]DMF solvent. [e]Determined by $^1$H NMR spectroscopy (> 95 % purity).

### 3.2.4 Heterogeneous Heck Cross-Coupling Reaction

The ability of the nanoparticle supported palladium species to catalyze Heck coupling was also examined. Aryl iodides with different functional groups were coupled with electron poor olefins like butyl acrylate and styrene at 100 ˚C using DMF as a solvent. Excellent yield was obtained with n-butyl acrylate within 2 h using catalyst **4** (Table **3-3**). Curiously, unlike the results in the Suzuki coupling (Table **3-1**), catalyst **3** was found to be significantly less reactive than catalyst **4**. Thus, **3** with dodecane sulfonate anion gave only 10% of n-butyl cinnamate while **4** with toluene sulfonate anion gave 99% of the product under similar conditions (entries 1and 2). With styrene, a high yield of the product was formed only when catalyst and base were stirred for 15 min at 100 ˚C before the introduction of reactants. Bromobenzene failed to react even under the modified condition. Catalyst degradation was observed when water was used as a co-solvent; however, high yield was obtained in 24 h when pure $^{i}$PrOH was the solvent (entry 6). So, benign solvent like $^{i}$PrOH can substitute the toxic solvent DMF in these reactions.

Table **3-3**: Heck cross-coupling reaction of aryl halides with olefins catalyzed by **4**[a].


| entry | R | X | R' | time (h) | yield (%)[b] |
|---|---|---|---|---|---|
| 1[c] | H | I | $C(O)O(CH_2)_3CH_3$ | 2 | 10 |
| 2 | H | I | $C(O)O(CH_2)_3CH_3$ | 2 | 99 |
| 3 | $OCH_3$ | I | $C(O)O(CH_2)_3CH_3$ | 2 | 97 |
| 4[d] | $COCH_3$ | I | $C(O)O(CH_2)_3CH_3$ | 2 | 98 |
| 5[e] | H | I | Ph | 4 | 94 |
| 6[f] | H | I | $C(O)O(CH_2)_3CH_3$ | 24 | 85 |
| 7 | H | Br | $C(O)O(CH_2)_3CH_3$ | 24 | - |

[a]Conditions: aryl halide (0.75 mmol), olefin (0.9 mmol), **4** (2 mol% Pd), $K_2CO_3$ (0.9 mmol), $Et_3N$ (0.9 mmol), DMF (5 mL), 100 ˚C. [b]Isolated by column chromatography. [c]Catalyst **3** was used. [d]Determined by $^1H$ NMR spectroscopy (> 95 % purity). [e]$K_2CO_3$ (3.75 mmol). [f]iPrOH, 70 ˚C.

### 3.2.5 Reusability of Silica Supported N-Heterocyclic Carbene-Pd Catalyst

Easy recyclability and prolonged retention of the catalytic activity are very important for the industrial applications. In order to check the reusability of the silica supported NHC-Pd complex, catalyst **3** was employed for the Suzuki coupling of 4-iodotoluene and phenylboronic acid using 1:1 $^{i}$PrOH:$H_2O$ as solvent. In the first cycle, 90% of 4-phenyl toluene was obtained. The nanoparticles were recovered by centrifugation, washed with water, acetone and dried at 50 ˚C for 4 h. The second cycle was started with the recovered catalyst and the process was repeated through five cycles without loss of productivity (Table **3-4**).

Table **3-4**: Reusability of silica nanoparticle supported NHC-Pd catalyst.

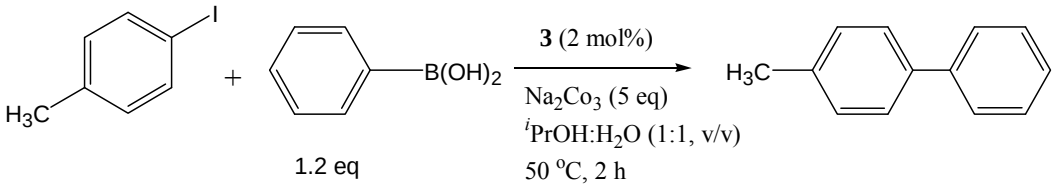


| no. of run | yield (%)[a] | catalyst recovered (%) |
|---|---|---|
| 1 | 90 | 85 |
| 2 | 90 | 98 |
| 3 | 92 | 98 |
| 4 | 95 | 97 |
| 5 | 91 | 91 |

[a]Isolated by column chromatography.

Finally, in order to verify that both the metal and the N-heterocyclic carbene ligand are essential for the catalysis, the reaction of 4-iodotoluene with phenylboronic acid was carried out in the presence of either the NHC precursor **1** or a mixture of n-octyl functionalized silica nanoparticles and $Pd(OAc)_2$, **5.** No product was formed with NHC precursor **1** showing the significance of the transition metal. With **5,** 82 % of the product was formed in the first cycle. However, the yield decreased to only 39 % in the second cycle, indicating significant loss of activity during recycling (Table **3-5**).

Table **3-5**: Suzuki coupling reaction in the absence of metal or carbene species.

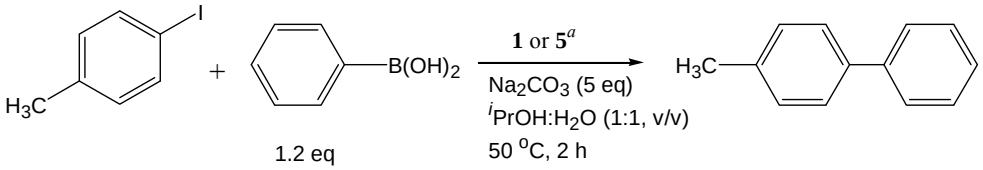


| entry | additives [no. of run] | yield (%)[b] |
|---|---|---|
| 1 | **1** | - |
| 2 | **5** [1] | 82 |
| 3 | **5** [2] | 39 |

[a]60 mg. [b]Isolated by column chromatography

### 3.3 Conclusion

In summary, we have described a new heterogeneous N-Heterocyclic Carbene-Pd catalyst immobilized on nano-sized silica particles. The catalyst showed excellent activity towards Suzuki coupling reaction of different aryl iodides and bromides with phenylboronic acid using $^{i}$PrOH:$H_2O$ as solvent. The catalyst was tolerant towards both electron withdrawing and electron donating functionalities. However, the catalyst was less effective towards aryl chloride. The catalyst was also effective for Heck coupling. Because of the very high surface area and small size of the nanoparticles, the catalysts remain suspended in a variety of solvents with the reactive sites readily accessible to the reactants. The NHC-Pd catalyst can be easily recovered and repeatedly reused without the loss of activity.

## 3.4 Experimental

### 3.4.1 Materials and Instrumentation

N-imidazole was purchased from Acros Organics and all other chemicals and materials were purchased from Aldrich and used without further purification. All reactions were carried out under air unless otherwise stated. $^{1}$H NMR spectra was recorded on Brucker DPX-300 (300 MHz) spectrometer. The TEM images were taken with JOEL 1200EXII operating at 80 kV. The sample was prepared by depositing 4 μL of the compound dispersed in toluene on carbon coated copper grid (300 mesh). Leeman Labs PS3000UV inductively coupled plasma spectrophotometer was used to determine the amount of Pd on the catalysts.

### 3.4.2 Preparation of 1-Decyl-3-(Triethoxysilyl Propyl) Imidazolium Salts Immobilized on Silica Nanoparticles

#### 3.4.2.1 Synthesis of 1-Decyl-3-(Triethoxysilyl Propyl) Imidazolium Chloride

The solution of imidazole (0.1 mol) in 80 mL THF was added drop wise to a slurry of NaH (0.12 mol) in 50 mL THF in a dry, inert atmosphere.[**14**] The mixture was stirred for 1 h at room temperature and a solution of tetrabutylammonium hydrogen sulfate (5 mmol) and decyl bromide (0.1 mol) in 50 ml THF was added. After stirring for 24 h, solids were filtered off and filtrate dried under vacuum. The product was purified by column chromatography using silica gel (0.035-0.070 mm, pore diameter 9 nm) and ethyl acetate. The resulting yields were in the range of 50-80%. A dry round bottomed flask with n-decyl imidazole (0.05 mol) and chloropropyl triethoxy silane (0.05 mol) was sealed and purged with $N_2$ for 20-25 min and then heated at 105 ˚C for 24 h. The resulting viscous liquid was washed with ether and dried under vacuum to give

71 % of 1-decyl-3-(triethoxysilyl propyl) imidazolium chloride. Both N-decyl imidazole and the ionic liquid were characterized by using $^{1}$H NMR spectroscopy. (Figure **3-5**) shows the $^{1}$H NMR spectra of N-decyl imidazole. The imidazole ring protons (a,b) appear between 6.90 and 7.30 ppm. The α-methylene proton (c) is at 3.94 ppm, while the remaining methylene and methyl protons (d,e,f) appear between 0.85 and 1.90 ppm.

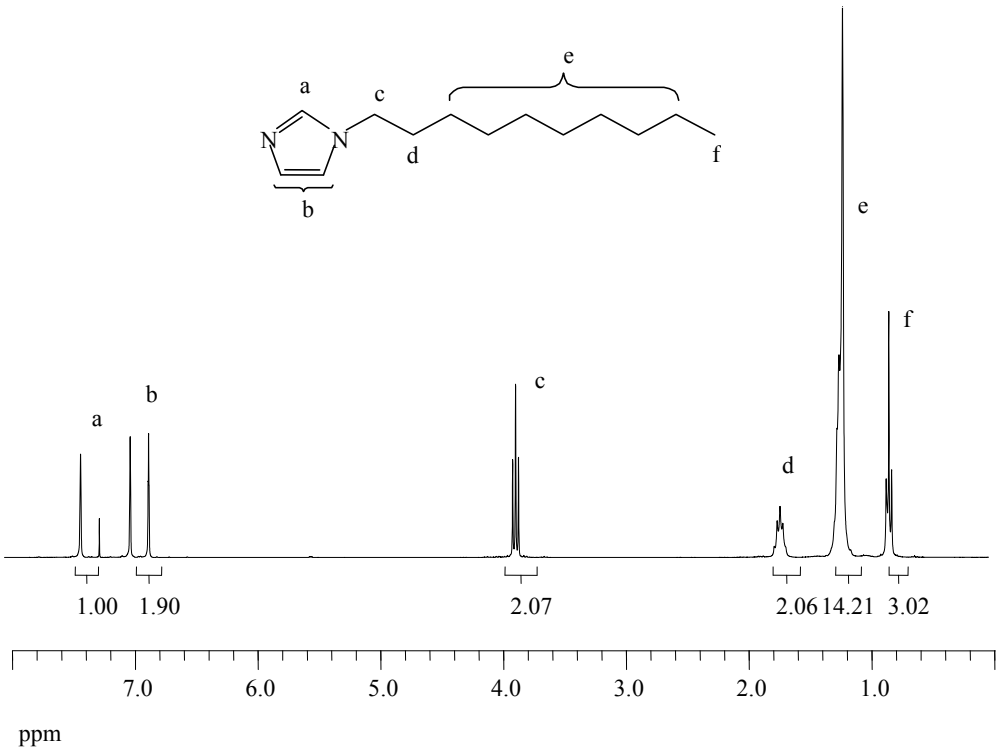


Figure **3-5**: $^{1}$H NMR (300 MHz, $CDCl_3$) spectrum of N-decyl imidazole.

When N-decyl imidazole was quaternized with chloropropyl triethoxy silane**,** the singlet of C-2 proton moves downfield at 10.64 ppm (a) due to de-shielding by the positive nitrogen (Figure **3-6**). The remaining imidazolium protons are seen at 7.12 and 7.20 ppm. The α-

methylene protons (c,c') is at 4.10 ppm followed by ethoxy methylene at 3.55 ppm. The remaining methylenes and methyls are between 0.29 and 1.86 ppm.

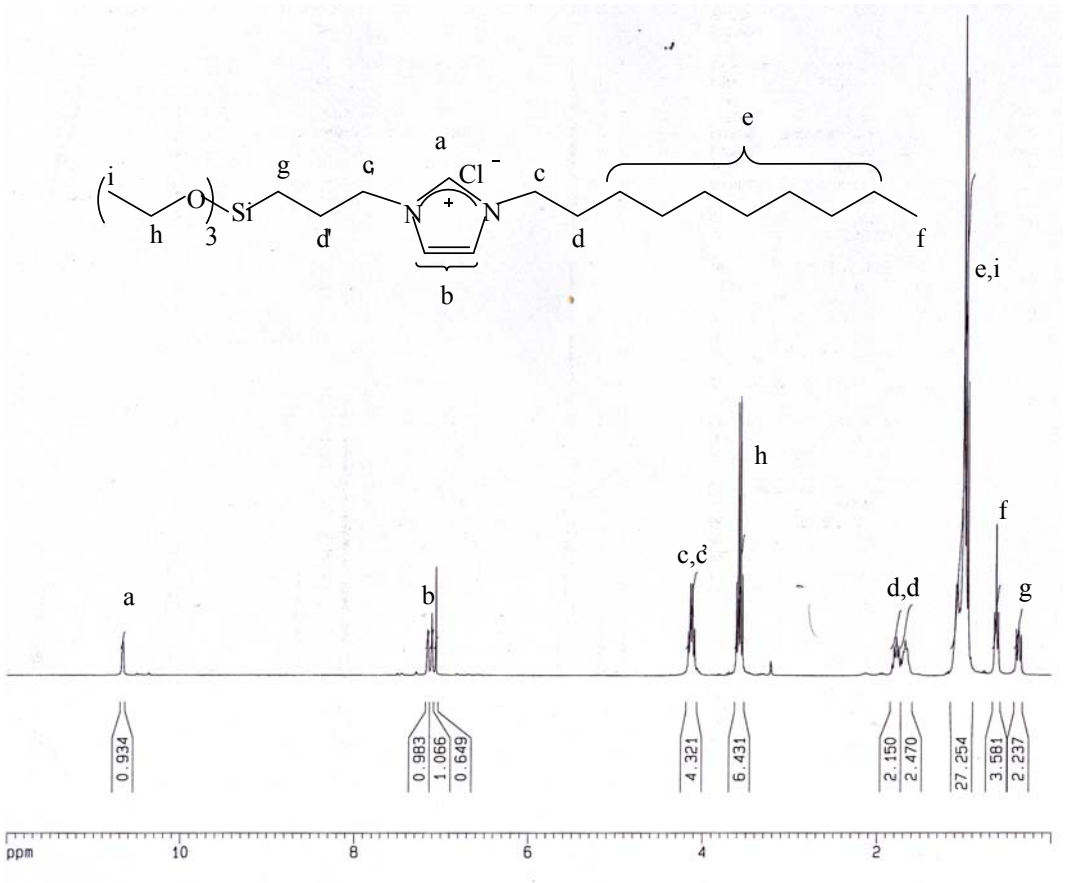


Figure **3-6**: $^{1}H$ NMR (300 MHz, $CDCl_3$) spectrum of 1-decyl-3-(triethoxysilyl propyl) imidazolium chloride.

### 3.4.2.2 NHC Precursor Covalently Bonded to Silica Nanoparticles

10.5 mL of Ludox colloidal silica (Ludox-SM, 30 wt % $SiO_2$, particle size 7 nm, pH 10) was diluted to 60 mL with deionized water.[**15**] To this, 1-decyl-3-(triethoxysilyl propyl) imidazolium chloride in 15 mL MeOH (40 wt %) was added. The white precipitate formed immediately was aged for 24 h with stirring at intervals. The precipitate was recovered by filtration washed with water, ethanol, and finally dried under vacuum. Chloride ions were replaced by heating the white particles (2 g) with an excess of corresponding sulfonate salt in water at 70 ˚C for 24 h. The particles were separated by filtration and washed with warm water, acetone and dried under vacuum to yield precursor **1** and **2**.

### 3.4.3 Preparation of Silica Supported N-Heterocyclic Carbene-Pd Complex

Silica nanoparticle supported NHC precursor **1** or **2** (1 g) and $Pd(OAc)_2$ (230 mg) were mixed in 40 mL toluene and heated at 50 ˚C for 8 h. The light brown colored catalyst **3** or **4** formed was separated and washed thoroughly with acetone and dried under vacuum. The catalysts were obtained in quantitative yield.

The amount of palladium loading was analyzed by Inductively Coupled Plasma-Atomic Emission Spectrophotometry (ICP-AES). 50 mg of the catalyst was mixed with 8 mL of $HCl:HNO_3$ (3:1, v/v) and heated at 75 ˚C for 4 h. The resulting orange colored solution was filtered, diluted to 50 mL with distilled water and analyzed.

### 3.4.4 General Procedure for Suzuki Coupling

Aryl halide (0.75 mmol), catalyst (2 mol % Pd), phenylboronic acid (0.9 mmol), $Na_2CO_3$ (3.75 mmol), $^{i}$PrOH /$H_2O$ (1:1, v/v) (10 mL) were mixed and heated at 50 ˚C for a specific period of time. Upon completion, catalyst was separated by filtration, and washed with 10 mL water. The product was extracted with ether, dried over anhydrous $Na_2SO_4$ and then solvent evaporated. The biaryl product was purified by flash chromatography using silica gel and hexane or 4% ethyl acetate in hexane and identified using $^{1}$H-NMR spectroscopy. $^{1}$H NMR spectrum of 4-acetylbiphenyl is illustrated in (Figure **3-7**). The aryl protons (a-e) appear in between 8.00 and 7.30 ppm while the singlet for the acetyl proton (f) is at 2.56 ppm.

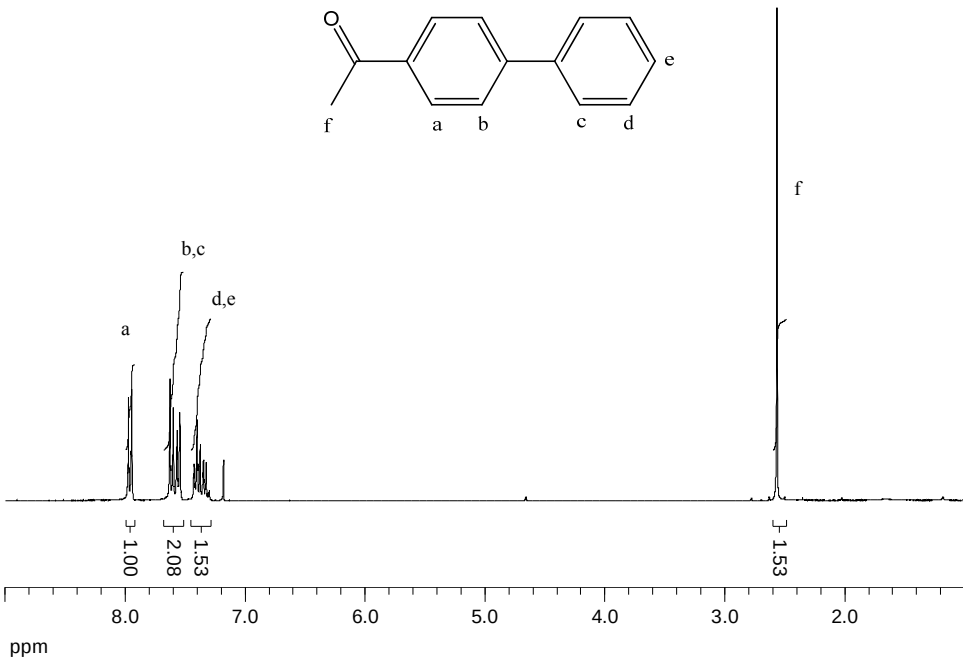


Figure **3-7**: $^{1}$H NMR (300 MHz, $CDCl_3$) spectrum of 4-acetylbiphenyl.

The peak positions as seen in $^1$H NMR spectra of remaining biaryl products are listed below.

**Biphenyl:** $^1$H NMR (300 MHz, $CDCl_3$, ppm): 7.52 (d, 4H), 7.36 (t, 4H), 7.27 (t, 2H).

**4-Phenyltoluene.** $^1$H NMR ($CDCl_3$, ppm): 7.50 (d, 2H), 7.41 (d, 2H), 7.35 (t, 2H), 7.25 (t, 1H), 7.18 (d, 2H), 2.30 (s, 3H).

**4-Nitrobiphenyl:** $^1$H NMR (300 MHz, $CDCl_3$, ppm): 8.22 (d, 2H), 7.64 (d, 2H), 7.55 (d, 2H), 7.40 (t, 3H).

**4-Methoxybiphenyl:** $^1$H NMR (300 MHz, $CDCl_3$, ppm): 7.45 (m, 4H), 7.34 (t, 2H), 7.22 (t, 1H), 6.90 (d, 2H), 3.71 (s, 3H).

**4-Phenylbenzaldehyde:** $^1$H NMR (300 MHz, $CDCl_3$, ppm): 9.99 (s, 1H), 7.88 (d, 2H), 7.69 (d, 2H), 7.58 (d, 2H), 7.40 (m, 3H).

**4-Hydroxybiphenyl:** $^1$H NMR (400 MHz, DMSO, ppm): 7.62 (d, 2H), 7.52 (d, 2H), 7.46 (t, 2H), 7.33 (t, 1H), 6.90 (d, 2H).

**4-Phenylbenzonitrile:** $^1$H NMR (300 MHz, $CDCl_3$, ppm): 7.62 (m, 4H), 7.52 (d, 2H), 7.38 (m, 3H).

**4-Phenylmethylbenzoate:** $^1$H NMR (400 MHz, $CDCl_3$, ppm): 8.00 (d, 2H), 7.58 (m,4H), 7.40 (t, 2H), 7.30 (d, 1H), 3.87 (s, 3H).

**2-Methoxybiphenyl:** $^1$H NMR (300 MHz, $CDCl_3$, ppm): 7.45 (d, 2H), 7.34 (t, 2H), 7.24 (m, 3H), 6.95 (m, 2H), 3.76 (s, 3H).

**2-Phenylnaphthalene:** $^1$H NMR (300 MHz, $CDCl_3$, ppm): 7.96 (s, 1H), 7.83 (m, 3H), 7.65 (m, 3H), 7.42 (m, 4H), 7.30 (t, 1H).

### 3.4.5 General Procedure for Heck Coupling

Aryl halide (0.75 mmol), catalyst (2 mol % Pd), olefin (0.9 mmol), $K_2CO_3$ (0.9 mmol), $Et_3N$ (0.9 mmol) and DMF (5 mL) were heated at 100 ˚C for a specific time. After the reaction was complete, catalyst was separated by filtration and washed with 10 mL water. The product was extracted with ether, dried over $Na_2SO_4$ and solvent evaporated. The cinnamate product was purified by column chromatography and identified by $^1$H-NMR spectroscopy. $^1$H NMR spectrum of n-butyl cinnamate is illustrated in (Figure **3-8**). The vinyl protons appear at 7.60 and 6.38 ppm (a,a'), while the aryl protons are at 7.48 and 7.30 ppm (b,b'). The α–methylene proton is at 4.18 ppm (c) due to de-shielding from the neighboring O. The remaining methylenes and terminal methyl (d,e) appear between 1.70 and 0.80 ppm.

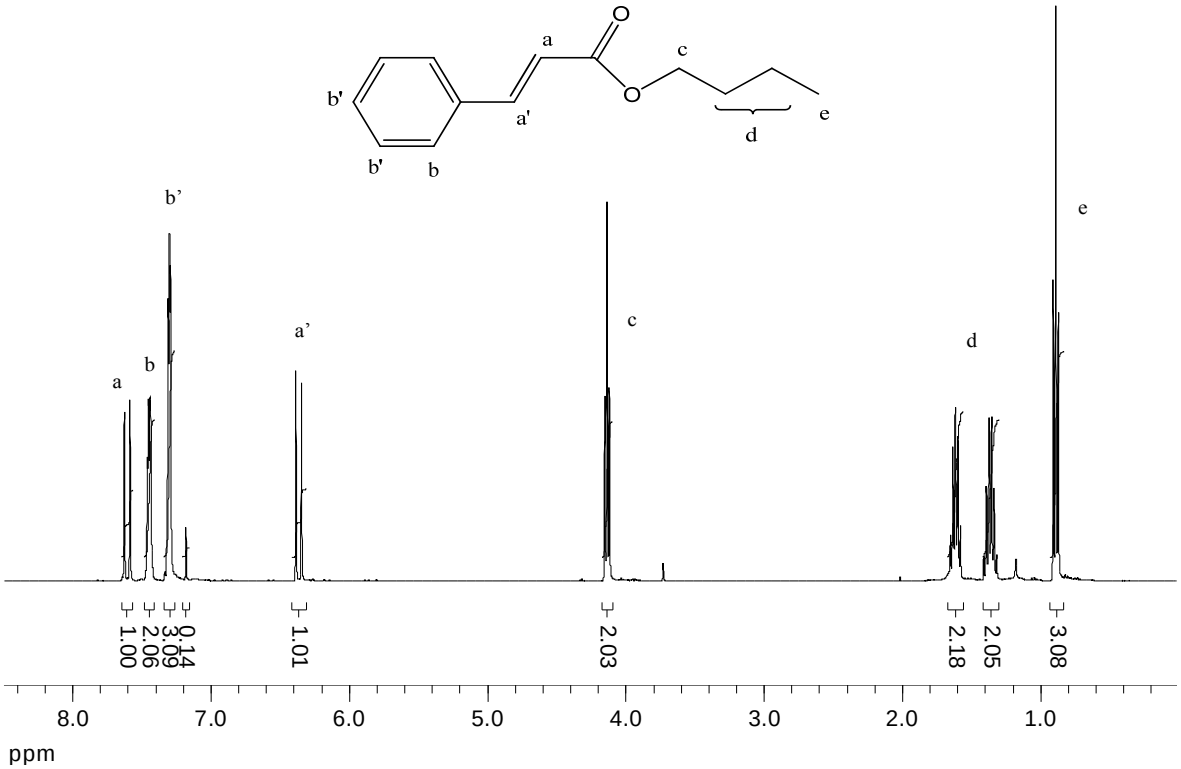


Figure **3-8**: $^{1}$H NMR (300 MHz, $CDCl_3$) spectrum of n-butyl cinnamate.

The peak positions as seen in $^{1}$H NMR spectra of different cinnamate products are listed below.

**3-(4-Methoxyphenyl) acrylic acid butyl ester:** $^{1}$H NMR (300 MHz, $CDCl_3$, ppm): 7.56 (d, 1H), 7.39 (d, 2H), 6.80 (d, 2H), 6.22 (d, 1H), 4.09 (t, 2H), 3.75 (s, 3H), 1.61 (m, 2H), 1.33 (m, 2H), 0.86 (t, 3H).

**3-(4-Acetylphenyl) acrylic acid butyl ester:** $^{1}$H NMR (300 MHz, $CDCl_3$, ppm): 7.89 (d, 2H), 7.63 (d, 1H), 7.55 (d, 2H), 6.44 (d, 1H), 4.14 (t, 2H), 2.55 (s, 3H), 1.60 (m, 2H), 1.35 (m, 2H), 0.89 (t, 3H).

**1,2-Diphenyl ethylene:** $^{1}$H NMR (300 MHz, $CDCl_3$, ppm): 7.42 (d, 4H), 7.28 (t, 4H), 7.18 (t, 2H), 7.03 (s, 2H).

### 3.4.6 Procedure for Recycling the Catalyst

4-Iodotoluene (0.75 mmol), catalyst **3** (2 mol %), phenylboronic acid (0.9 mmol), $Na_2CO_3$ (3.75 mmol), $^{i}$PrOH /$H_2O$ (1:1, v/v) (10 mL) were heated at 50 ˚C for 2 h. The catalyst was then separated by centrifuging at 750 rpm and then washed with 2 x 8 mL water, 8 mL acetone and dried at 50 ˚C for 4 h. The product was isolated by extraction with ether and purifying with flash chromatography. Recovered catalyst was reused for 4 more cycles of the same reaction.

**3.5 References**

**1.** Ardeungo, A. J. III; Harlow, R. L.; Kline, M. *J. Am. Chem. Soc*. **1991**, *113*, 361-363.

**2.** Viciu, M. S.; Nolan, S. P. *Top Organomet. Chem*. **2005**, *14*, 241-278.

**3.** Scott, N. M.; Nolan, S. P. *Eur. J. Inorg. Chem*. **2005**, 1815-1828.

**4.** Singh, R.; Viciu, M. S.; Kramareva, N.; Navarro, O.; Nolan, S. P. *Org. Lett*. **2005**, *7*, 1829-1832.

**5.** Billingsley, K. L.; Anderson, K. W.; Buchwald, S. L. *Angew. Chem. Int. Ed*. **2006**, *45*, 3484-3488.

**6.** Schneider, S. K.; Roembke, P.; Julius, G. R.; Loschen, C.; Raubenheimer, H. G.; Frenking, G.; Herrmann, W. A. *Eur. J. Inorg. Chem*. **2005**, 2973-2977.

**7.** Schneider, S. K.; Herrmann, W. A.; Herdtweck, E. *J. Mol. Cat. A: Chem*. **2006**, *245*, 248-254.

**8.** Schonfelder, D.; Nuyken, O.; Weberskirch, R. *J. Organomet. Chem*. **2005**, *690*, 4648-4655.

**9.** Kim, J-H.; Kim, J-W.; Shokouhimehr, M.; Lee, Y-S. *J. Org. Chem*. **2005**, *70*, 6714-6720.

**10.** Schwarz, J.; Bohm, V. P. W.; Gardiner, M. G.; Grosche, M.; Harrmann, W. A.; Hieringer, W.; Raudaschl-Sieber, G. *Chem. Eur. J*. **2000**, *6*, 1773-1780.

**11.** Byun, J-W.; Lee, Y-S. *Tetrahedron Lett*. **2004**, *45*, 1837-1840.

**12.** Kim, J-W.; Kim, J-H.; Lee, D-H.; Lee, Y-S. *Tetrahedron Lett.* **2006**, *47*, 4745-4748.

**13.** Karimi, B.; Enders, D. *Org. Lett*. **2006**, *8*, 1237-1240.

**14.** Tandukar, S.; Sen, A. *J. Mol. Catal. A:Chem*. **2007**, *268*, 112-119.

**15.** Montanari, F.; Penso, M.; Quici, S.; Vigano, P. *J. Org. Chem.* **1985**, *50*, 4888-4893.

**16.** Bourlinos, A. B.; Herrera, R.; Chalkias, N.; Jiang, D. D.; Zhang, Q.; Archer, L. A.; Giannelis, E. P. *Adv. Mater*. **2005**, *17*, 234-237.

## Chapter 4

# Palladium Crosslinked Poly(allylamine): Recyclable Green Catalyst for High Yield C-C Coupling Reactions

### 4.1 Introduction

Palladium-mediated cross coupling reactions like Suzuki-Miyaura, Mizoroki-Heck, and Sonogashira find extensive use in organic synthesis.[**1**],[**2**] Homogeneous catalysts that are often employed for their high activity are difficult to separate and reuse. Heterogeneous catalysts, in which the transition metal species are anchored on polymer or inorganic supports,[**3-13**] can be recovered and recycled but the loss of activity and leaching of the catalyst from the support are always the issues. Recently, we reported N-heterocyclic carbene-palladium (NHC-Pd) complexes immobilized on silica nanoparticles for Suzuki and Heck coupling reactions.[**13**] Because of the very high surface area and small size, the catalyst sites are readily accessible to the reactants and are effective for a wide range of substrates under mild conditions. They can be readily separated by filtration and reused repeatedly without loss of activity.

Nevertheless, the preparation of these and other reported supported heterogeneous catalysts involve tedious multistep processes involving ligand synthesis, incorporation of the metal, followed by immobilization on the solid support. There are also examples of polymer incarceration [**14**],[**15**],[**16**],[**17**] which is based on microencapsulation of the metal followed by crosslinking of the polymer chains of the copolymer; however, an external ligand is needed for effective coupling reaction.[**16**],[**17**] Colloidal palladium nanoparticles stabilized by a polymer have also been used for Suzuki [**18**],[**19**],[**20**] and Heck [**21-26**] coupling. Copolymer stabilized nanoparticles, which act as ‘homogeneous’ catalyst during the reaction, requires specific treatments for catalyst separation.[**20**],[**23**] The loss of activity due to catalyst leaching has also

been reported.[**19**],[**22**],[**26**] Thus, it is still relevant to develop a simple method for the preparation of the heterogeneous catalyst and the resulting catalyst should exhibit and retain excellent activity. Here, we report a simple one step synthesis of heterogeneous palladium catalyst formed by crosslinking commercially available poly(allylamine) (PAA) with a palladium salt. The resulting air and moisture stable PAA-Pd complex can effectively catalyze Suzuki, Heck and Sonogashira reactions without any additional ligand. The reactions can be carried out with excellent yields in benign solvents, including water. Moreover, the catalyst is easily separated and used repeatedly without loss of activity. Further, based on the reusability of the catalyst, a continuous reactor system was developed for facile separation of the product.

## 4.2 Results and Discussion

### 4.2.1 Synthesis of Heterogeneous PAA-Pd Catalyst

PAA-Pd was formed instantly by the addition of $Na_2PdCl_4$ to PAA in methanol at room temperature (Figure **4-1**). The resulting yellow cross-linked polymer was insoluble in common reaction solvents and stable at ambient atmosphere and was directly used for catalysis. This simple method minimized the time and cost involved in the tedious multistep reaction normally followed for the heterogeneous catalyst synthesis. Two compositions, PAA-Pd-**1** and PAA-Pd-**2** containing 10 and 20 mol % added Pd were prepared. The amount of palladium in PAA-Pd-**2**, as determined by inductively coupled plasma-atomic emission spectroscopy (ICP-AES), was found to be 17.4 mol %. A TEM image (Figure **4-2**) of PAA-Pd-**2** revealed a uniform particle distribution in the polymer matrix and particle diameter of 6.3 nm with narrow size distribution (standard deviation of 0.8 nm).

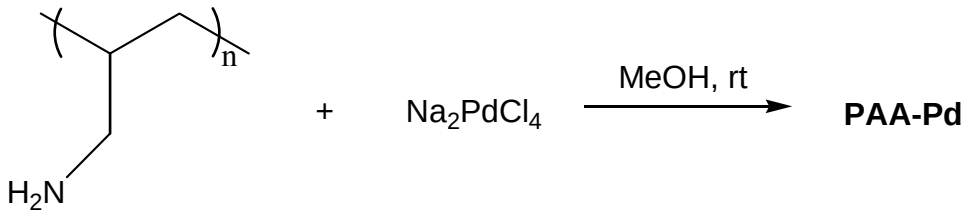


Figure **4-1**: Synthesis of palladium cross-linked poly(allylamine) PAA-Pd catalyst.

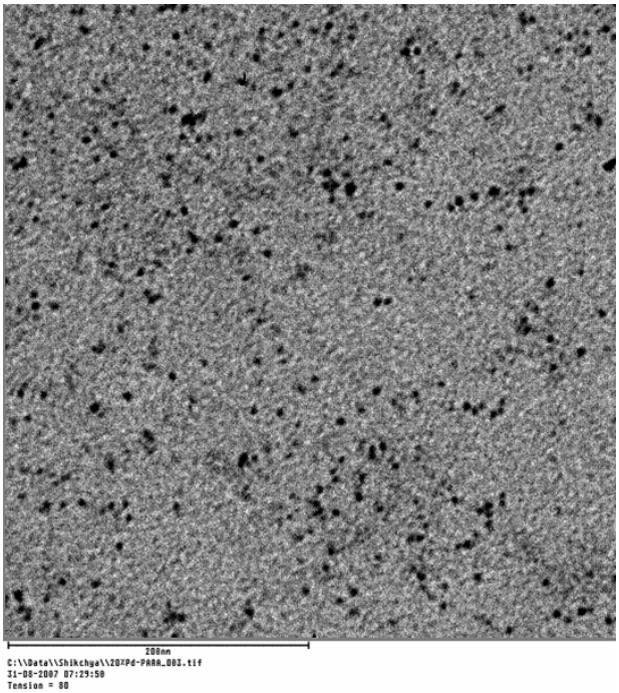


Figure **4-2**: TEM image of PAA-Pd-**2** catalyst.

### 4.2.2 Heterogeneous Suzuki Cross-Coupling Reaction

The catalytic activity of PAA-Pd was initially examined in the reaction of iodobenzene with phenylboronic acid at 75 ˚C using 1:1 (v/v) of isopropanol ($^{i}$PrOH) and water as solvent (Table **4-1**). The catalyst PAA-Pd-**2** with higher mol % of Pd gave a better result in 4 h. Since the polymer itself is basic, catalysis in the absence of added base was attempted but proved less effective (entry 3).

Table **4-1**: Optimization of the catalytic condition[a].

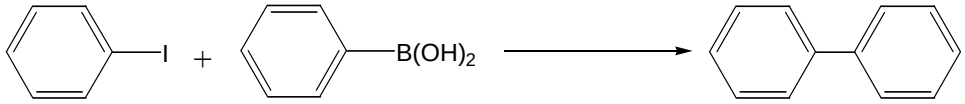


| entry | catalyst | base | time (h) | yield (%)[b] |
|---|---|---|---|---|
| 1 | PAA-Pd-**1** | $Na_2CO_3$ | 6 | 56 |
| 2 | PAA-Pd-**2** | $Na_2CO_3$ | 4 | 84 |
| 3 | PAA-Pd-**2** | - | 4 | 21 |

[a]Conditions: aryl halide (0.5 mmol), phenylboronic acid (0.7 mmol), $Na_2CO_3$ (2.5 mmol), $^{i}$PrOH /$H_2O$ (1:1, v/v, 10 mL), 75 ˚C. [b]Isolated by column chromatography.

The complex PAA-Pd-**2** was then used for the heterogeneous cross coupling reaction of a range of aryl halides with $PhB(OH)_2$ (Table **4-2**). Excellent yields were obtained with both iodo- and bromo- substrates with electron withdrawing (entries 3, 6, and 7) and electron donating (entry 4) functionalities. Satisfactory yield was obtained with chlorobenzene within 21 h. It is also noteworthy that the coupling reaction could also be carried out in neat water with good yield (entry 2). To test the possibility of catalyst leaching from the solid support, the mother liquor

from entry 1 (Table **4-2**), after removing the catalyst and the product, was again used for coupling reaction with a fresh batch of reactants. GC analysis revealed no product formation even after 7.5 h (entry 9), thereby indicating that the catalyst did not leach out during the course of the reaction. The non-leaching nature of the catalyst was further confirmed by ICP-AES analysis. The amount of Pd in the mother liquor from entry 1 was below the detection limit (1 ppm) of the instrument.

Table **4-2**: Suzuki cross coupling reaction of aryl halides with phenylboronic acid catalyzed by PAA-Pd-**2**[a].

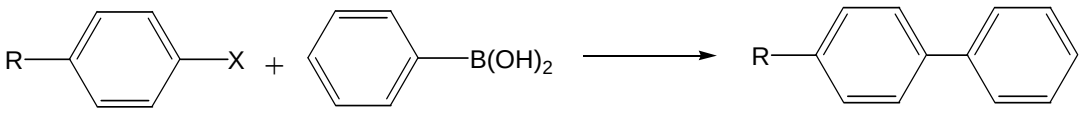


.

| entry | R | X | time (h) | yield (%)[b] |
|---|---|---|---|---|
| 1 | H | I | 4 | 86 |
| 2[c] | OH | I | 4 | 76 |
| 3 | $CH_3CO$ | I | 4 | 90 |
| 4 | $CH_3O$ | I | 4 | 98 |
| 5 | H | Br | 24 | 89 |
| 6 | $CH_3CO$ | Br | 24 | 93 |
| 7 | CHO | Br | 24 | 44 |
| 8 | H | Cl | 21 | 57 |
| 9[d] | H | I | 7.5 | - |

[a]Conditions: aryl halide (0.5 mmol), phenylboronic acid (0.7 mmol), PAA-Pd-**2** (0.17 mmol Pd), $Na_2CO_3$ (2.5 mmol), $^i$PrOH/$H_2O$ (1:1, v/v) (10 mL), 75 ˚C. [b]Isolated by column chromatography. [c]$H_2O$ as solvent. [d]No catalyst, only solvent from entry 1.

The coupling reaction of iodobenzene and phenylboronic acid was also carried out at varying ratios of PAA-Pd-**2** catalyst and aryl halide to check the reactivity of the catalyst. The catalyst showed high activity with as low as 1 mol % of Pd in the reaction medium (Table **4-3**).

Table **4-3**: Reactivity of PAa-Pd-**2** catalyst[a].

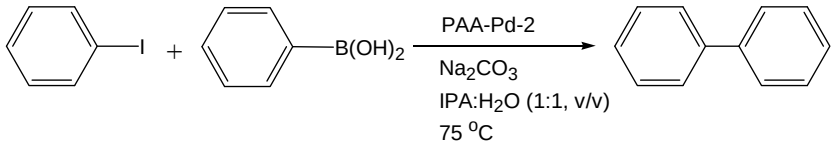


| entry | Pd:PhI (mmol) | Pd (mol %) | time (h) | yield (%)[b] |
|---|---|---|---|---|
| 1 | 0.17:1.0 | 17 | 4 | 86 |
| 2 | 0.17:1.5 | 11 | 4 | 85 |
| 3 | 0.17:2.8 | 6 | 4 | 87 |
| 4 | 0.17:5.6 | 3 | 5 | 80 |
| 5[a] | 0.17:8.4 | 2 | 8 | 82 |
| 6[a] | 0.17:17 | 1 | 9 | 79 |

[a]Conditions: aryl iodide (1.0 equivalent), phenylboronic acid (1.2 equivalent), $Na_2CO_3$ (5.0 equivalent), $^{i}PrOH/H_2O$ (1:1, v/v, 10 mL). [a]3.0 equivalent base and 12 mL solvent. [b]Isolated by column chromatography.

### 4.2.3 Heterogeneous Heck and Sonogashira Cross-Coupling Reactions

Next, the ability of PAA-Pd-**2** to catalyze other carbon-carbon coupling reactions was examined by catalyzing Heck and Sonogashira reactions. (Table **4-4)** lists the results of a number of Heck reactions. Aryl iodides with different functional groups were coupled with electron poor alkenes like butyl acrylate and styrene at 100 ˚C using DMF as a solvent. An excellent yield was obtained with n-butyl acrylate within 4 h (entries 1and 3), whereas with styrene, a high yield required 24 h (entry2). Bromobenzene also gave a high yield in 24 h (entry 4) but chlorobenzene failed to react under similar conditions (entry 5). PAA-Pd-**2** is also an effective catalyst for copper-free Sonogashira reaction (Figure **4-3**). 90 % yield of diphenyl acetylene was obtained from the coupling reaction of iodobenzene and phenyl acetylene.

Table **4-4**: Heck cross coupling reaction of aryl halides with alkenes catalyzed by PAA-Pd-**2**[a].

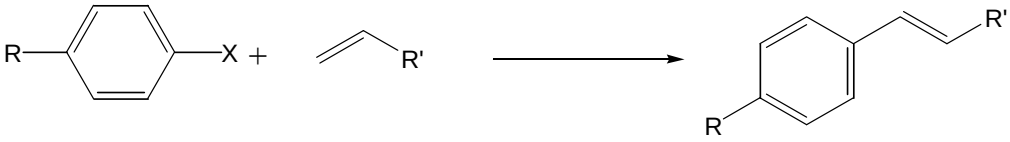


| entry | R | X | R’ | time (h) | yield (%)[b] |
|---|---|---|---|---|---|
| 1 | H | I | $COO(CH_2)_3CH_3$ | 4 | 93 |
| 2 | H | I | $C_6H_5$ | 24 | 82 |
| 3 | $CH_3O$ | I | $COO(CH_2)_3CH_3$ | 4 | 95 |
| 4 | H | Br | $COO(CH_2)_3CH_3$ | 24 | 87 |
| 5 | H | Cl | $COO(CH_2)_3CH_3$ | 24 | - |

[a]Conditions: aryl halide (0.5 mmol), alkene (0.7 mmol), catalyst PAA-Pd-**2** (0.17 mmol Pd), $K_2CO_3$ (1.5 mmol), $Et_3N$ (1 mmol), DMF (5 mL), 100 ˚C. [b]Isolated by column chromatography.

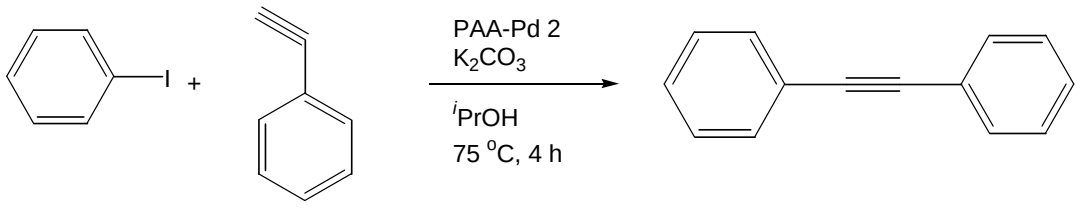


Figure **4-3**: Sonogashira reaction using PAA-Pd **2**.

### 4.2.4 Reusability of PAA-Pd Catalyst

Further, the reusability of PAA-Pd-**2** was checked for the Suzuki coupling reaction of iodobenzene with phenylboronic acid (Table **4-5**). In the first cycle, 86% yield of biphenyl was obtained. The catalyst was recovered by centrifugation, washed with water and immediately used for the next cycle. The process was repeated through seven cycles without loss of activity.

Table **4-5**: Recycling of PAA-Pd-**2** catalyst.

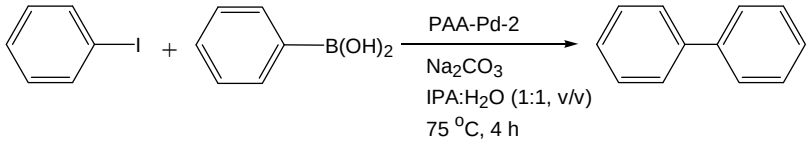


| no. of run | yield (%)[a] |
|---|---|
| 1 | 86 |
| 2 | 91 |
| - | - |
| 6 | 92 |
| 7 | 92 |

[a]Isolated by column chromatography.

### 4.2.5 Continuous Reactor System

The easy preparation, ambient atmosphere stability, non-leaching nature and the retention of the catalytic activity of PAA-Pd-**2** prompted us to design a continuous reactor system. The concept was to continuously add the reaction mixture at a specific rate to the top of a heated column pre-packed with the catalyst and to collect the product from the bottom (Figure **4-4**). A quantitative amount of biphenyl was obtained when iodobenzene and $PhB(OH)_2$ in basic 1:1 (v/v) $^{i}$PrOH and water were fed into the column. The collected biphenyl needed no further purification other than the simple removal of the solvent and washing with water to remove the inorganic salts.

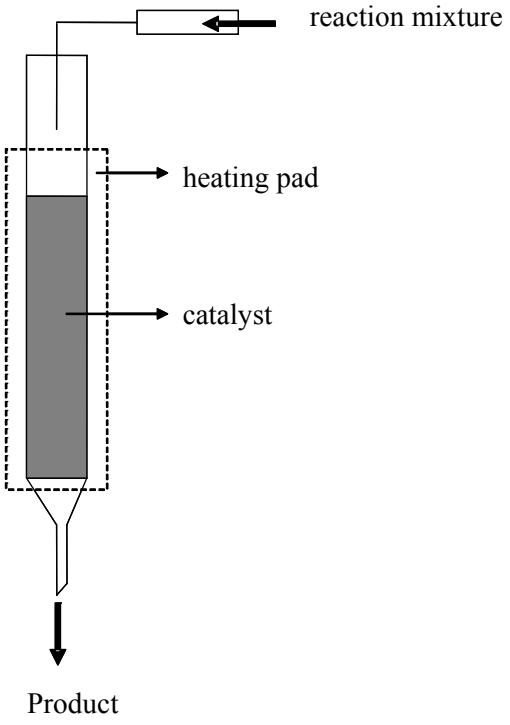


Figure **4-4**: Schematic representation of a continuous column reactor.

## 4.3 Conclusion

In summary, we have described a simple one-step route to the synthesis of a heterogeneous palladium catalyst by crosslinking commercially available polymer with the corresponding metal salt. The catalyst exhibited excellent activity toward Suzuki coupling of different aryl halides and phenylboronic acid in $^{i}$PrOH:$H_2O$. The reaction also proceeded in good yield in aqueous media. The catalyst was recovered easily and recycled without losing any activity and ICP analysis showed no Pd leaching. The catalyst was also effective for Heck and Sonogashira couplings. Finally, a continuous-flow reactor was designed that allowed facile product isolation.

## 4.4 Experimental

### 4.4.1 Materials and Instrumentation

All chemicals were purchased from Aldrich and used without further purification. The reactions were carried out under air. $^{1}H$ and $^{13}C$ NMR spectra were recorded on Bruker DPX-300 (300 MHz) and DRX-400 (400 MHz) spectrometers. Chemical shifts are referenced to $CDCl_3$ unless otherwise stated. The TEM images were taken with JOEL 1200EXII operating at 80 kV. The sample was prepared by depositing 4 μL of the compound dispersed in toluene on carbon coated copper grid (300 mesh). Perkin-Elmer Ultima 5300 ICP (inductively coupled plasma emission spectrometer) was used to determine the amount of Pd on the catalyst. Molecular mass analysis were performed on Waters LCT Premier time of flight mass spectrometer with dual electrospray and chemical ionization (ESCI) and Waters CGT time of flight mass spectrometer with electron impact ionization (EI). GC analysis was performed on Hewlett Packard-5890 with a FID detector and 95% dimethyl- and 5% diphenyl- polysiloxane column.

### 4.4.2 Preparation of Palladium Crosslinked Poly(allylamine) PAA-Pd-2

0.2 mmol $Na_2PdCl_4$ in 1 mL MeOH was added dropwise to 1 mmol PAA (obtained after neutralizing PAA.HCl, $M_W \sim 15{,}000$, with KOH in MeOH and removing the insoluble salt) [**27**] in 2 mL MeOH. The yellow precipitate, formed immediately, was stirred for 15 min, separated by centrifugation and washed with 2x10 mL reaction solvent. The catalyst was then directly used in reactions.

The amount of palladium loading was analyzed by ICP-AES. The catalyst, prepared as above, was mixed with 8 mL of $HCl:HNO_3$ (3:1, v/v) and heated at 100 ˚C for 6 h. The resulting orange colored solution was filtered, diluted to 50 mL with distilled water and analyzed.

### 4.4.3 General Procedure for Suzuki Coupling

Aryl halide (0.5 mmol), phenylboronic acid (0.7 mmol), $Na_2CO_3$ (2.5 mmol), catalyst PAA-Pd-**2** (0.17 mmol Pd), $^{i}$PrOH /$H_2O$ (1:1, v/v, 10 mL) were mixed and heated at 75 ˚C for a specific period of time. Upon completion, catalyst was separated by centrifugation, and washed with 10 mL each of ether and water. The product was extracted with ether, dried over anhydrous $Na_2SO_4$ and then the solvent evaporated. The biaryl product was purified by flash chromatography using silica gel and hexane or 4% ethyl acetate in hexane.

$^{1}$H NMR spectrum of 4-phenylbenzaldehyde is illustrated in (Figure **4-5**). The singlet for the aldehyde proton (f) is at 9.97 ppm while the aryl protons (a-e) appear between 7.30 and 7.90 ppm. Figure **4-6** represents the $^{13}$C NMR spectrum of 4-phenylbenzaldehyde. LC-MS (*m/z* $[M+H]^+$: 183.1) confirmed the mass of the product.

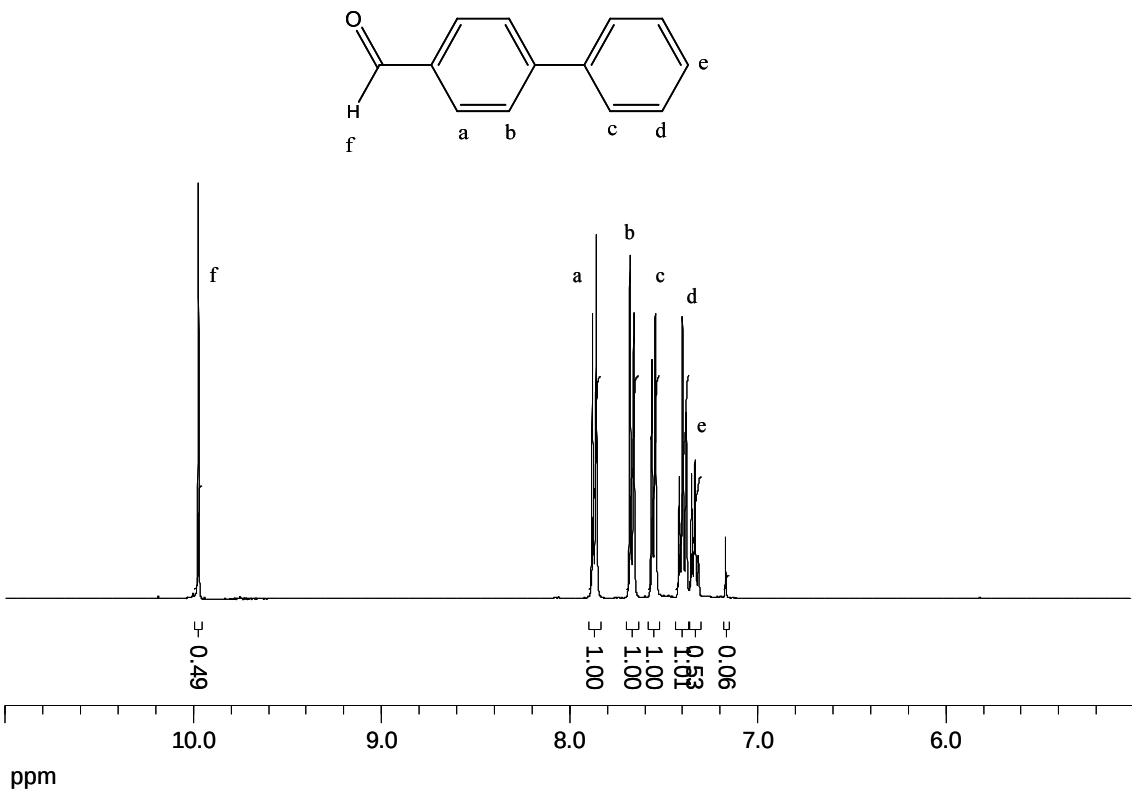


Figure **4-5**: $^{1}H$ NMR (400 MHz, $CDCl_3$) spectrum of 4-phenylbenzaldehyde.

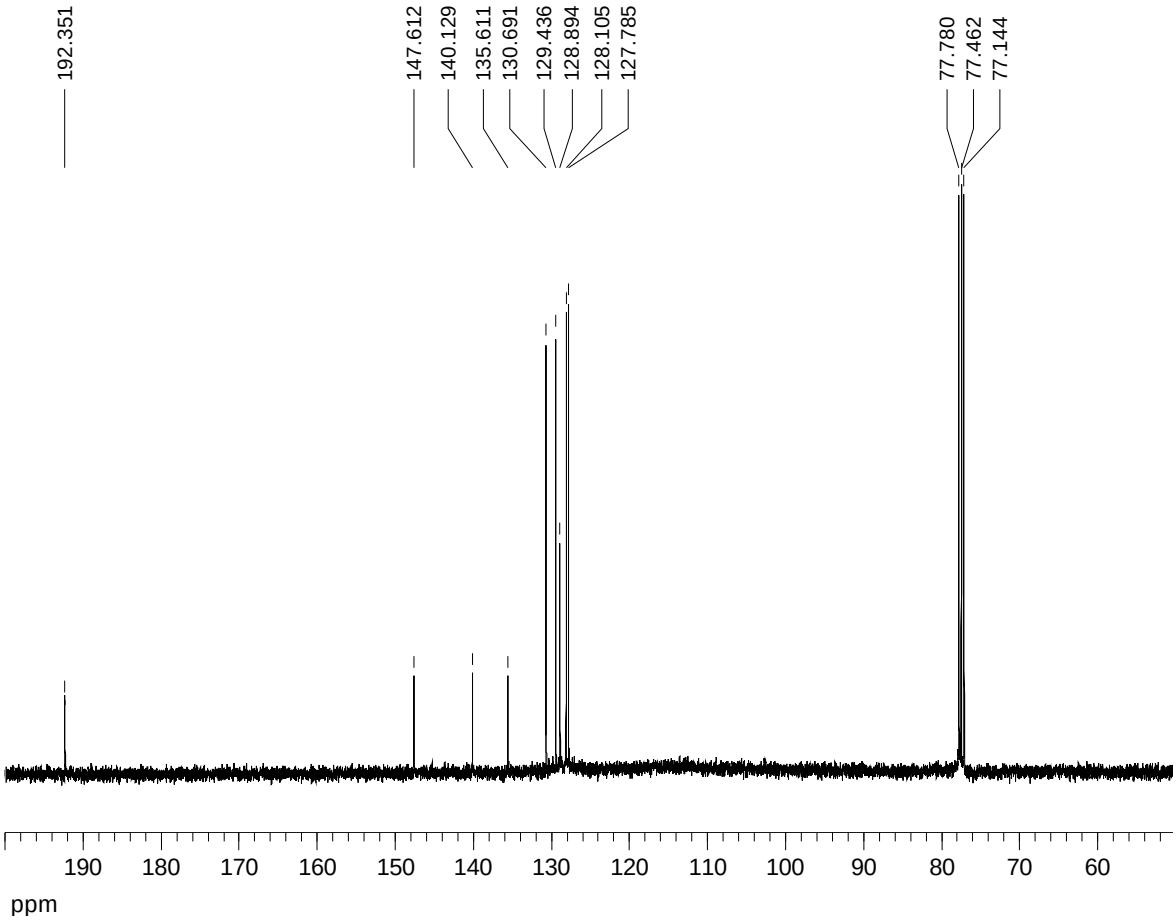


Figure **4-6**: $^{13}C\{^{1}H\}$ NMR (100 MHz, $CDCl_3$, ppm) of 4-phenylbenzaldehyde.

The spectral data of the remaining biaryl products characterized similarly are listed below.

**Biphenyl:** $^{1}H$ NMR (400 MHz, $CDCl_3$, ppm): 7.50 (d, 4H), 7.35 (t, 4H), 7.25 (t, 2H). $^{13}C\{^{1}H\}$ NMR (100 MHz, $CDCl_3$, ppm): 140.2, 127.7, 126.2, 126.1. GC-MS: *m/z* $[M^+]$: 154.

**4-Hydroxybiphenyl:** $^{1}H$ NMR (400 MHz, $CH_3OD$, ppm): 7.52 (d, 2H), 7.43 (d, 2H), 7.36 (t, 2H), 7.24 (t, 1H), 6.85 (d, 2H). $^{13}C\{^{1}H\}$ NMR (100 MHz, $CH_3OD$, ppm): 161.1, 145.4, 136.8, 132.6, 131.9, 130.3, 130.3, 119.5. LC-MS: *m/z* $[M-H]^-$: 169.1.

**4-Acetylbiphenyl:** $^{1}$H NMR (300 MHz, $CDCl_3$, ppm): 7.96 (d, 2H), 7.61 (d, 2H), 7.55 (d, 2H), 7.40 (t, 2H), 7.31 (t, 1H), 2.56 (s, 3H). $^{13}C\{^{1}H\}$ NMR (75 MHz, $CDCl_3$, ppm): 198.1, 146.2, 140.3, 136.3, 129.4, 129.3, 128.6, 127.7, 127.6, 27.1. LC-MS: *m/z* $[M+H]^+$: 197.1.

**4-Methoxybiphenyl:** $^{1}$H NMR (400 MHz, $CDCl_3$, ppm): 7.45 (m, 4H), 7.32 (t, 2H), 7.22 (t, 1H), 6.89 (d, 2H), 3.75 (s, 3H). $^{13}C\{^{1}H\}$ NMR (100 MHz, $CDCl_3$, ppm): 159.6, 141.3, 134.2, 129.1, 128.6, 127.2, 127.1, 114.6, 55.8. GC-MS: *m/z* $[M^+]$: 184.

### 4.4.4 General Procedure for Heck Coupling

Aryl halide (0.5 mmol), alkene (0.7 mmol), $K_2CO_3$ (1.5 mmol), $Et_3N$ (1.0 mmol), catalyst PAA-Pd-**2** (0.17 mmol Pd) and DMF (5 mL) were heated at 100 ˚C for a specific time. After the reaction was complete, catalyst was separated by centrifugation, and washed with 2x10 mL ether. The ether fractions were combined, dried over anhydrous $Na_2SO_4$ and the solvent evaporated. The cinnamate product was purified by column chromatography using silica gel and 4% ethyl acetate in hexane.

$^{1}$H NMR spectrum of 1,2-diphenylethylene is illustrated in (Figure **4-7**). The aryl protons (a-d) appear between 7.00 and 7.50 ppm. Figure **4-8** represents the $^{13}$C NMR spectrum of 1,2-diphenylethylene. GC-MS (*m/z* $[M^+]$: 180) confirmed the mass of the product.

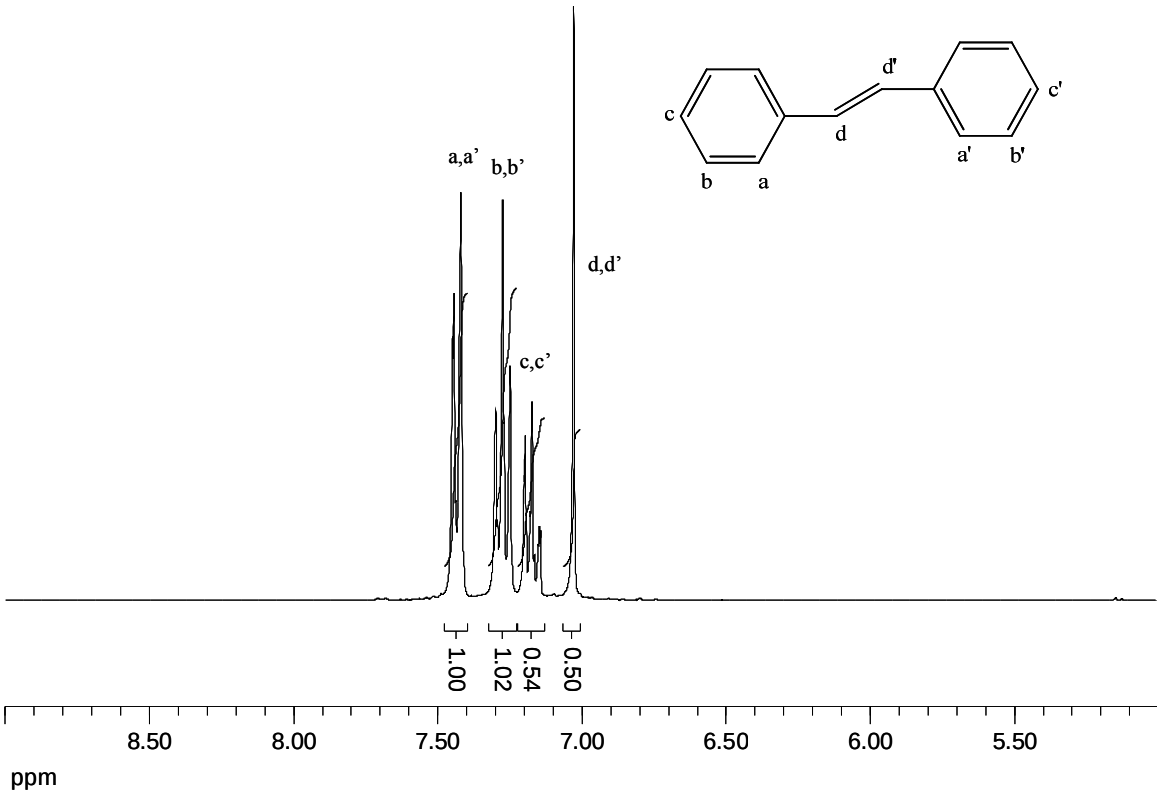


Figure **4-7**: $^{1}H$ NMR (300 MHz, $CDCl_3$) spectrum of 1,2-diphenylethylene.

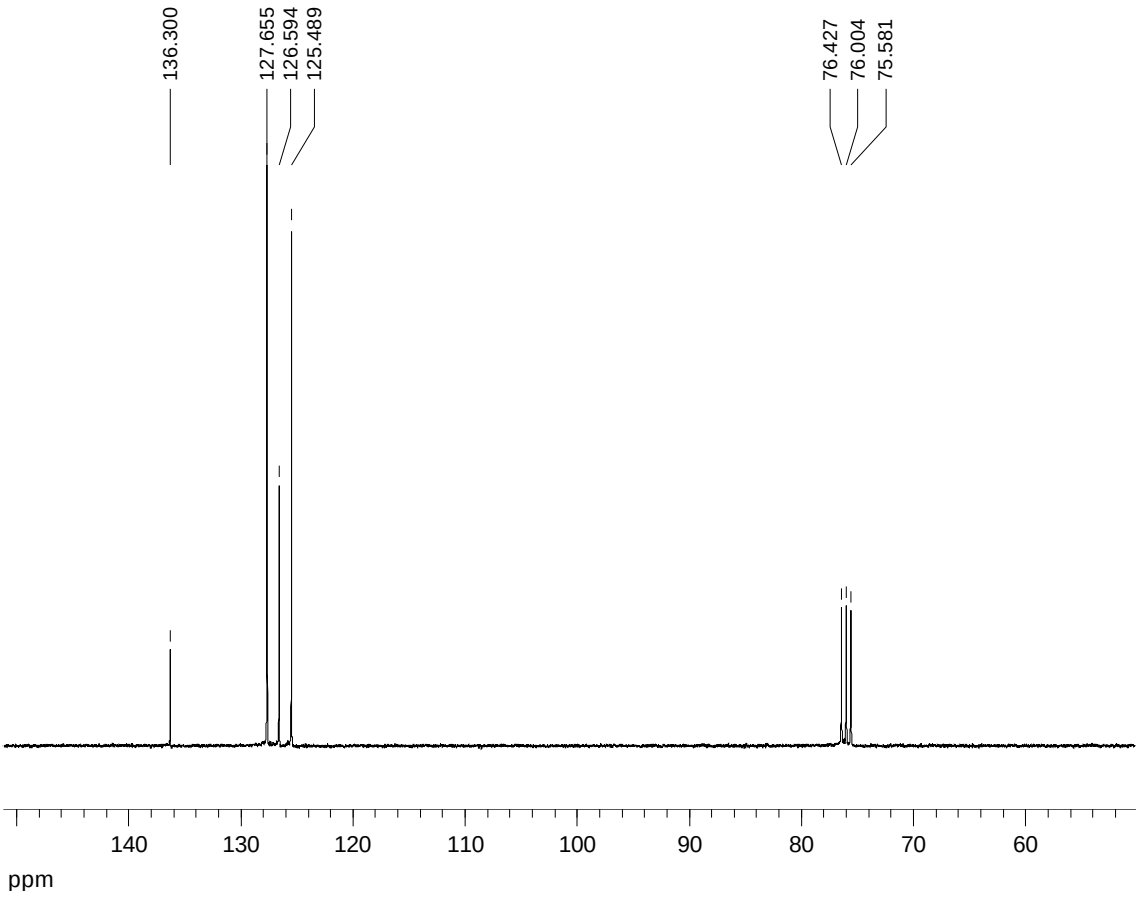


Figure **4-8**: $^{13}C\{^{1}H\}$ NMR (75 MHz, $CDCl_3$, ppm) of 1,2-diphenylethylene.

The spectral data of the remaining cinnamate products characterized similarly are listed below.

**n-Butyl cinnamate:** $^{1}H$ NMR (400 MHz, $CDCl_3$, ppm): 7.61 (d, 1H), 7.45 (m, 2H), 7.30 (t, 3H), 6.37 (d, 1H), 4.14 (t, 2H), 1.62 (p, 2H), 1.36 (m, 2H), 0.91 (t, 3H). $^{13}C\{^{1}H\}$ NMR (100 MHz, $CDCl_3$, ppm): 167.5, 144.9, 134.9, 130.6, 129.3, 128.4, 118.7, 64.8, 31.2, 19.6, 14.2. LC-MS: *m/z* $[M+H]^+$: 205.1.

**3-(4-Methoxyphenyl) acrylic acid butyl ester:** $^{1}$H NMR (300 MHz, $CDCl_3$, ppm): 7.56 (dd, 1H), 7.39 (d, 2H), 6.80 (d, 2H), 6.24 (d, 1H), 4.12 (t, 2H), 3.85 (s, 3H), 1.61 (m, 2H), 1.37 (m, 2H), 0.88 (t, 3H). LC-MS: *m/z* $[M+H]^+$: 235.2.

### 4.4.5 General procedure for Sonogashira coupling

Aryl halide (0.5 mmol), phenyl acetylene (0.7 mmol), $K_2CO_3$ (2.5 mmol), catalyst PAA-Pd-**2** (0.17 mmol Pd) and $^{i}$PrOH (8 mL) were heated at 75 ˚C for 4 h. After the reaction was complete, catalyst was separated by centrifugation, and washed with 2x10 mL ether. The ether fractions were combined, dried over anhydrous $Na_2SO_4$ and the solvent evaporated. The product was purified by column chromatography using silica gel and hexane. $^{1}$H NMR spectrum of 1,2-diphenylacetylene is illustrated in (Figure **4-9**). The aryl protons appear between 7.30 and 7.70 ppm. (Figure **4-10)** represents the $^{13}$C NMR spectrum of 1,2-diphenylacetylene. GC-MS (*m/z* $[M^+]$: 178) confirmed the mass of the product.

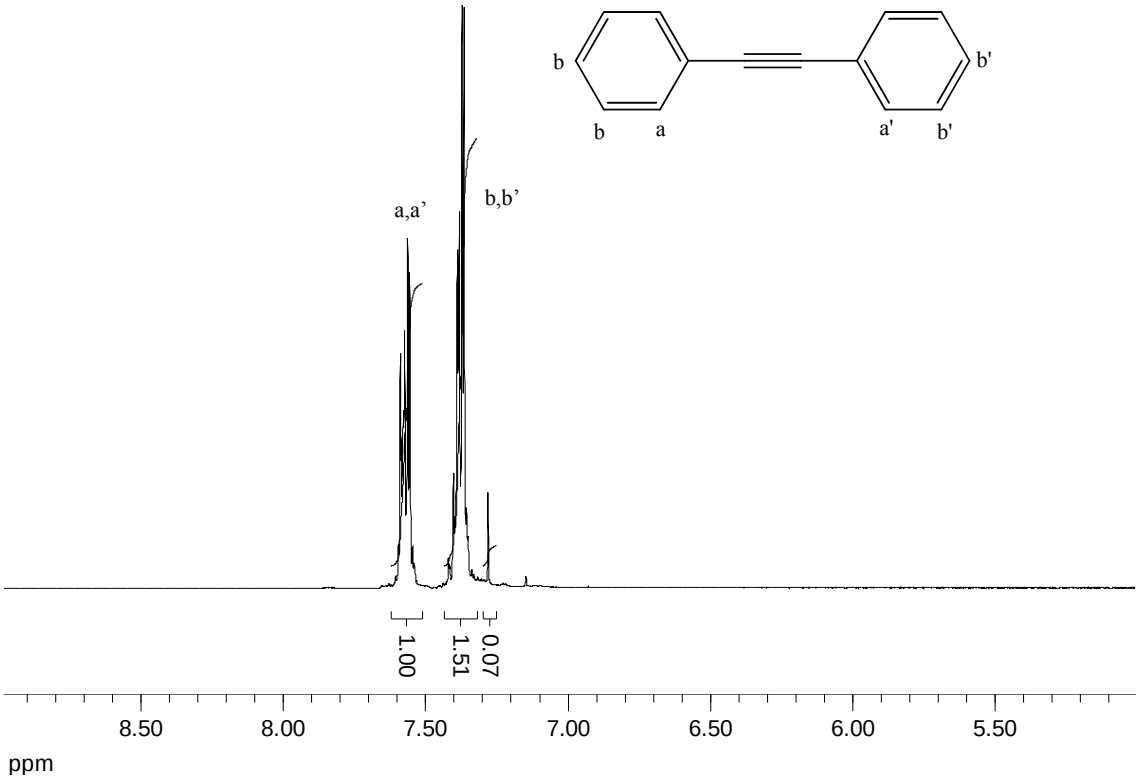


Figure **4-9**: $^{1}H$ NMR (400 MHz, $CDCl_3$) spectrum of 1,2-diphenylacetylene.

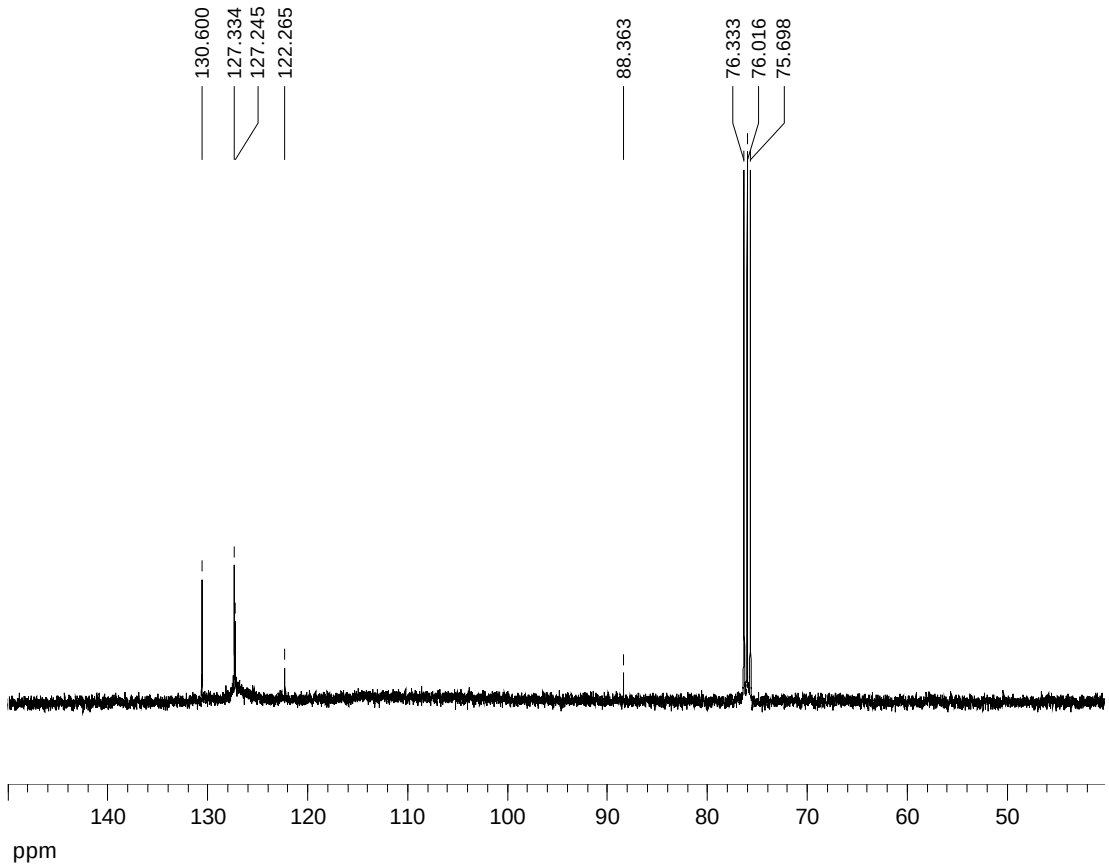


Figure **4-10**: $^{13}C\{^{1}H\}$ NMR (100 MHz, $CDCl_3$, ppm) of 1,2-diphenylacetylene.

### 4.4.6 Procedure for Recycling the Catalyst

Iodobenzene (0.5 mmol), phenylboronic acid (0.7 mmol), $Na_2CO_3$ (2.5 mmol), catalyst PAA-Pd-**2** (0.17 mmol Pd), $^{i}$PrOH /$H_2O$ (1:1, v/v, 10 mL) were heated at 75 ˚C for 4 h. The catalyst was then separated by centrifugation and washed with 10 mL ether, 10 mL water and subsequently directly used for the next cycle. The product was isolated by extraction with ether and purified by flash chromatography. Recovered catalyst was reused for 7 more cycles of the same reaction.

### 4.4.7 Procedure for Continuous Column Reactor

The column (length, 20 cm; diameter, 1.7 cm) was tightly packed with PAA-Pd-**2** catalyst, wrapped with a heating tape and heated to 75 ˚C. The reaction mixture (PhI: $PhB(OH)_2$: $Na_2CO_3$, 1: 1.4: 5; $^{i}$PrOH/$H_2O$, 1: 1, v/v) was added continuously from the top at the rate of 2 drops/min. The white crystals of biphenyl were collected at the other end along with the solvent.

**4.5 References**

**1(a).** Tsuji, J. *Palladium Reagents and Catalysts: Innovations in Organic Synthesis*, Wiley, UK, 1995. **(b).** Heck, R. F. *Comprehensive Organic Synthesis*; Trost, B. M.; Fleming, I., Eds.; Pergamon: Oxford, 1991. **(c).** Negishi, E. (Ed.), *Handbook of Organipalladium Chemistry for Organic Synthesis*, Wiley, New York, 2002.

**2(a.)** Miyaura, N.; Suzuki, A. *Chem. Rev*. **1995**, *95*, 2457-2483. **(b).** Sonogashira, K. *J. Organomet. Chem.* **2002**, *653,* 46-49. **(c).** Singh, R.; Viviu, M. S.; Kramareva, N.; Navarro, O.; Nolan, S. P. *Org. Lett.* **2005**, *7,* 1829-1832. **(d).** Billengsley, K. L.; Anderson, K. W.; Buchwald, S. L. *Angew. Chem. Int. Ed.* **2006**, *45,* 3484-3488.

**3.** McNamara, C. A.; Dixon, M. J.; Bradley, M. *Chem. Rev.* **2002**, *102,* 3275-3300.

**4**. Viciu, M. S.; Nolan, S. P. *Top Organomet. Chem.* **2005**, *14,* 241-278.

**5.** Yin, L.; Liebscher, J. *Chem. Rev.* **2007**, *107,* 133-173.

**6.** Kim, J-H.; Kim, J-W.; Shokouhimehr, M.; Lee, Y-S. *J. Org. Chem.* **2005**, *70,* 6714-6720.

**7.** Schwarz, J.; Bohm, V. P. W.; Gardiner, M. G.; Grosche, M.; Harrmann, W. A.; Hieringer, W.; Raudaschl-Sieber, G. *Chem. Eur. J.* **2000**, *6,* 1773-1780.

**8.** Gil-Molto, J.; Karlstrom, S.; Najera, C. *Tetrahedron* **2005**, *61*, 12168-12176.

**9.** Karimi, B.; Enders, D. *Org. Lett.* **2006**, *8,* 1237-1240.

**10.** Stevens, P. D.; Li, G.; Fan, J.; Yen, M.; Gao, Y. *Chem. Commun.* **2005**, 4435-4437.

**11.** Dahan, A.; Portnoy, M. *J. Am. Chem. Soc.* **2007**, *129,* 5860-5869.

**12.** Pittelkow, M.; Moth-Poulsen, K.; Boas, U,; Christensen, J. B. *Langmuir* **2003**, *19*, 7682-7684.

**13.** Tandukar, S.; Sen, A. *J. Mol. Cat. A: Chem.* **2007**, *268,* 112-119.

**14.** Akiyama, R.; Kobayashi, S. *J. Am. Chem. Soc.* **2003**, *125,* 3412-3413.

**15.** Okamoto, K.; Akiyama, R.; Kobayashi, S. *J. Org. Chem.* **2004**, *69,* 2871.

**16.** Okamoto, K.; Akiyama, R.; Kobayashi, S. *Org. Lett.* **2004**, *6,* 1987-1990.

**17.** Oyamada, H.; Akiyama, R.; Hagio, H.; Mailto, T.; Kobayashi, S. *Chem. Commun.* **2006**, 4297-4299.

**18.** Reetz, M. T.; Breinbauer, R.; Wanninger, K. *Tetrahedron Lett.* **1996**, *37,* 4499-4502.

**19.** Li, Y.; Hong, X. M.; Collard, D. M.; El-Sayed, M. A. *Org. Lett*. **2000**, *2*, 2385-2388.

**20.** Zhang, M.; Zhang, W. *J. Phys. Chem. C* **2008**, *112*, 6245-6252.

**21.** Klingelhofer, S.; Heitz, W.; Greiner, A.; Oestreich, S.; Forster, S.; Antoniette, M. *J. Am. Chem. Soc.* **1997**, *119,* 10116-10120.

**22.** Okamoto, K.; Akiyama, R.; Yoshida, H.; Yoshida, T.; Kobayashi. S. *J. Am. Chem. Soc*. **2005**, *127*, 2125-2135.

**23.** Beletskaya, I. P; Kashin, A. N.; Litvinov, A. E.; Tyurin, V. S.; Valetsky, P. M.; van Koten, G. *Organometallics* **2006**, *25*, 154-158.

**24.** Beletskaya, I. P.; Khokhlov, A. R.; Tarasenko, E. A.; Tyurin, V. S. *J. Organomet. Chem*. **2007**, *692*, 4402-4406.

**25.** Panziera, N.; Pertici, P.; Barazzone, L.; Caporusso, A. M.; Vitulli, G.; Salvadori, P.; Borsacchi, S.; Geppi, M.; Veracini, C. A.; Martra, G.; Bertinetti, L. *J. Catal.* **2007**, *246*, 351-361.

**26.** Miao, S.; Zhang, C.; Liu, Z.; Han, B.; Xie, Y.; Ding, S.; Yang, Z. *J. Phys. Chem. C* **2008**, *112*, 774-780.

**27.** Seo, T.; Kajihara, T.; Iijima, T. *Makromol. Chem*. **1987**, *188*, 2071-2082.

# Chapter 5

# Synthesis of Dialkyl Ethers: Catalytic Reductive Etherification

## 5.1 Introduction

The unsymmetrical dialkyl ether moieties are one of the most common sub-structure found in organic compounds. Ether is traditionally synthesized by Williamson's reaction using strong bases and forming stoichiometric amount of salt byproducts.**[1]** It can also be made by catalytic reduction of ketones or aldehydes with alcohol; however, the methods employ harsh reaction conditions. The typical procedure requires a large excess of acidic alcohol and uses platinum oxide.**[2]** Pd/C can carry out the reaction in acid free medium but only at high hydrogen pressure or under the hydrogen flow in an apparatus designed to remove water continuously. **[3],[4]** Alternatively, alkyl- and alkoxy- silanes also reduce the carbonyl compounds in acidic alcohol.**[5]** Recently, a mild reaction protocol has been reported for reductive etherification of ketones with primary and secondary alcohols at ambient hydrogen pressure and acid free condition but needs specific Degussa platinum on charcoal catalyst for high yield.**[6]** Pd/C showed almost negligible catalytic activity under the mentioned condition. At this time, there is a high synthetic interest in this area as reactants, ketones and alcohols can be produced from biomass. The growing research in renewable resources has facilitated the production of ketones, phenols, and aldehydes from lignin, an abundantly found biomass.**[7],[8],[9]** A protocol that will allow the synthesis of ethers using these biomass derived carbonyl compounds and different alcohols under mild reaction conditions would be very significant. Here, we report Pd/C catalyzed etherification of carbonyl compounds like ketones and phenols with a range of alcohols in the presence of only catalytic amount of acid. The presence of catalytic amount of both protic and solid Lewis acid led to the high yield of ether in a solvent free medium.

## 5.2 Results and Discussion

### 5.2.1 Catalytic Reductive Etherification of Cyclohexanone with 1˚ Alcohol

In order to define the optimal reaction condition for the etherification of the carbonyl compounds, cyclohexanone was taken as a model substrate. Pd/C is a commercially available heterogeneous catalyst and can be recycled by simple filtration. In a typical reaction, 1:1.5 molar ratios of cyclohexanone and alcohol, catalytic amounts of Pd/C and the acids in a stainless steel autoclave was charged with hydrogen and heated to 65 ˚C. No solvent was used for the reaction. The GC analysis performed at the end of the reaction shows the formation of desired product, alkyl cyclohexyl ether (**1**) along with cyclohexanol (**2**) and dicyclohexyl ether (**3**) (Figure **5-1**). The products were further confirmed by GC-MS. The ratio of the products depends on the amount of the acid added.

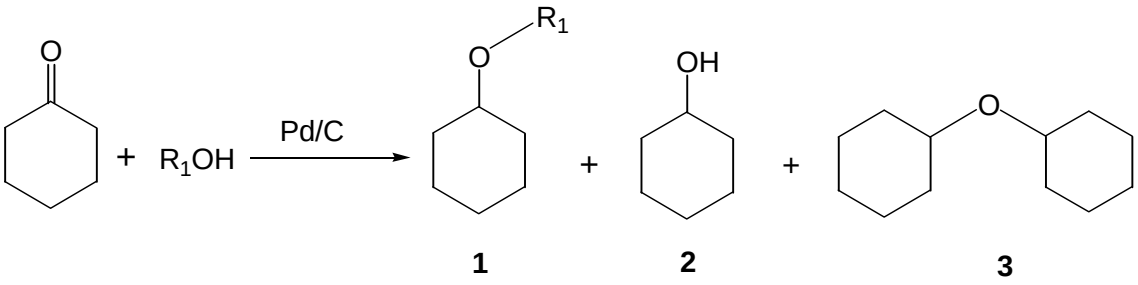


Figure **5-1**: Synthesis of ether from ketone and alcohol.

When the catalytic reaction was carried out with 5 mol % Pd and 200 psi of $H_2$ for 16 h without any acid, the rate of hydrogenation exceeded etherification yielding cyclohexanol and n-butyl cyclohexyl ether in 2:1 ratio; whereas, the rate was reversed with the addition of catalytic amount of HCl (Table **5-1**, entries 1 and 2). Similar result was obtained when the pressure was decreased to 60 psi of $H_2$ and catalyst to 3 mol % Pd (entry 3) and this milder condition was implied henceforth. It has been reported that water formed during the reaction can be detrimental to the etherification.**[6]** Adding molecular sieves (3 Å MS) to the reaction increased the yield of **1** from 60.1 to 65.4 % (entry 4). The highest yield of 84 % for cyclohexyl butyl ether was achieved when catalytic amount of Lewis acid $Al_2O_3$ was also added to the reaction (entry 5). It would be beneficial to catalyze the reaction with solid acids as they can be recycled and do not corrode. However, Lewis acid alone was unable to deliver the same result (entry 6). Further, decreasing the reaction time or hydrogen pressure led to lower conversion of cyclohexanone (entries 7-9). It is to be noted that when ambient hydrogen pressure (created by a gas balloon) was maintained during the reaction, contrary to other results hydrogenation is negligible and dicyclohexyl ether is formed as the main side product (entry 8). This optimized reaction condition employed in entry 5 was then employed for etherification of cyclohexanone with secondary and tertiary alcohols.

Table **5-1**: Catalytic etherification of cyclohexanone with n-butanol ($R_1OH$)[a].

| entry | HCl (mmol) | $Al_2O_3$ (mmol) | 3 Å MS (g) | conversion (%) | yield of 1 (%) | 2 (%) | 3 (%) |
|---|---|---|---|---|---|---|---|
| 1[b] | - | - | - | 100 | 33.9 | 66.1 | - |
| 2[b] | 0.9 | - | - | 100 | 60.5 | 39.4 | - |
| 3 | 0.9 | - | - | 100 | 60.1 | 37.7 | 2 |
| 4 | 0.9 | - | 0.5 | 100 | 65.4 | 32.9 | 1.6 |
| 5 | 0.9 | 0.6 | 0.5 | 100 | 84 | 16 | - |
| 6 | - | 1.2 | 0.5 | 99 | 42 | 54 | 2.5 |
| 7[c] | 0.9 | 0.6 | 0.5 | 83 | 56.3 | 26.5 | - |
| 8[d] | 0.9 | 0.6 | 0.5 | 85 | 63.7 | 1.9 | 19.2 |
| 9[e] | 0.9 | 0.6 | 0.5 | 54 | 40 | 14.3 | - |

[a]Conditions: ketone (10 mmol), alcohol (15 mmol), Pd/C (3 mol % Pd), 60 psi $H_2$, 65 ˚C, 16 h. [b]200 psi $H_2$, Pd/C (5 mol % Pd). [c]7 h. [d]~1 atm $H_2$. [e]15 psi $H_2$. Conversion and yield calculated with reference to the internal standard, decane.

### 5.2.2 Catalytic Reductive Etherification of Cyclohexanone with 2˚ and 3˚Alcohols

The product analysis of the reaction of cyclohexanone with isopropanol ($^{i}$PrOH) and tertiary butanol ($^{t}$BuOH) employing the optimal condition for the primary alcohol showed that mainly hydrogenation was occurring with the highest yield of cyclohexanol ( Table **5-2**, entries 1 and 6). The volume of alcohol as well as HCl was altered to improve the yield of ether. When the amount of isopropanol was increased to three equivalents along with increase in HCl to 2.4 mmol, the yield of ether increased to 47.5 % (entry 3).

Table **5-2**: Catalytic etherification of cyclohexanone with 2˚ and 3˚ alcohol[a].

| entry | alcohol | HCl (mmol) | $Al_2O_3$ (mmol) | conversion (%) | yield of 1 (%) | 2 (%) | 3 (%) |
|---|---|---|---|---|---|---|---|
| 1 | i-PrOH | 0.9 | 0.6 | 100 | 9.3 | 79 | 11.7 |
| 2[b] | i-PrOH | 0.9 | 0.6 | 100 | 18.5 | 73.4 | 8.1 |
| 3[c] | i-PrOH | 2.4 | 0.6 | 100 | 47.5 | 52.5 | - |
| 4[c] | i-PrOH | 3.6 | 0.6 | 100 | 16 | 76 | 7.3 |
| 5[d] | i-PrOH | 2.4 | 0.6 | 100 | 20.6 | 74 | 5.3 |
| 6 | t-BuOH | 0.9 | 0.6 | 100 | 2.1 | 88.3 | 9.3 |

[a]Condition: ketone (10 mmol), alcohol (15 mmol), Pd/C (3 mol % Pd), 3 Å MS (0.5 g), 60 psi $H_2$, 65 ˚C, 16 h. [b]alcohol (30 mmol). [c]alcohol (40 mmol). [d]alcohol (50 mmol). Conversion and yield calculated with reference to the internal standard, decane.

### 5.2.3 Etherification Reactions with Other Substrates

For the diversity of this reaction protocol, other substrates were also used. 1:2 molar ratios of phenol and n-butanol were reacted at the pressure of 200 psi of hydrogen and temperature of 65 ˚C using Pd/C catalyst and 0.9 mmol HCl. At the end of 16 h, phenol was completely converted into butyl cylcohexyl ether (61 %), cyclohexanol (32 %) (Figure **5-2 (a)**). It is also interesting that the studied condition can be used for substituting the methoxy group with bulkier alkoxy group. Anisole under this condition reacts to yield butyl cyclohexyl ether (69 %), cyclohexyl methyl ether (24 %) and cyclohexanol (8 %) (Figure **5-2 (b)**). However, cyclohexanol failed to react under the studied reaction condition.

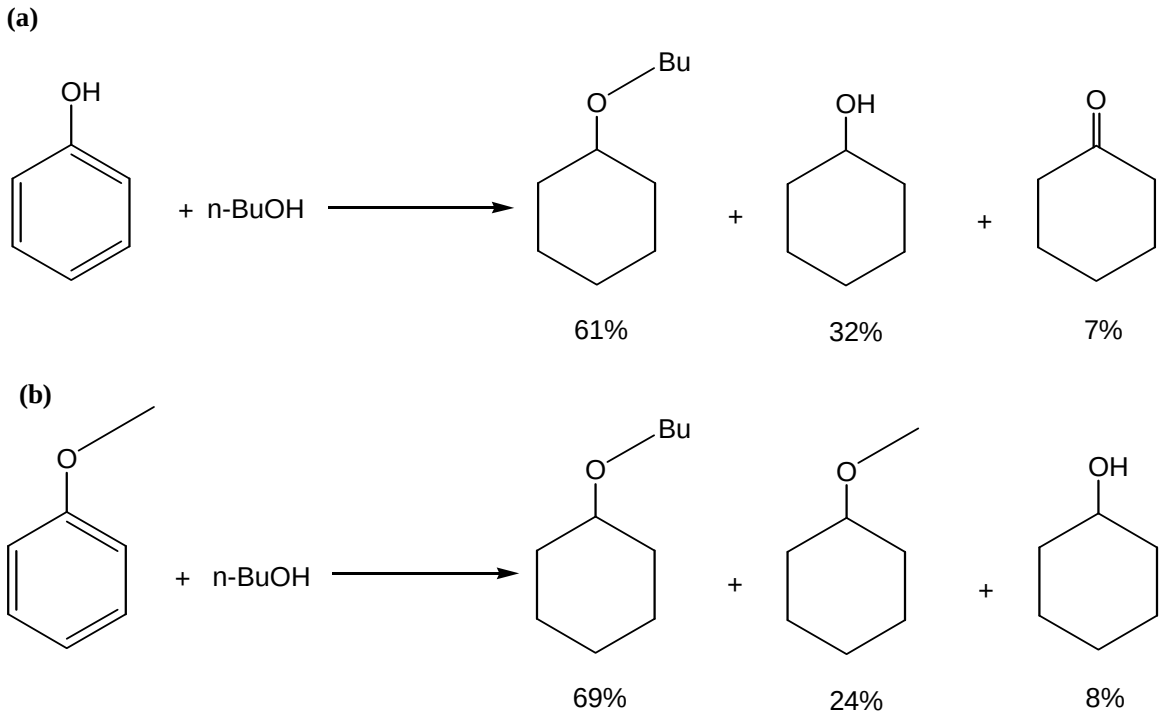


Figure **5-2**: Catalytic etherification of (a) phenol and (b) anisole with n-butanol.

## 5.3 Conclusion

We have reported a mild reaction protocol for the reductive etherification of carbonyl compounds into unsymmetrical ethers using catalytic amount of mineral and solid acids. The method is applicable for the reaction of different substrates like cyclohexanone, phenol and anisole with both primary and secondary alcohols. The reported method can also be used to substitute simple methoxy group with bulkier butoxy groups in ether. The reaction employed heterogeneous catalyst, Pd/C in a mild reaction condition. Moreover, the reactions were solvent free.

## 5.4 Experimental

### 5.4.1 Materials and Instrumentation

n-Butanol was purchased from Acros. All other chemicals were purchased from Aldrich and used without further purification. Molecular mass analysis was performed on Waters CGT time of flight mass spectrometer with electron impact ionization (EI). GC analysis was performed on Hewlett Packard-5890 with a FID detector and 95% dimethyl- and 5% diphenyl- polysiloxane column.

### 5.4.2 Synthesis of Butyl Cyclohexyl Ether

The reactions were carried out in a stainless steel autoclave with a glass liner. Cyclohexanone (10 mmol), alcohol (15 mmol), HCl (0.9 mmol), $Al_2O_3$ (0.6 mmol), molecular sieves (0.5 g), Pd/C (3 mol % Pd) was reacted at 65 ˚C and 60 psi of $H_2$. At the end of the reaction, a small fraction of the reaction mixture was diluted with $CH_2Cl_2$. A known volume of an internal standard, decane was added and the products were analyzed by both GC and GC-MS. The yields were calculated with reference to the internal standard, decane.

## 5.5 References

**1.** March, J. *Advanced Organic Chemistry*, 6th ed; Wiley: New York, 2007, 529-531.

**2.** Verzele, M.; Acke, M.; Anteunis, M. *J. Chem Soc*. **1963**, 5598-5600.

**3.** Bethmont, V.; Fache, F.; Lemaire, M. *Tetrahedron Lett*. **1995**, *36*, 4235-4236.

**4.** Bethmont, V.; Montassier, C.; Marecot, P. *J. Mol. Catal. A:Chem*. **2000**, *152*, 133-140.

**5.** Doyle, M. P.; DeBruyn, D. J.; Kooista, D. A. *J. Am .Chem. Soc*. **1972**, 3659-3661.

**6.** Gooβen, L. J.; Linder, C. *Synlett* **2006**, *20*, 3489-3491.

**7.** Kleinert, M.; Barth, T. *Chem. Eng. Technol*. **2008**, *31*, 736-745.

**8.** Kleinert, M.; Barth, T. Energy & Fuels **2008**, *22*, 1371-1379.

**9.** Yan, N.; Zhao, C.; Dyson, P. J.; Wang, C.; Liu, L.; Kou, Y. *ChemSusChem* **2008**, *1*, 626-629.

# Chapter 6

# One Step Conversion of Cellulose into Liquid Fuels by High Temperature Water and Rhodium Catalyst

## 6.1 Introduction

The need for alternate fuel source is the basis of much research these days. The driving force is the energy independence, decrease in the greenhouse gas effect and the creation of jobs. The worldwide investment in the renewable fuel increased from $5 billion in 1995 to $38 billion in 2005 and is expected to be more than $100 billion by 2010.**[1]** The commonly used biofuel, i.e. ethanol, is made by the fermentation of plant matter; mainly, corn, soybean and sugarcane. These resources are renewable and the combustion of biofuel is considered to generate lower greenhouse gas than the fossil fuel considering the $CO_2$ consumption during their subsequent regrowth.**[2]** However, the increasing use of food crops to fill our tanks has a net effect of worldwide food shortage and record high prices. In this context, biomass, which is abundant and renewable, is a promising new raw material for producing fuels, chemicals and energy.**[3],[4],[5],[6],[7]** Both chemical and biological processes are employed for biomass conversion.

Cellulose is the most abundant source of biomass. It is a highly crystalline polymer of D-glucose linked together by $\beta$-1,4-glycoside bonds. The intra- and inter-molecular hydrogen bonding greatly stabilizes the polymer. It can be broken down into glucose by acid hydrolysis and then hydrogenated to sorbitol and other polyols.**[3-7]** These carbohydrate monomers are then converted to liquid fuels, energy and chemicals. However, the mineral acids are corrosive and the recovery and proper disposal of the acid is always an issue. Alternatively, cellulose breakdown by the enzymes take place in mild reaction conditions, but the process is slow and enzymes are expensive.**[8]**

Fukuoka and coworker have reported the conversion of cellulose to sorbitol and mannitol using Ru and other metal catalysts supported on solid acids**[5]** but the yields are low, mainly due to the poor access of highly stable polymeric chains to the surface acid sites. Ionic liquid, like 1-butyl-3-methylimidazolium chloride can dissolve up to 25 wt % of cellulose. The cellulose conversion to sorbitol has been performed using mineral acid and Ru nanoclusters in ionic liquids.**[9],[10]** The efficiency due to the dissolved cellulose is, however, outdone by the difficulty to separate the ionic liquid from the products. It seems that the hydrolysis of cellulose is best done by liquid acids but the balance between the reaction conditions and product yield has to be properly analyzed. Recently, Mascal and coworkers have reported a direct, high yield conversion of cellulose into biofuel.**[6]** The cellulose is acid hydrolyzed in the presence of LiCl and the furanic product formed was continuously extracted with an organic solvent. Although, the reported method gave isolated yield of over 80 %, the use of a large amount of concentrated acid and long reaction time are the drawbacks.

Water at elevated temperatures (above 200 ˚C) generates $H^+$ ions which can perform acid catalyzed reactions and at ambient temperatures, these in situ formed $H^+$ ions disappear.**[7],[11],[12]** This reversible method of acid formation from hot water eliminates the need of the acid recovery and disposal associated with using conventional acids. Liu and coworkers have reported the cellulose conversion into polyols using such conditions and Ru/C catalyst.**[7c]** The conversion of 85 % was obtained in 30 min with 39 % yield of hexitols (sorbitol and mannitol) and the rest being lower alcohols. The authors suggest that the aqueous alcohol solution can then be converted directly into hydrogen and synthetic gas. Here, we report the one step conversion of cellulose into liquid fuels using reversibly formed acid in water at high temperature and rhodium catalyst. Within 2.5 h, there is a 100 % conversion of cellulose into dehydrated hexitols which is further hydrogenolyzed into alcohols, furans, pyrans and $C_6$ compounds. The method gave high yield when toluene was used as an extracting solvent. These

products can be used as liquid fuel or as fuel additives. The most appealing aspect of this process is that no mineral acid is used for hydrolysis. Rather, acid hydrolysis of the celluloses is performed by $H^+$ ions generated from water at high temperature. At ambient temperature, these insitu formed $H^+$ ions disappear thereby eliminating the need for acid recovery and disposal.

## 6.2 Results and Discussion

### 6.2.1 Reaction Set-up

Cellulose was converted in a single step into liquid fuels by the $H^+$ ions formed from water at high temperature and $RhCl_3$ catalyst. The reaction was carried out in a stainless steel autoclave with a glass liner (Figure **6-1**). Cellulose, $RhCl_3$ and water at 900 psi $H_2$ was reacted at (215-240) ˚C. At the end of the reaction, the aqueous layer was extracted with benzene or toluene. Better results were obtained when toluene was present in the reactor to extract the organic products formed during the reaction. Rhodium chloride was the most efficient catalyst out of the three transition metal catalysts tested. Ruthenium chloride was comparatively less efficient while both Pd/C and $Na_2PdCl_4$ failed to deliver the desired product.

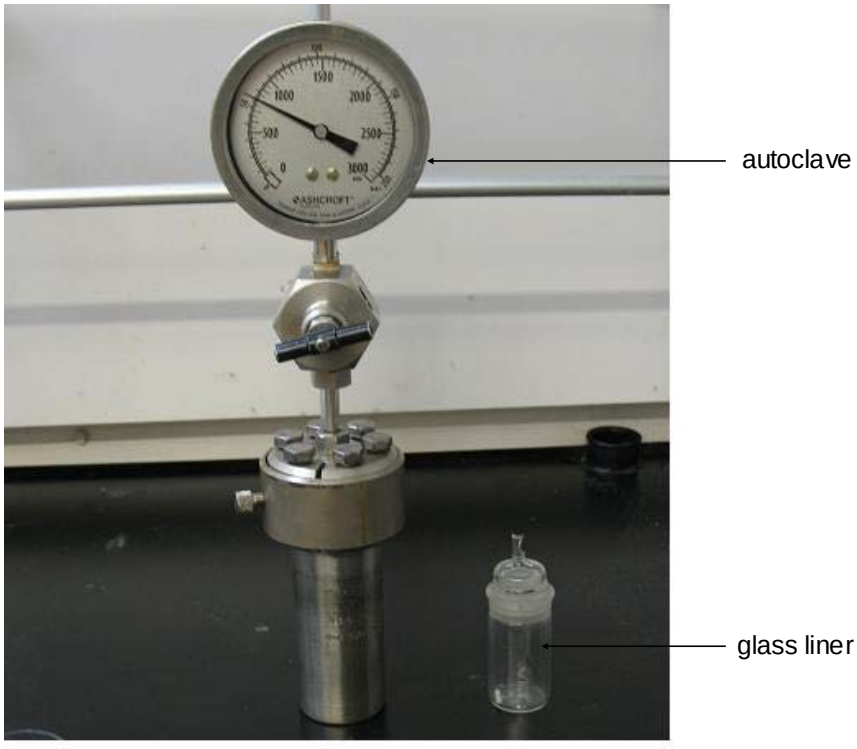


Figure **6-1**: Pressure reactor used for cellulose conversion.

### 6.2.2 Conversion of Cellulose to Polyols

As shown in (Table **6-1)**, the cellulose reacted rapidly to hexitols (**1**) (sorbitol and mannitol); 29 % conversion and 19.6 % hexitols in 30 min at 180 ˚C (entry 1). Electrospray Ionization-Mass Spectrometry (ESI-MS) of the aqueous layer showed m/z of 183 $[M+H]^+$, 200 $[M+NH_4]^+$ and 205 $[M+Na]^+$ corresponding to the molecular weight of hexitols-182 (Figure **6-2**). When the temperature was increased to 240 ˚C, the conversion was 66 % and the yield of hexitols was 62.5 % in 30 min (entry 2). The high selectivity of the hexitols reflects the immediate

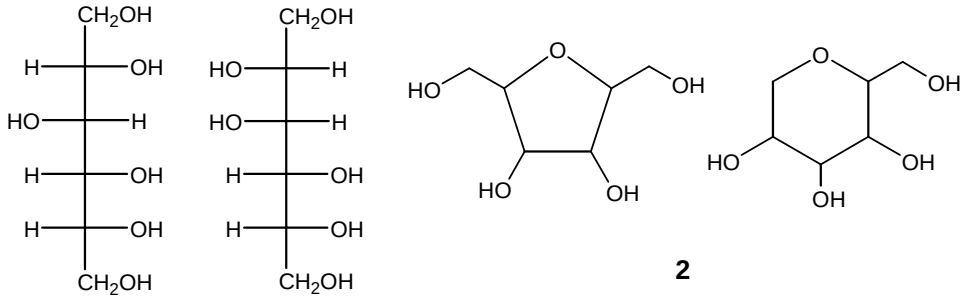


Sorbitol Mannitol

**1** **2**

hydrogenation of the glucose formed from the acid hydrolysis of cellulose. Upon prolonged reaction time of 2.5 h, the cellulose conversion was 100 % and the linear polyols dehydrated to five and six member heterocyclic dehydrated hexitols (**2**) (entry 3). ESI-MS of the aqueous layer showed m/z of 165 $[M+H]^+$, 182 $[M+NH_4]^+$ and 187 $[M+Na]^+$ corresponding to the molecular weight of dehydrated hexitols-164 (Figure **6-3**). No liquid fuel was formed at this point as revealed by the analysis of the organic phase after extracting the aqueous layer.

Table **6-1**: Catalytic conversion of cellulose into hexitols[a].

| entry | temp (˚C) | time (h) | cellulose conversion (%)[b] | yield of hexitols (%)[c] |
|---|---|---|---|---|
| 1 | 180 | 0.5 | 29 | 19.6 |
| 2 | 240 | 0.5 | 66 | 62.5 |
| 3 | 240 | 2.5 | 100 | - |

[a]Conditions: cellulose (1 mmol), $RhCl_3.xH_20$ (10 mol %), $H_20$ (10 mL), 900 psi $H_2$. [b]calculation based on unreacted cellulose. [c]analyzed by ESI-MS and yield determined by $^1$H-NMR.

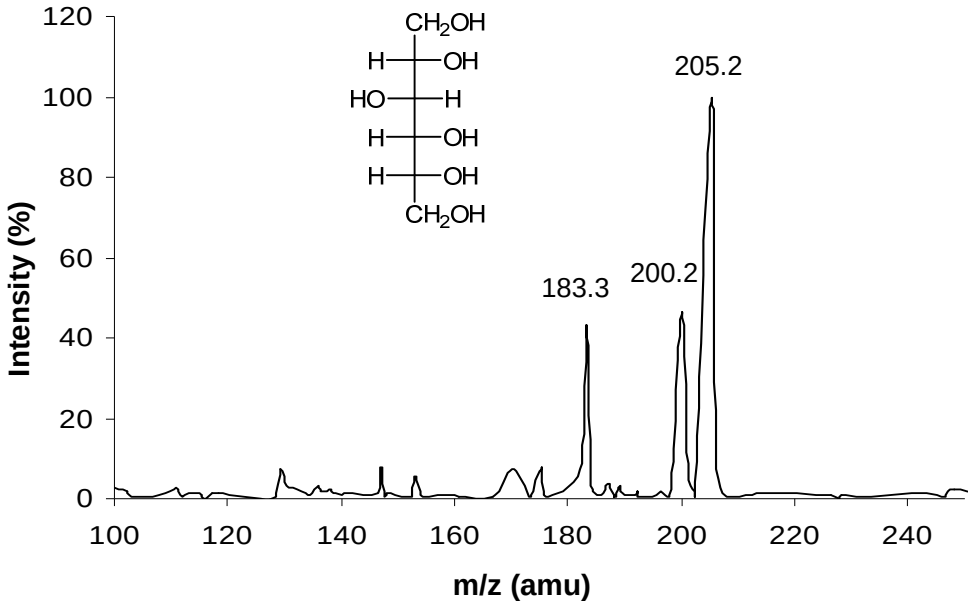


Figure **6-2**: ESI-MS spectrum of hexitol formed at the end of 0.5 h.

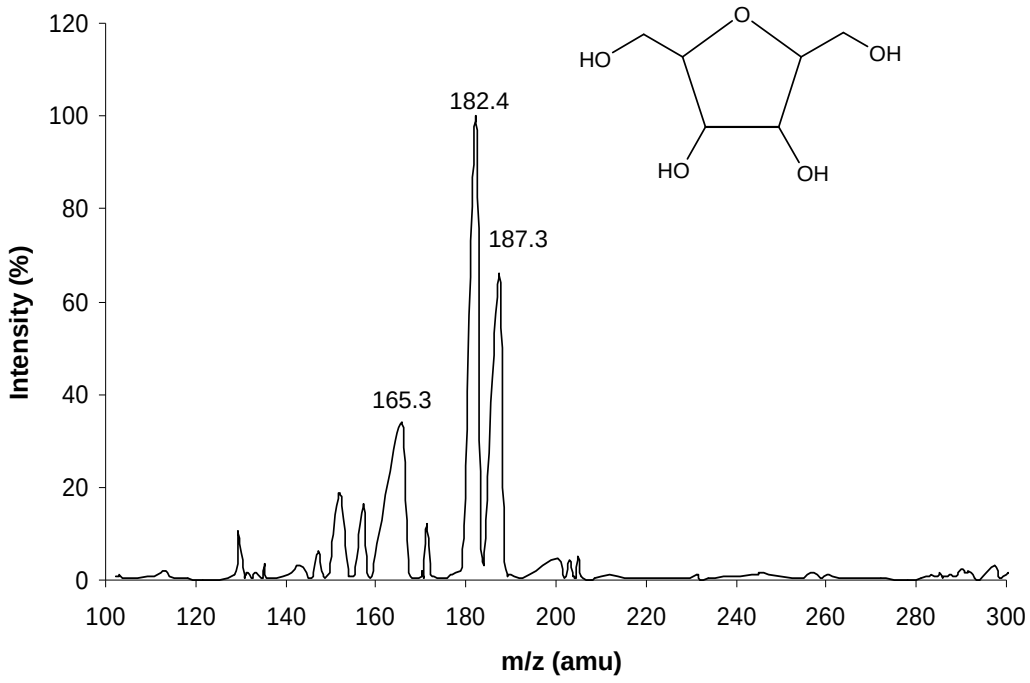


Figure **6-3**: ESI-MS spectrum of dehydrated hexitol formed at the end of 2.5 h.

### 6.2.3 Conversion of Cellulose to Fuels

Ethanol, dimethyl tetrahydrofuran and other mono-oxygenated hydrocarbons are valuable chemicals that can be produced from the dehydrated hexitols. Ethanol has been used alone or mixed with petroleum gasoline in automotives. Recently, dimethylfuran derived from carbohydrates was reported to have good fuel qualities as high energy density, low water solubility.**[4d]** However, DMF is an unsaturated hydrocarbon. Our group has recently reported the one step synthesis of DMTHF from carbohydrates. DMTHF is a saturated hydrocarbon with high energy density, low solubility in water, high boiling point and good stability for transportation and storage making it an excellent candidate for automotive fuel.**[13]**

When the reaction time was prolonged, the dehydrated hexitols undergo hydrogenolysis of C-O bond over Rh catalyst. The ring opening and further degradation of the hydrogenolyzed products also occur as indicated form the study. As seen in (Table **6-2,** entry 5), when the reaction time was increased to 10 h, the overall yield of the liquid fuels was 15 % with the highest selectivity of 47 % for the cis- and trans- iosmers of 2,5-dimethyl tetrahydrofuran (**3**) (DMTHF) followed by the selectivity of 26.5 % for 2-methyl tetrahydropyran (**4**) (MTHP), the structural isomer of DMTHF. DMTHF undergo C-C bond cleavage to form 2-methyl tetrahydrofuran (**5**) with a selectivity of 16 % and the rest are linear, mono-oxygenated $C_6$ compounds and tetrahydropyran (**6**). With the increase in reaction pressure to 1400 psi, the yield increased to 20.4 % in 5.5 h as compared to 15 % in 10 h, however, the selectivity for DMTHF decreased (entry 6). The employed condition has similar selectivity of about 20 % for 2,5- dimethyl tetrahydrofuran **3**, methyl tetrahydropyran (**4**) and hexanone (**7**) (1:1 ratio of 2- and 3-ketone), 11.3 % selectivity for 2- methyl cyclopentanone (**8**) and the rest being the liner $C_6$ and cyclic $C_5$ mono-oxygenated products. The liner $C_6$ compounds in these reactions must have been formed by the ring opening of the furanic and pyranic compounds. This hypothesis is supported by the result that there are no

linear hexitols in the reaction medium by 2.5 h (as indicated by the absence of adducts of molecular weight 182 in Figure **6-3**). The reaction pressure of over 900 psi was not further pursued as it lowered the selectivity and thus, to increase the overall yield of the products, an organic solvent was used as an extracting solvent during the reaction.

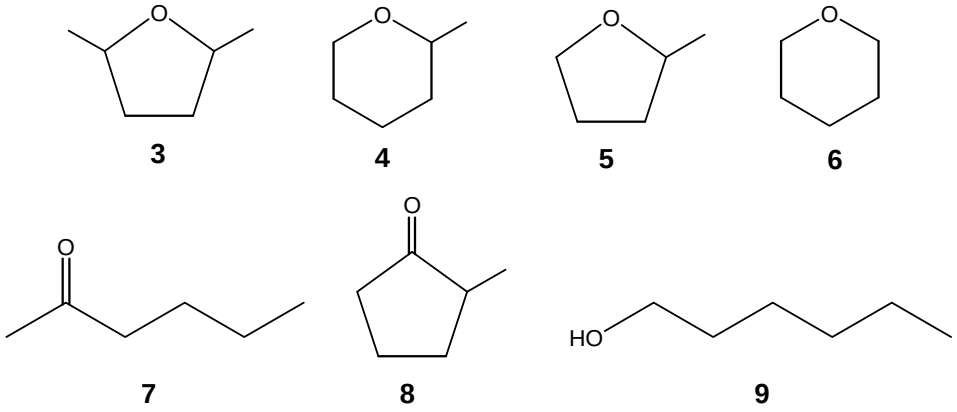


When toluene was used as an extracting solvent in the autoclave, excellent yield of the liquid fuels was obtained (entry 1). Toluene was placed outside the glass vial carrying the reaction mixture. The temperature was also lowered to 215 ˚C to minimize the side reactions associated with long reaction time. After a reaction time of 18 h, 82.4 % liquid fuels was formed with the highest selectivity of 27.9 % for 2,5-DMTHF (**3**). Ethanol that was not observed previously was formed with a selectivity of 15.3 % and similar selectivity was seen for hexanone (**7**) (2.5:1 ratio of 2- and 3-ketone) and MTHP (**4**). The employed condition also hydrogenates about half of the used toluene to mostly methyl cyclohexane and some methylcyclohex-1-ene.With water and toluene as a biphasic reaction medium (entry 2), the selectivity for ethanol increased to 42.8 % while the selectivity for DMTHF (**3**) increases slightly to 30.1 %. However, the yield decreased almost half to 42.8 %. It was also noted during the analysis that almost all of the toluene used was hydrogenated to methyl cyclohexane. The lower yield acquired with the biphasic system can be due to the competitive side reaction, the hydrogenation of toluene.

The selectivity of DMTHF and DMTHP decreased during the long reaction time. The efficient removal of DMTHF and MTHP from the aqueous medium as it is formed can suppress the side reactions and increase the selectivity. The addition of the salt to the reactive aqueous phase has been shown to improve the extraction of similar products into an organic phase.**[4d]** In this context, a reaction was carried out in 35 wt % NaCl solution (entry 3). Unfortunately, the addition of NaCl has detrimental effect in the reaction. A lot of coke was formed and the yield of valuable chemicals was only 3.0 % with the highest selectivity of 36.6 % for 1- hexanol (**9**). The reason for such adverse effect of the salt in the condition studied is not fully understood.

Table **6-2**: Cellulose conversion and selectivity using water at high temperature and Rh catalyst[a].

| | **1** | **2** | **3** | **4** | **5** | **6** |
|---|---|---|---|---|---|---|
| conversion (%)[b] | 100 | 100 | - | 100 | 100 | 100 |
| yield (%)[c] | 82.4 | 45.8 | 3.0 | 17.8 | 15.0 | 20.4 |
| selectivity (%)[c] | | | | | | |
| 2,5-dimethyltetrahydrofuran | 27.9 | 30.1 | 18.6 | 34.8 | 47.0 | 21.8 |
| methyl tetrahydropyran | 13.1 | 9.2 | 16.6 | 11.7 | 26.5 | 20.1 |
| 2- & 3- hexanone | 14.4 | 2.2 | - | 14.0 | 1.4 | 26.2 |
| 1-hexanol | 4.6 | - | 36.6 | - | 2.7 | 6.1 |
| 1-hexanal | 2.9 | - | - | - | 2.8 | 7.4 |
| 2-methyl tetrahydrofuran | 3.7 | 5.2 | 26.6 | 10.6 | 16.0 | 2.2 |
| tetrahydropyran | 7.2 | - | - | 12.9 | 3.4 | 4.0 |
| methyl cylcopentanone | 5.5 | - | - | - | - | 11.3 |
| ethanol | 15.3 | 42.8 | - | 4.5 | - | 1.1 |
| methanol | 2.8 | 10.5 | - | 7.3 | - | - |
| cyclohexanone | 2.5 | - | - | - | - | - |
| methyl-2.5-dihydrofuran | - | - | - | 3.9 | - | - |

[a]Condition: cellulose (1 mmol), $RhCl_3.xH_2O$ (10 mol %), $H_2O$ (4 mL), 900 psi $H_2$, 215 ˚C, 18 h. GC-MS was used for product identification. [b]calculation based on unreacted cellulose. [c]yield and selectivity calculated using GC with reference to the internal standard, nitromethane.

**1**-toluene as extracting solvent in the autoclave.
**2**-$H_2O$ and toluene used for biphasic condition.
**3**-35 wt % NaCl added to the reaction and toluene as extracting solvent.
**4**-n-butanol as extracting solvent in the autoclave.
**5**-240 ˚C, 10 h, no extracting solvent in the autoclave.
**6**-240 ˚C, 5.5 h, 1400 psi $H_2$, no extracting solvent in the autoclave.

In an effort to eliminate the competing hydrogenation of toluene, n-butanol was substituted for toluene as the extracting solvent in the autoclave (entry 4). Moreover, n-butanol can be produced from biomass derived carbohydrates making it greener than toluene.**[14],[15]** Under similar reaction condition, only 17.8 % yield was obtained with n-butanol as an extracting solvent as compared to 82.4 % with toluene, however, the selectivities were similar. It has a highest selectivity of 34.8 % for 2,5-DMTHF (**3**). MTHP (**4**), 2-methyl tetrahydrofuran (**5**), tetrahydropyran (**6**) and hexanone (**7**) (2.4:1 ratio of 2- and 3-ketone) have selectivity in the range of 10-14 %. Further, the solvent undergoes reductive etherification to form di-butylether. This competitive etherification reaction might have decreased the overall yield of the product.

These results show that our approach can completely convert cellulose initially into dehydrated hexitols which further undergoes hydrogenolysis to form useful products. No/negligible amount of coke was formed during the reaction. The highest yield of 82.4 % was obtained with toluene as the extracting solvent; however, it would be ideal to increase the selectivity of one of the products say DMTHF or ethanol. The selectivity can be increased by analyzing other transition metal catalysts or designing more selective C-O bond breaking catalyst. Further, the optimal solvent should be chosen which is inert during the reaction.

### 6.2.4 Reaction Pathway for the Conversion of Cellulose into Liquid Fuels

The rationale for converting cellulose into liquid fuels is illustrated in (Figure **6-4**). Under the reaction condition, cellulose is initially hydrolyzed into glucose by the reversibly formed acid from water at high temperature. The glucose immediately undergoes hydrogenation forming hexitols. As previously described in section 6.2.2, ESI-MS analysis (Figure **6-2**) confirmed the formation of hexitols. It is also evident from ESI-MS analysis of the reaction mixture at the end of 2.5 h that the hexitols lose a molecule of water to form dehydrated hexitols (Figure **6-3**). Finally, hydrogenolysis over Rh catalyst breaks the C-O bond to yield DMTHF and DMTP. These products can further undergo C-C bond cleavage to form methyl tetrahydrofuran and tetrahydropyran respectively. The liner compounds are also formed by the ring opening and degradation reactions of the furanic and pyranic compounds. This hypothesis is supported by the ESI-MS result that there are no linear hexitols seen in the reaction medium by 2.5 h. No/negligible coke is formed during the reaction.

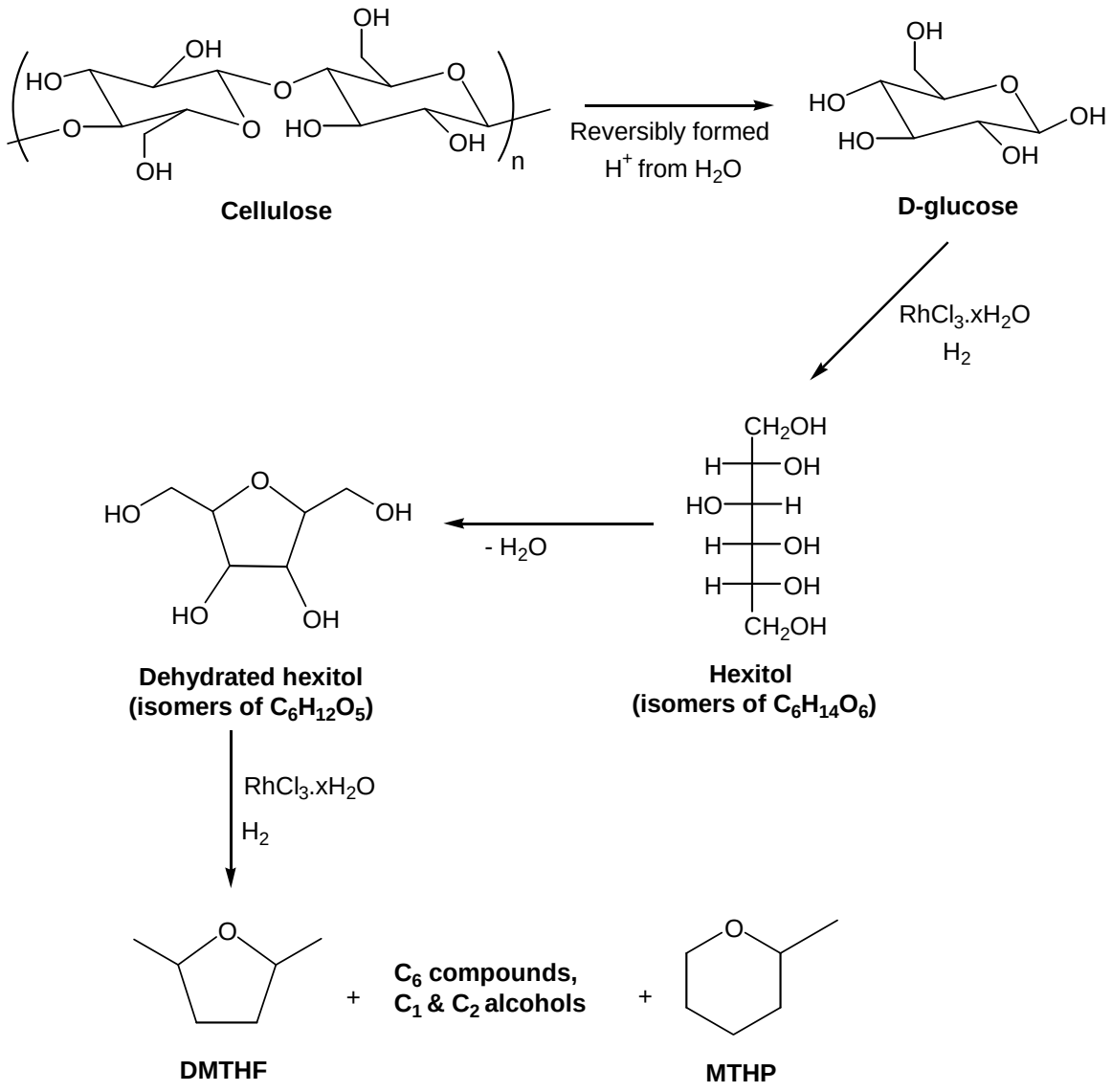


Figure **6-4**: Conversion of cellulose into liquid fuels.

## 6.3 Conclusion

We have reported an efficient conversion of cellulose into liquid fuels in a single step using reversibly formed acid from water at high temperature and rhodium catalyst. This method allows complete conversion of cellulose and the highest yield of 82.4 % was obtained with toluene as the extracting solvent. Liquid fuels like DMTHF, MTHP and ethanol is formed by the acid hydrolysis and subsequent hydrogenolysis over Rh catalyst. However, it would be ideal to increase the selectivity of one of the products say DMTHF or ethanol. Further work is needed to increase the selectivity. This is also a green approach as the in situ formed acid at higher temperature vanishes at ambient temperature, thus eliminating the need for the acid recovery and disposal.

## 6.4 Experimental

### 6.4.1 Materials and Instrumentation

$RhCl_3.xH_2O$ was purchased from Alfa Aesar. All other chemicals were purchased from Aldrich and used without further purification. $^1H$ spectra were recorded on Bruker DPX-300 (300 MHz) spectrometer. Molecular mass analysis of water soluble fractions were performed on Waters LCT Premier time of flight mass spectrometer with electrospray ionization (ESI) and organic soluble fractions were analyzed on Waters CGT time of flight mass spectrometer with electron impact ionization (EI). GC analysis was performed on Hewlett Packard-5890 with a FID detector and 95% dimethyl- and 5% diphenyl- polysiloxane column.

### 6.4.2 Conversion of Cellulose to Liquid Fuels

The reactions were carried out in a stainless steel autoclave with a glass liner. Cellulose (1 mmol), $RhCl_3.xH_2O$ (0.1 mmol), $H_2O$ (4 mL) was reacted at 215 ˚C and 900 psi $H_2$ for a specific period of time. Toluene was outside of the glass liner in the autoclave when used as an extracting solvent. At the end of the reaction, the two phases were collected. The aqueous layer was filtered to separate any reduced catalyst. The diluted aqueous phase products were analyzed by ESI-MS. The components of the organic phase were identified by GC-MS and quantified by GC. The yield and selectivity were calculated with reference to the internal standard, nitromethane using GC. The conversion was based on the weight of cellulose before and after the reaction.

## 6.5 References

**1.** Grunwald, M. *Time* **2008**, *April 7*, 40-45.

**2.** Klass, D. L. *Biomass for Renewable Energy, Fuels, and Chemicals*, Academic Press: San Diego, 1998.

**3.** Klemm, D.; Heublien, B.; Fink, H-P.; Bohn, A. *Angew. Chem. Int. Ed*. **2005**, *44*, 3358-3393.

**4.** (a) Huber, G. W.; Iborra, S.; Corma, A. *Chem. Rev*. **2006**, *106*, 4044-4098. (b) Chheda, J. N.; Huber, G. W.; Dumesic, J. A. *Angew. Chem. Int. Ed*. **2007**, *14*, 7164-7183. (c) Huber, G. W.; Chheda, J. N.; Barrett, C. J.; Dumesic, J. A. *Science* **2005**, *308*, 1446-1450. (d) Roman-Leshkov, Y.; Barrett, C. J.; Liu, Z. Y.; Dumesic, J. A. *Nature* **2007**, *447*, 982-985.

**5.** Fukuoka, A.; Dhepe, P. L. *Angew. Chem. Int. Ed*. **2006**, *45*, 5161-5163.

**6.** Mascal, M.; Nikitin, E. B. *Angew. Chem. Int. Ed*. **2008**, *47*, 7924-7926.

**7.** (a) Yu, Y.; Lou, X.; Wu, H. *Energy & Fuels* **2008**, *22*, 46-60. (b) Mochidzuki, K.; Sakoda, A.; Suzuki, M. *Adv. Env. Res*. **2003**, *7*, 421-428. (c) Luo, C.; Wang, S.; Liu, H. *Angew. Chem. Int. Ed***. 2007**, *46*, 7636-7639.

**8.** U. S. Department of Energy, Energy Efficiency and Renewable Energy. http://www.eere.energy.gov/biomass (accessed on January 24, 2007).

**9.** Yan, Y.; Zhao, C.; Luo, C.; Dyson, P. J.; Liu, H.; Kou, Y. *J. Am. Chem. Soc*. **2006**, *128*, 8714-8715.

**10.** Zhao, Z. K.; Li, C. *Adv. Synth. Catal*. **2007**, *349*, 1847-1850.

**11.** Sasaki, M.; Fang, Z.; Fukushima, Y.; Adschiri, T.; Arai, K. *Ind. Eng. Chem. Res*. **2000**, *39*, 2883-2890.

**12.** (a) Chamblee, T. S.; Weikel, R. R.; Nolen, S. A.; Liotta, C. L.; Eckert, C. A. *Green Chem*. **2004**, *6*, 382-386. (b) Nolen, C. A.; Liotta, C. L.; Eckert, C. A.; Glaserb, R. *Green Chem*. **2003**, *5*, 663-669.

**13.** Yang, W.; Sen, A. submitted to *Angew. Chem. Int. Ed*. **2008**.

**14.** Jones, D. T.; Woods, D. R. *Microbiol. Rev*. **1986**, *50*, 484-524.

**15.** Ramey, E. D. US patent US5753474, **1998**.

# VITA

## Shikchya Tandukar

Shikchya Tandukar received her Master of Science (M. Sc.) from Tribhuvan University, Kathmandu, Nepal. She joined the Department of Chemistry at The Pennsylvania State University; University Park in fall 2003 to pursue Ph. D. degree under the supervision of Dr. Ayusman Sen. She started her graduate study with antibacterial compounds and continued to work on heterogeneous catalyst for various coupling reactions. Her research also includes a green method for high conversion of cellulose to valuable chemicals. She will be joining Intel Corporation at Hillsboro, OR as a process development engineer.